AD-A040 760 COLD REGIONS RESEARCH AND ENGINEERING LAB HANOVER N H F/G 13/9
MECHANICS OF CUTTING AND BORING. PART 4. DYNAMICS AND ENERGETIC--ETC(U)
APR 77 M MELLOR

UNCLASSIFIED CRREL-77-7 NL

1 OF 2
AD A040760

CRREL REPORT 77-7

Mechanics of cutting and boring
Part IV: Dynamics and energetics of parallel motion tools

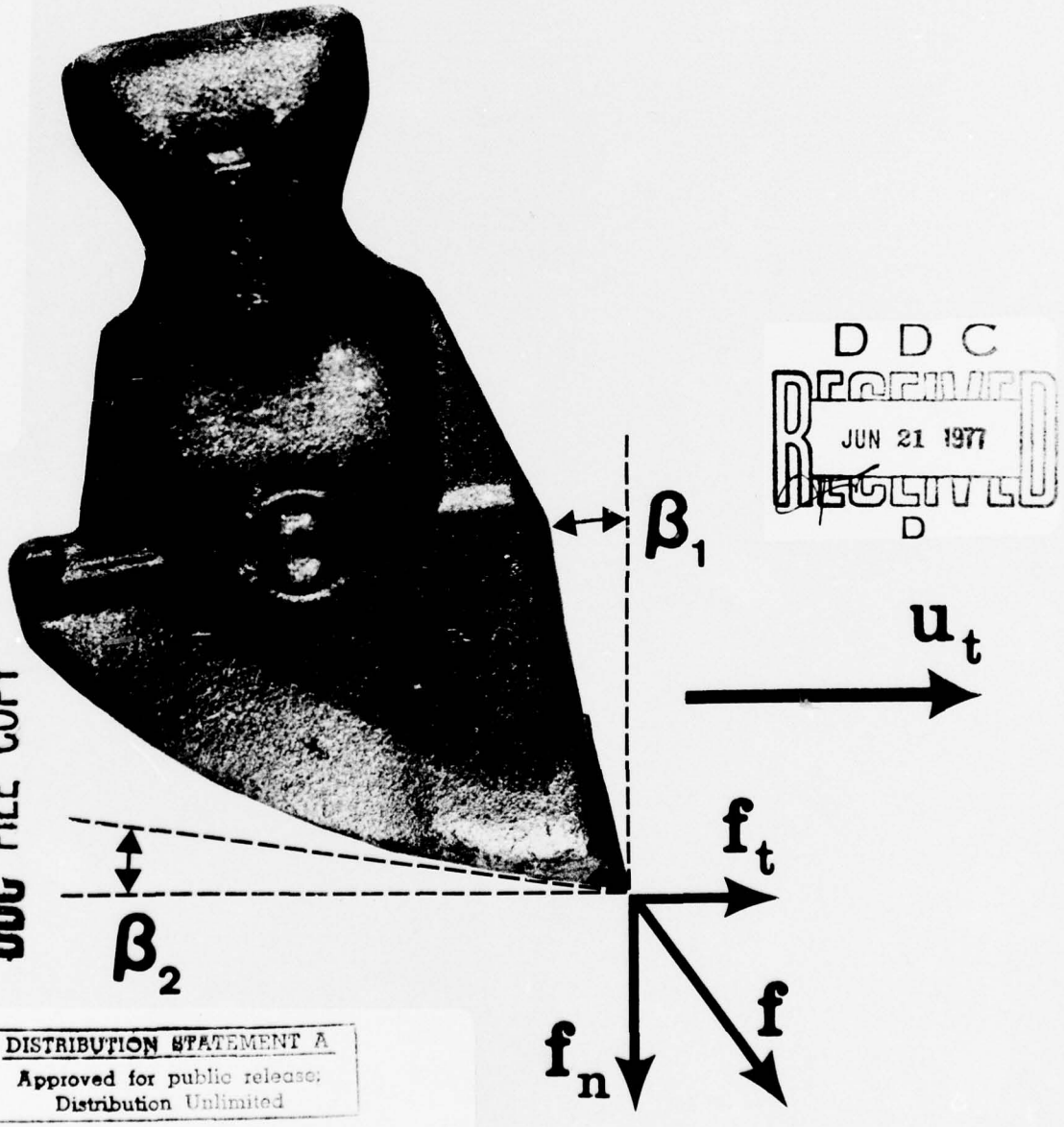

CRREL Report 77-7

Mechanics of cutting and boring
Part IV: Dynamics and energetics of parallel motion tools

Malcolm Mellor

April 1977

Prepared for
DIRECTORATE OF FACILITIES ENGINEERING
OFFICE, CHIEF OF ENGINEERS
By
CORPS OF ENGINEERS, U.S. ARMY
COLD REGIONS RESEARCH AND ENGINEERING LABORATORY
HANOVER, NEW HAMPSHIRE

Approved for public release; distribution unlimited.

Unclassified

SECURITY CLASSIFICATION OF THIS PAGE (When Data Entered)

REPORT DOCUMENTATION PAGE

READ INSTRUCTIONS BEFORE COMPLETING FORM

1. REPORT NUMBER: CRREL Report 77-7	2. GOVT ACCESSION NO.
3. RECIPIENT'S CATALOG NUMBER	
4. TITLE (and Subtitle): MECHANICS OF CUTTING AND BORING, Part 4, Dynamics and Energetics of Parallel Motion Tools	5. TYPE OF REPORT & PERIOD COVERED
	6. PERFORMING ORG. REPORT NUMBER
7. AUTHOR(s): Malcolm Mellor	8. CONTRACT OR GRANT NUMBER(s)
9. PERFORMING ORGANIZATION NAME AND ADDRESS: U.S. Army Cold Regions Research and Engineering Laboratory, Hanover, New Hampshire 03755	10. PROGRAM ELEMENT, PROJECT, TASK AREA & WORK UNIT NUMBERS: ~~DA Project~~ 4A762719AT42, Technical Area 02, Work Unit 004
11. CONTROLLING OFFICE NAME AND ADDRESS: Directorate of Facilities Engineering, Office, Chief of Engineers, Washington, D.C. 20314	12. REPORT DATE: April 1977
	13. NUMBER OF PAGES: 96
14. MONITORING AGENCY NAME & ADDRESS (if different from Controlling Office)	15. SECURITY CLASS. (of this report): Unclassified
	15a. DECLASSIFICATION/DOWNGRADING SCHEDULE

16. DISTRIBUTION STATEMENT (of this Report)

Approved for public release; distribution unlimited.

17. DISTRIBUTION STATEMENT (of the abstract entered in Block 20, if different from Report)

18. SUPPLEMENTARY NOTES

19. KEY WORDS (Continue on reverse side if necessary and identify by block number)

Boring machines	Ice cutting
Drills	Machine design
Excavating machines	Permafrost excavation
Excavation	Rock cutting

20. ABSTRACT (Continue on reverse side if necessary and identify by block number)

The report deals with the cutting of rock and similar materials by parallel motion tools. It examines cutting forces and energy requirements, taking into consideration tool geometry, wear, operating conditions, and material properties. After an introductory discussion of terminology, some general principles are outlined, and relevant theoretical ideas on metal cutting and rock cutting are reviewed. The next section, which is the heart of the report, reviews experimental data on the magnitudes and directions of cutting forces. There is a graphical compilation of data, including some from obscure or unpublished sources. The variables covered include chipping depth, rake angle, relief angle, side rake, base angle, tool width, tool compliance, tool speed, tool wear, tool interactions, and material properties.

DD FORM 1 JAN 73 1473 EDITION OF 1 NOV 65 IS OBSOLETE

Unclassified

SECURITY CLASSIFICATION OF THIS PAGE (When Data Entered)

037100

20. Abstract (cont'd)

The second major part of the report treats the energetics of cutting. It begins with a short discussion of relevant principles, and continues with a compilation and review of experimental data, covering the same independent variables as the force section. The report ends with a concise summary of general behavior for parallel motion tools.

PREFACE

This report was prepared by Dr. Malcolm Mellor, Physical Scientist, Experimental Engineering Division, U.S. Army Cold Regions Research and Engineering Laboratory. The work was done under DA Project 4A762719AT42, *Design, Construction and Operations Technology for Cold Regions*, Technical Area 02, *Soils and Foundations Technology*, Work Unit 004, *Excavation in Frozen Ground*.

The author is indebted to many individuals and organizations for the data compiled here. He is particularly grateful to Professor Frank Roxborough and colleagues for providing copies of unpublished reports, and to Mr. M.P. O'Reilly of the Transport and Road Research Laboratory (U.K.) for granting permission to abstract data from these reports. Unpublished results were also generously provided by Mr. Kihachiro Furumi of Komatsu Ltd. Valuable professional courtesies were extended by Dr. Ivor Evans, Mr. John Barker, and Dr. Peter Kenny of the Mining Research and Development Establishment, National Coal Board (U.K.), by Mr. Belin and Mr. A. Valantin of the Centre d'Etudes et Recherches des Charbonnages de France, and by Mr. D. Fourmaintraux of the Laboratoire Central des Ponts et Chaussées (Paris). Last, but certainly not least, the author gratefully acknowledges the "real world" explanations provided by engineers and equipment operators at various construction sites, mines, and tunnels.

Paul V. Sellmann of CRREL and Dr. Ivor Hawkes provided technical reviews of the manuscript.

CONTENTS

ILLUSTRATIONS

Figure Page

Figure Page

MECHANICS OF CUTTING AND BORING

FOREWORD

There are a multitude of tasks that involve the cutting, drilling, or excavating of natural ground materials and massive structural materials. The required technology varies with the properties of the materials and with the scale of operations, but a broad distinction can be made on the basis of the strength, cohesion, and ductility of the material that is to be worked. In weak materials that have little cohesion (e.g. typical soils) the forces and energy levels required for separation and disaggregation are often small compared with the forces and energy levels required for acceleration and transport, and materials handling technology dominates the consideration. By contrast, in strong materials that exhibit brittle fracture characteristics (e.g. rock, concrete, ice, frozen ground) the forces and energy levels required for cutting and breaking are high compared with those required for handling the broken material, and the technical emphasis is on cutting and breaking processes.

CRREL has long been concerned with excavating and drilling in ice and frozen ground, and over the past decade systematic research has been directed to this technical area. The research has covered a wide range of established technologies and novel concepts but, for short term applications, interest has necessarily centered on special developments of proven concepts. In particular, there has been considerable concern with direct mechanical cutting applied to excavation, cutting, and drilling of frozen soils, glacier ice, floating ice, and dense snow. During the course of this work, numerous analyses and design exercises have been undertaken, and an attempt is now being made to develop a systematic analytical scheme that can be used to facilitate future work on the mechanics of cutting and boring machines.

In the industrial sector, rock-cutting machines are usually designed by applying standard engineering methods in conjunction with experience gained during evolution of successive generations of machines. This is a very sound approach for gradual progressive development, but it may not be appropriate when there are requirements for rapid development involving radical departures from established performance characteristics, or for operations in unusual and unfamiliar materials. A distinct alternative is to design more or less from first principles by means of theoretical or experimental methods, but this alternative may not be practically feasible in its more extreme form.

There are numerous difficulties in attempting a strict scientific approach to the design of rock-cutting machines. The relevant theoretical rock mechanics is likely to involve controversial fracture theories and failure criteria, and to call for detailed material properties that are not normally available to a machine designer. Direct experiments are costly and time-consuming, and experimental data culled from the literature may be unsuitable for extrapolation, especially when (as is sometimes the case) they are described by relationships that violate the basic physics of the problem. Comprehensive mechanical analyses for rock-cutting machines have not yet

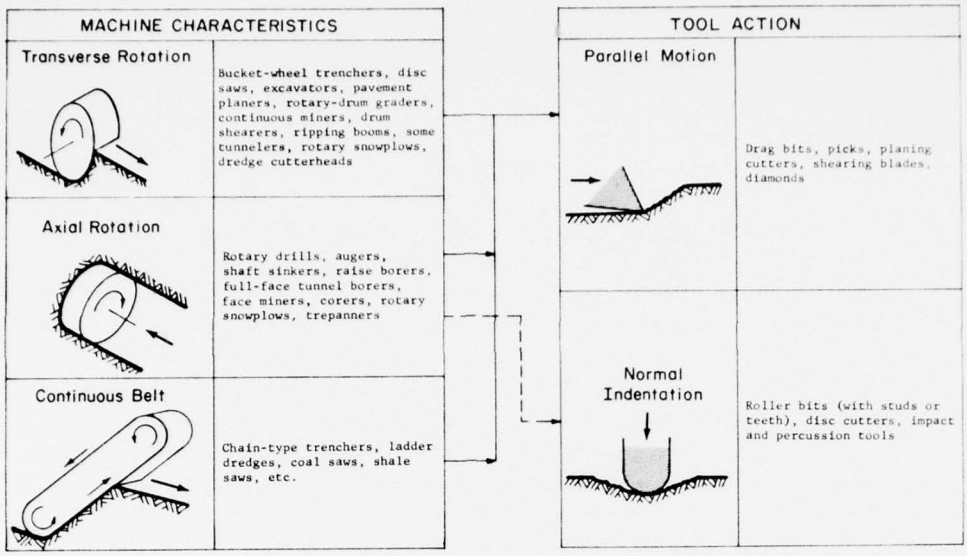

Classification of machines and cutting tools for analytical purposes.

evolved, and while established design principles for metal-cutting machine tools may be helpful, they do not cover all pertinent aspects. For example, there are usually enormous differences in forces and power levels between machine tools and excavating machines, and force components that can be almost ignored in a relatively rigid machine tool may be crucial design factors for large mobile rock cutters that are highly compliant.

In dealing with cold regions problems where neither outright empiricism nor highly speculative theory seem appropriate, some compromise approaches have been adopted. While simple and practical, these methods have proved useful for analysis and design of cutting and boring machines working under a wide range of conditions in diverse materials, and it seems possible that they might form the basis for a general analytical scheme. The overall strategy is to examine the kinematics, dynamics and energetics for both the cutting tool and the complete machine according to a certain classification, adhering as far as possible to strict mechanical principles, but holding to a minimum the requirements for detailed information on the properties of the material to be cut.

Kinematics deals with the inherent relationships defined by the geometry and motion of the machine and its cutting tools, without much reference to the properties of the material being cut. *Dynamics* deals with forces acting on the machine and its cutting tools, taking into account machine characteristics, operating procedures, wear effects, and material properties. *Energetics* deals largely with specific energy relationships that are determined from power considerations involving forces and velocities in various parts of the system, taking into account properties of the materials that are being cut.

These mechanical principles are applied in accordance with a classification based on the characteristic motions of the major machine element and the actual cutting

tools, as illustrated above. Machines are classified as *transverse rotation, axial rotation,* or *continuous belt,* while the action of cutting tools is divided into *parallel motion* and *normal indentation.*

Transverse rotation devices turn about an axis that is perpendicular to the direction of advance, as in circular saws. The category includes such things as bucket-wheel trenchers and excavators, pavement planers, rotary-drum graders, large disc saws for rock and concrete, certain types of tunneling machines, drum shearers, continuous miners, ripping booms, some rotary snowplows, some dredge cutterheads, and various special-purpose saws, millers and routers. *Axial rotation* devices turn about an axis that is parallel to the direction of advance, as in drills. The category includes such things as rotary drills, augers and shaft-sinking machines, raise borers, full-face tunnel boring machines, corers, trepanners, some face miners, and certain types of snowplows. *Continuous belt* machines represent a special form of transverse rotation device, in which the rotor has been changed to a linear element, as in a chain saw. The category includes "digger chain" trenchers, ladder dredges, coal saws, shale saws, and similar devices.

In tool action, *parallel motion* denotes an active stroke that is more or less parallel to the surface that is being advanced by the tool, i.e. a planing action. Tools working this way include drag bits for rotary drills and rock-cutting machines; picks for mining and tunneling machines; teeth for ditching and dredging buckets; trencher blades; shearing blades for rotary drills, surface planers, snowplows, etc.; diamond edges for drills and wheels; and other "abrasive" cutters. *Normal indentation* denotes an active stroke that is more or less normal to the surface that is being advanced, i.e. one which gives a pitting or cratering effect such as might be produced by a stone chisel driven perpendicular to the surface. Tools working this way include roller rock bits for drills, tunneling machines, raise borers, reamers, etc.; disc cutters for tunneling machines; and percussive bits for drills and impact breakers.

A few machines and operations do not fit neatly into this classification. For example, certain roadheaders and ripping booms used in mining sump-in by axial rotation and produce largely by transverse rotation, and there may be some question about the classification of tunnel reamers and tapered rock bits. However, the classification is very satisfactory for general mechanical analysis.

Complete treatment of the mechanics of cutting and boring is a lengthy task, and in order to expedite publication a series of reports dealing with various aspects of the problem will be printed as they are completed. The main topics to be covered in this series are:

1. Kinematics of transverse rotation machines (Special Report 226, May 1975)
2. Kinematics of axial rotation machines (CRREL Report 76-16, June 1976)
3. Kinematics of continuous belt machines (CRREL Report 76-17, June 1976)
4. Dynamics and energetics of parallel-motion tools
5. Dynamics and energetics of normal indentation tools
6. Dynamics and energetics of transverse rotation machines
7. Dynamics and energetics of axial rotation machines
8. Dynamics and energetics of continuous belt machines.

MECHANICS OF CUTTING AND BORING
PART 4: DYNAMICS AND ENERGETICS OF PARALLEL MOTION TOOLS

by

Malcolm Mellor

INTRODUCTION

Parallel motion tools are used in a wide variety of cutting and boring devices, from hand tools to giant machines. Simple examples include knives, chisels, planes and hand saws. Other applications are found in woodworking and metal-working machines, such as saws, lathes, millers and drills. On a larger scale, parallel motion tools are fitted to construction machines and agricultural machines that work in soils. However, in this report the main concern is with tools that are used for cutting and boring in rock, concrete, mineral deposits, frozen ground and ice (Fig. 1). The types of machines that carry the tools include rotary drills and corers, mining machines and tunnel borers, wheel trenchers and ladder trenchers, chain saws and disc saws, milling and planing drums, tractor rippers, dredges, and excavator buckets. In these applications the cutting tools themselves are usually known as *drag bits*, *picks*, or *cutting teeth*. On a different scale, cutting diamonds are also parallel-motion tools, and some grinding abrasives can probably be included in the same category.

The object of this report is to examine the forces developed, and the energy consumed, when parallel motion tools cut various types of rock, taking into account modes of operation, tool geometry, cutting speed, wear, and compliance. The first part deals with general characteristics of cutting tools and relevant theoretical considerations; the second part summarizes and reviews available experimental data on tool forces, and the final section covers energy considerations and experimental data on variations of specific energy. No attempt is made to consider the complex tool motions that occur when tools are fitted to various machines, since these motions, and their influences on tool geometry, have already been treated in Parts 1-3 of this series.

A major effort has gone into compiling as much experimental data as could be obtained, much of it from relatively obscure sources. A thorough compilation was judged necessary for understanding of the interrelationships between the many variables, and for resolution of some apparent contradictions between different sets of data.

TERMINOLOGY

A *kerf* is the groove or slot gouged out by a cutting tool. Parallel kerfs swept out by adjacent tools may overlap, or they may be separated by uncut *ribs*. In brittle materials a kerf usually has sloping sides resulting from overbreak.

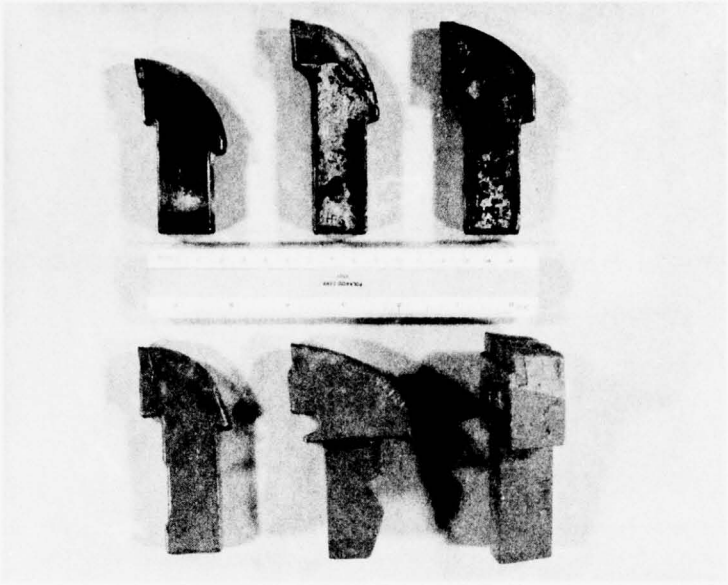

a. Small picks for mining machines, all tipped with tungsten carbide inserts.

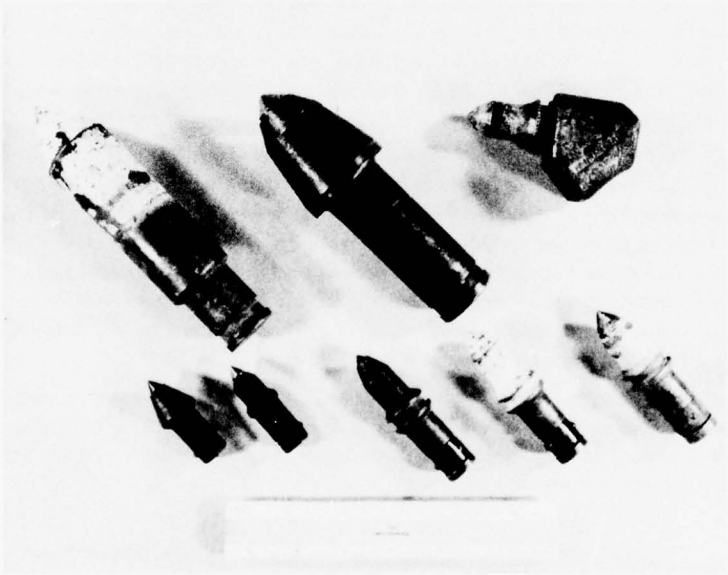

b. Rotationally symmetrical tools known variously as "bullet bits," "plumb-bob bits," "pencil bits," "conical bits," "point attack bits." The tungsten carbide insert is set in a similar manner to the lead of a pencil.

Figure 1. Examples of parallel-motion tools for cutting rock and other brittle materials.

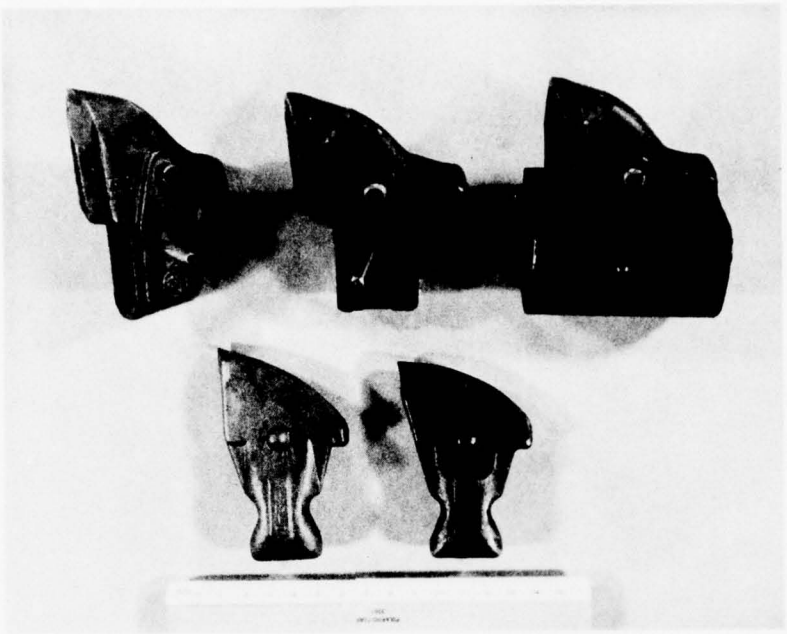

c. Medium size "parrot beak" picks for mining and rock-cutting machines.

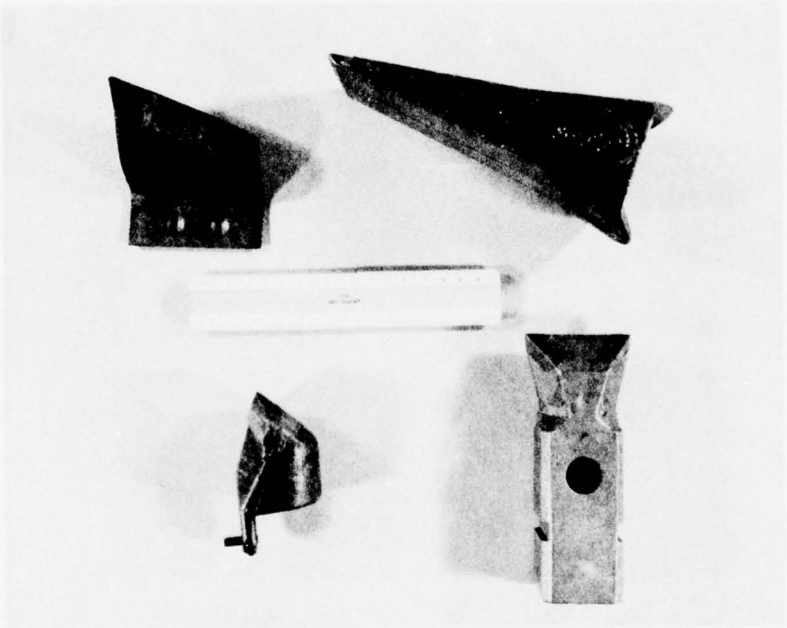

d. Clockwise from upper left: small hard-faced blade for a ladder-type soil trencher; large tooth for use on heavy auger drills, bucket wheel trenchers or excavator buckets; heavy pick for tunneling machines; hollow rock-cutting pick for "spigot" mounting.

Figure 1 (cont'd).

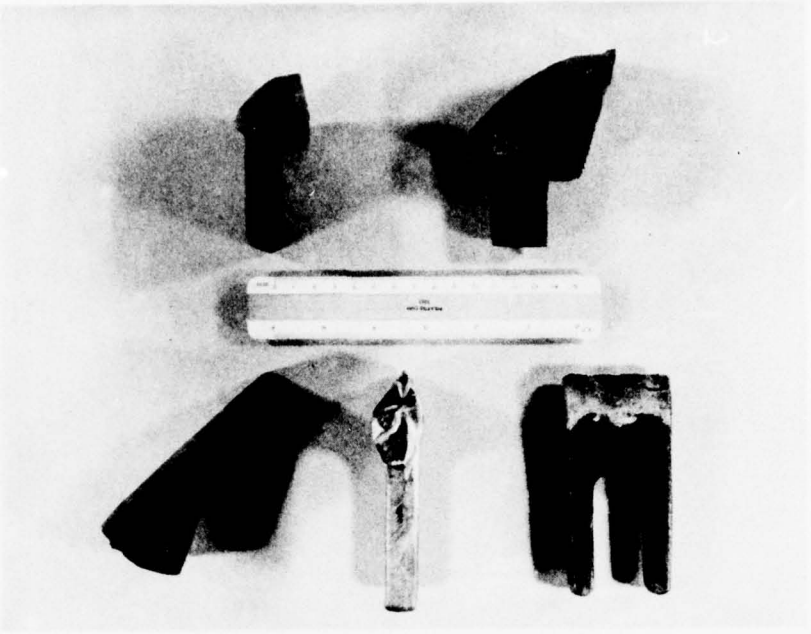

e. Teeth for heavy augers boring in soils and weak rocks.

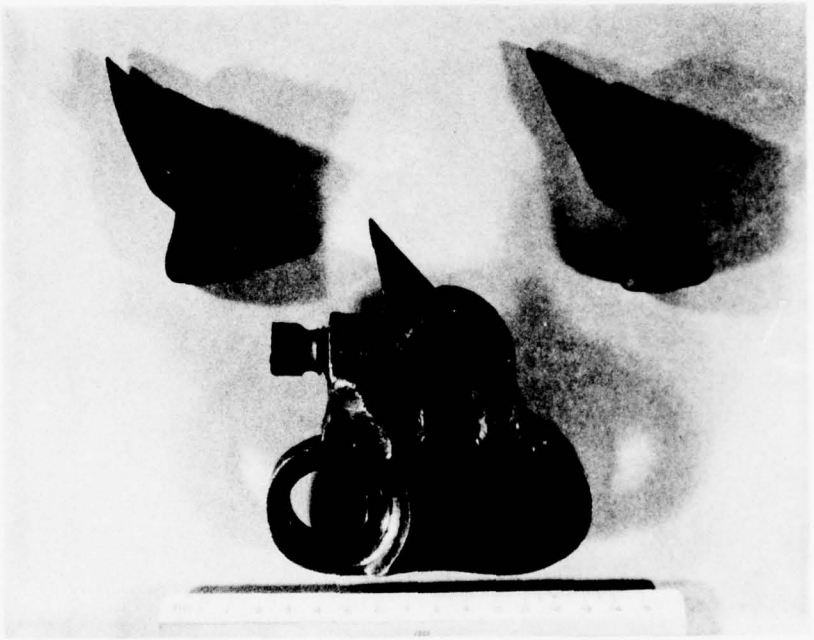

f. Coal-cutter bits with very high relief angle; lower item is a link from the chain of a small coal saw.

Figure 1 (cont'd). Examples of parallel-motion tools for cutting rock and other brittle materials.

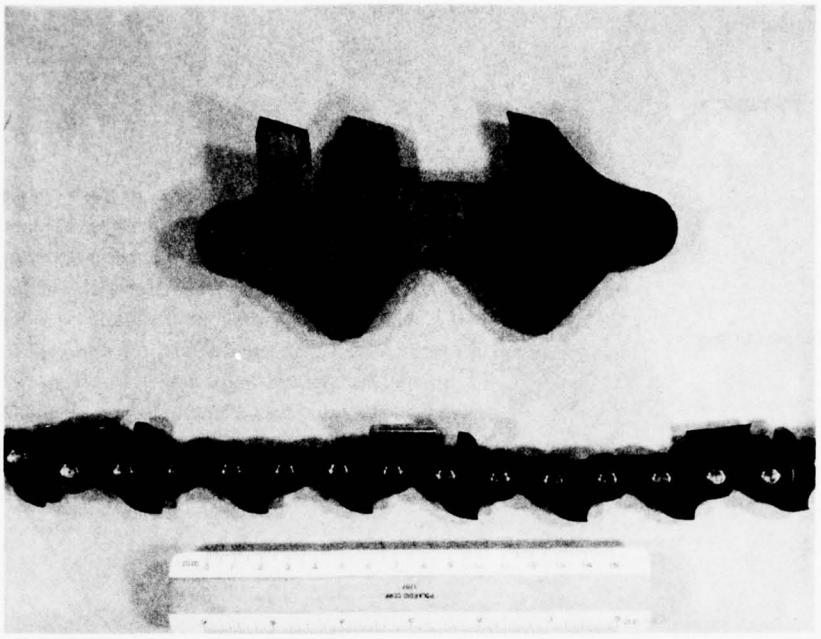

g. Chain-saw teeth, designed for wood-cutting and modified to cut ice.

Figure 1 (cont'd).

The difference between the width of a tool and the width of the kerf it produces is termed *overbreak*. Overbreak usually gives sloping sides to the kerf; the inclination of the sideslope to the normal direction is known as the *overbreak angle* ϕ.

Chipping depth ℓ is the penetration of the tool into the work, measuring in a normal direction from the current surface to the tool tip (Fig. 2). It is equivalent to "uncut chip thickness" in machine tool terminology.

Deep cutting involves penetration of the tool to a depth significantly greater than the radius of the tool tip r (Fig. 9). It allows tool rake to have some influence on the cutting process.

Shallow cutting involves penetration of the tool to a depth that is comparable to, or less than, the radius of the tip r (Fig. 9). The apparent rake of the tool is largely irrelevant to the cutting process in shallow cutting.

Orthogonal cutting takes place when a straight-edge cutting tool moves in such a way that the cutting edge is perpendicular to the direction of motion (Fig. 4). With a wide tool, orthogonal cutting can be idealized as a two-dimensional process. Direct scraping with a bulldozer blade is an example of orthogonal cutting.

Oblique cutting takes place when the edge of a cutting tool is not perpendicular to the direction of motion (Fig. 4). There may be more than one cutting edge involved in this slicing action, as in a V-face tool. Angle-dozing with a side-angled bulldozer blade is an example of oblique cutting.

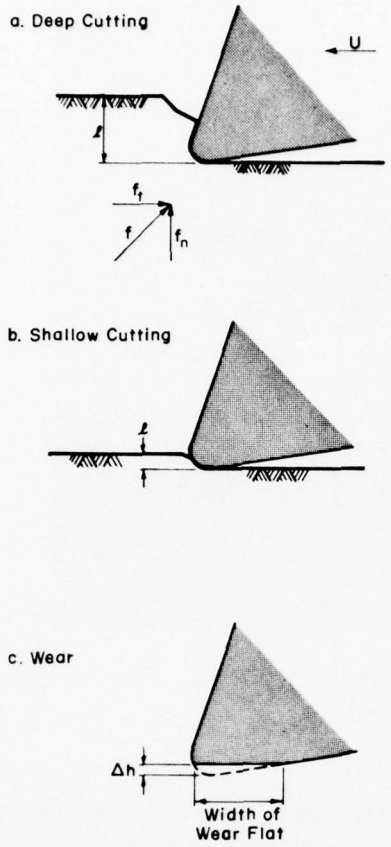

Figure 2. Cutting terminology. a) Deep cutting, in which the chipping depth ℓ is significantly greater than the radius of the tool tip r. Force components f (resultant), f_n (normal) and f_t (tangential) are illustrated. b) Shallow cutting, in which the chipping depth ℓ is comparable to, or smaller than, the radius of the tool tip, making the rake angle largely irrelevant. c) Wear flat on the relief face (flank wear). Note that the wear flat is not always exactly parallel to the tangential direction; it sometimes inclines slightly, giving initial negative relief angle of a few degrees.

The *cutting force* exerted by a tool is the force required to actually cut or break chips. It does not include forces associated with chip clearance or with unnecessary friction of trailing parts of the tool. The *resultant cutting force f* is inclined at some angle to the work surface, and it is convenient to resolve it into components parallel and perpendicular to the surface, the *tangential component* f_t and the *normal component* f_n respectively (Fig. 2a). The unqualified term "cutting force" is used by some writers to denote the tangential component only. In this report, primes are used to denote force per unit width (f', f_t', f_n'), and bars are used to denote mean values ($\bar{f}$, $\bar{f}_t$, $\bar{f}_n$) where force fluctuates with time.

Specific energy for the cutting process is the energy required to cut or break unit mass or unit volume of material. In this report, specific energy E_s is taken as energy per unit volume (it is also equal to the cutting power divided by volumetric cutting rate); this gives a quantity that has the dimensions of stress. Unless stated otherwise, it does not include energy consumed in displacing or accelerating cuttings. The reciprocal of specific energy, termed *energy effectiveness*, is used by some writers to express energetic efficiency.

The *angle of friction* ψ in cutting theory is the angle between the resultant cutting force and a normal to the rake face of the tool (Fig. 6). It is often regarded as being the friction angle for sliding of rock (or other material) against the tool face, but this physical interpretation seems dubious.

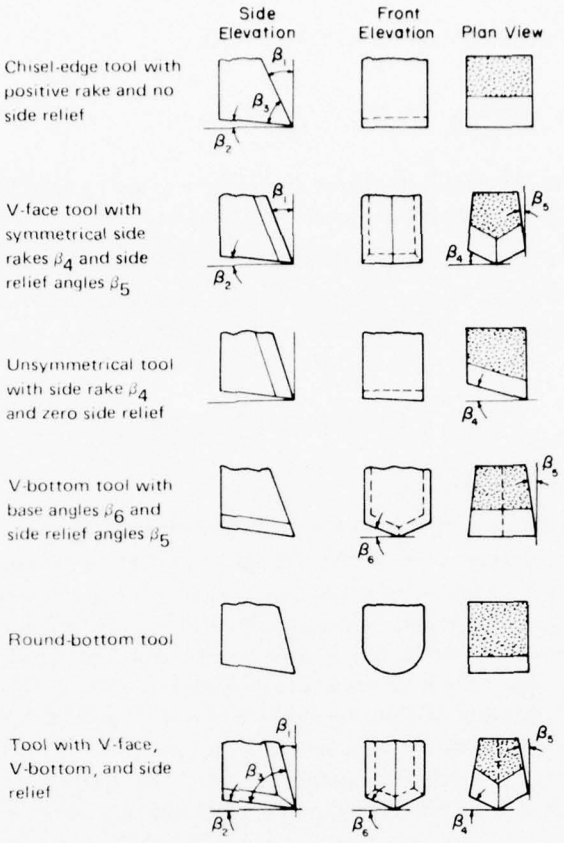

Figure 3. Tool geometry – designation of tool angles.

The *angle of internal friction* ϕ is the inclination of a linear Mohr envelope for rock that fails in conformance with the Coulomb-Mohr criterion.

The *shear angle* θ is the inclination, relative to the surface plane, of a hypothetical shear plane developed during formation of cuttings or chips (see Fig. 5).

The *rake angle* of a cutting tool β_1 is the angle between the leading face of the tool and a normal to the surface of the work (Fig. 3).

The *relief angle* of a cutting tool β_2 is the angle between the lower surface of the tool (the "flank" in machine tool terminology) and a plane parallel to the surface of the work (Fig. 3).

The *included angle* of a cutting tool β_3 is the angle between the rake face and the relief face, i.e. $\beta_3 = 90^\circ - (\beta_1 + \beta_2)$.

The *side rake angle* β_4 is the angle between the leading face of the tool and a normal to the travel direction, measuring in a plane parallel to the work surface (Fig. 3).

The *side relief angle* β_5 is the angle between the side of the tool and the travel direction, measuring in a plane parallel to the work surface (Fig. 3).

The *base angle* β_6 is the angle between the base of the leading face and the plane of the work surface, measuring in a plane that is normal to the travel direction (Fig. 3).

The *tip radius* of a cutting tool r is the radius of curvature of the cutting edge when viewed in side elevation.

The *face profile* of a cutting tool is the shape of the rake face when viewed in front elevation (Fig. 3).

A *wear flat* on a cutting tool is an abraded area, typically almost parallel to the work surface (Fig. 2). The term "wear land" is used in machine tool technology.

Tool speed u is the linear speed of the cutting tool in a direction parallel to the work surface.

The *compliance* of a tool in any given direction is the tool deflection divided by the applied force. Compliance is the reciprocal of *stiffness* (force divided by deflection).

PRINCIPLES OF CUTTING

Forces acting on a single cutter

Parallel-motion tools all work by some kind of planing or abrading action; in some materials the action is more or less continuous, so that the cuttings tend to be long shavings or uniform powders, while in other materials the action is discontinuous, and the cuttings tend to be discrete chips with associated smaller fragments. In a planing motion, the tool is usually driven across the work in a direct symmetrical way, such that its axes of symmetry are parallel or normal to the direction of motion (Fig. 4). The alternative is for the tool to slice sideways while it thrusts forward, so that there is a lateral component of relative motion when reference axes are symmetrical with respect to the tool (Fig. 4). For basic analytical purposes the direct symmetrical action is the one that is usually treated, since it lends itself to two-dimensional idealization. This mode of action is termed *orthogonal cutting* in the analysis of metal-cutting machine tools (the alternative mode is referred to as *oblique cutting*).

A rock-cutting drag bit or similar tool can perhaps be envisaged as an inclined indenter, or chisel, that is scraped continuously across the advancing surface while being held forcibly into the work. It experiences a direct indentation resistance that is inclined at some angle to the advancing surface, plus a frictional resistance that is more or less tangential to the tip trajectory. In orthogonal cutting, the force imposed on the rock by the tool, and the equal and opposite reaction on the tool itself, can be resolved into a tangential component f_t and a normal component f_n (Fig. 2), directions being taken with reference to the plane of the advancing surface. Both the absolute and relative magnitudes of f_t and f_n vary with chipping depth, rock properties, and tool angles, and they also change with time as progressive wear changes the shape of the tool tip.

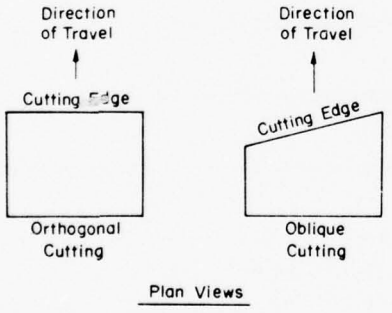

Figure 4. Orthogonal cutting and oblique cutting.

Tool forces also fluctuate over short periods. In the cutting of brittle materials this is always the case, since the process is inherently one of repetitive chipping. With more ductile materials, which can be cut continuously, force fluctuations are more directly attributable to the characteristics of the machines, i.e. to what extent it is compliant ("soft") or rigid ("stiff"). The compliance of the tool and the machine also influences the cutting mode, in that a very rigid tool can readily maintain

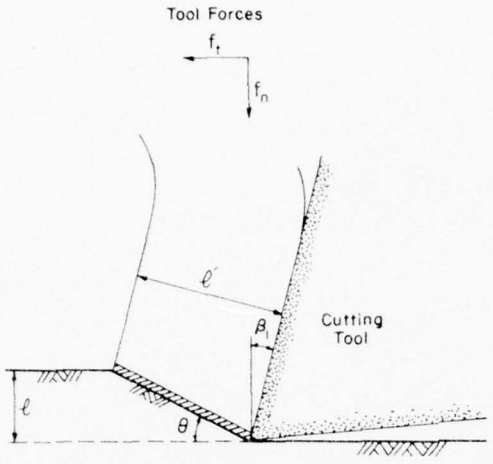

Figure 5. Idealized geometry for metal cutting by a parallel motion tool.

constant chipping depth, whereas a highly compliant tool tends to deflect or to ride up in response to fluctuations in cutting resistance.

Theoretical ideas on cutting

Theoretical ideas on cutting with parallel-motion tools originate in the analytical work that has been done in connection with machining of metals. In orthogonal metal-cutting, three modes of cutting are distinguished, depending on the type of chip that is formed.* In Type I a discontinuous, or segmental, chip is formed by the tool when the material behaves in a more or less brittle manner. In Type II a continuous chip is formed; this is favored by ductile behavior of the material and by low friction between the chip and the rake face of the tool. Type III also involves formation of a continuous chip, but a built-up nose or edge of metal adheres to the rake face of the tool near its tip, creating a false cutting edge and giving high chip friction. In all of these cutting modes it is considered that chips are formed by shearing along a plane, or within a zone, that extends from the tool tip to the free surface, the plane or zone having a characteristic inclination to the direction of tool motion (Fig. 5). The main object of theoretical analysis is to relate tool forces to material properties, tool geometry, and operating conditions.

Inclination of the shear plane (θ), termed the "shear angle," has been considered in various theoretical analyses of metal cutting. In the pioneering Ernst-Merchant theory (Ernst 1938, 1951, Merchant 1945), application of a maximum shear stress hypothesis led to a value of shear angle that can be expressed as

$$\theta = 1/2\,(\pi/2 + \beta_1 - \psi) \tag{1}$$

or

$$\theta = 1/2\,[\pi/2 - \tan^{-1}\,(f_n'/f_t')] \tag{2}$$

where β_1 is a positive rake angle of the cutting tool, ψ is an "angle of friction" between the metal chip and the rake face, and f_t' and f_n' are tangential and normal components of cutting force (per unit width) respectively (see Fig. 6). This did not give good agreement with experimental data, and Merchant modified the approach by adopting a yield criterion equivalent to the Coulomb-Mohr failure criterion:

---

* Three analogous modes of chip formation are considered in orthogonal cutting of wood with parallel motion tools (Koch 1964). Type I is a discontinuous mechanism involving cleavage parallel to the free surface, followed by cantilever failure. Type II is a continuous mechanism involving compression and shear, terminating at a definite shear plane. Type III also involves compression and shear, but there is less of a peeling action and more tendency to cyclic repetition. As in metals, Type III chip formation in wood can involve a built-up nose of material that cannot escape.

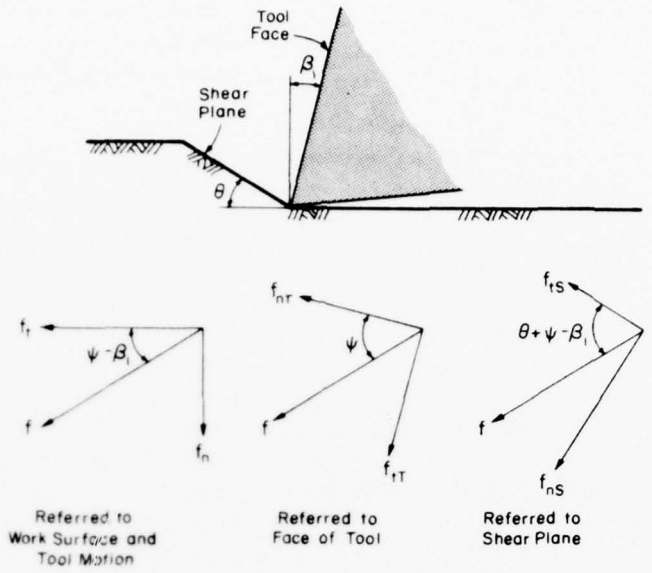

Figure 6. Force vectors for a cutting tool, showing resolution of orthogonal force components in three different sets of directions

$$\tau_s = \tau_0 + k\sigma_s \tag{3}$$

where τ_s and τ_0 are tangential and normal stresses on the shear plane, τ_0 is the tangential stress when $\sigma_s = 0$, and k is a constant. The value of shear angle derived with this assumption can be expressed as

$$\theta = 1/2\ (\cot^{-1} k + \beta_1 - \psi) \tag{4}$$

or

$$\theta = 1/2\ (\pi/2 - \phi + \beta_1 - \psi) \tag{5}$$

or

$$\theta = 1/2\ [\pi/2 - \phi - \tan^{-1}\ (f_n/f_t)] \tag{6}$$

where ϕ is the "angle of friction" for the more familiar form of the Coulomb-Mohr criterion, using the substitution $\tan\phi = k$. Merchant used the term "machining constant" for $\cot^{-1} k$. Later developments involved application of plasticity theory. Assuming that the metal behaves as an ideal rigid-plastic material, Lee and Shaffer (1951) obtained a value for the shear angle that can be expressed as

$$\theta = \pi/4 + \beta_1 - \psi \tag{7}$$

or

$$\theta = \pi/4 - \tan^{-1}(f'_n/f'_t). \tag{8}$$

This relation is obviously limited to conditions where $f'_n < f'_t$.

The effective shear angle has been determined experimentally by measuring the thickness or length of a continuous chip relative to the depth or length of cut for a wide orthogonal cutter. Referring to Figure 5, the shear angle is given by

$$\theta = \tan^{-1}\left(\frac{r_t \cos\beta_1}{1 - r_t \sin\beta_1}\right) \tag{9}$$

where

$$r_t = \ell/\ell' = L'/L$$

β_1 is the rake angle of the cutting tool, ℓ is uncut chip thickness, ℓ' is chip thickness after cutting, L is tool travel distance, and L' is the corresponding chip length.

Knowing θ from experimental determination (e.g. eq 9), having a relation between θ and (f'_n/f'_t), such as in eq 2, 6 or 8, and knowing the yield strength of the material (according to some failure criterion), then values of f'_t and f'_n can be estimated by resolving along the shear plane. For example, taking a simple yield strength Y that is unaffected by normal stress, resolution along the shear plane gives

$$f'_t \cos\theta - f'_n \sin\theta = Y\ell/\sin\theta \tag{10}$$

and eq 2 gives

$$f'_n/f'_t = \cot 2\theta. \tag{11}$$

If Y and θ are known, then f'_t and f'_n can be determined from eq 10 and 11:

$$f'_t = 2Y\ell \cot\theta \tag{12}$$

$$f'_n = 2Y\ell \cot\theta \cot 2\theta = Y\ell(\cot^2\theta - 1). \tag{13}$$

For some reason the expression for f'_t is usually expressed in a mixture of implicitly related variables as:

$$f'_t = \frac{Y\ell \cos(\psi - \beta_1)}{\sin\theta \cos(\theta + \psi - \beta_1)}. \tag{14}$$

This is actually identical to eq 12.

The only general point that need be made about this rather tortuous semi-theoretical estimate is that it predicts direct proportionality between cutting force and the chip depth ℓ.

So far, theoretical approaches have not provided a reliable basis for quantitative analysis of cutting forces, and so the usual expedient in metal-cutting analysis is to adopt empirical equations that relate cutting force f_t to depth of cut, feed rate, tool geometry, and material properties. Only the

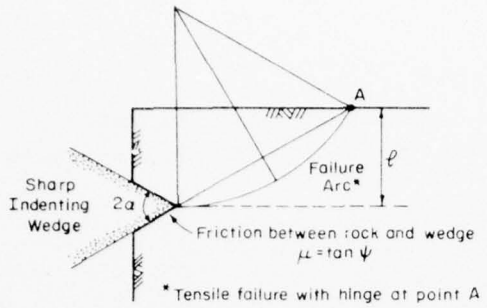

Figure 7. Penetration by a sharp symmetrical wedge in proximity to a secondary free face — Evans' theory.

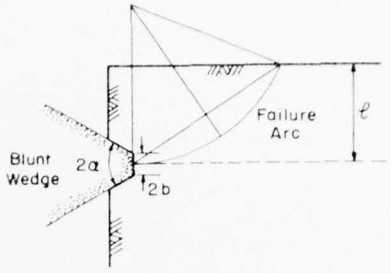

Figure 8. Penetration by a blunt symmetrical wedge in proximity to a secondary free face — Evans' theory.

tangential component f_t is considered under normal circumstances, presumably because the normal component f_n makes no significant contribution to the power consumption, and because adequate reaction to f_n can be provided easily.* Some widely used empirical relations of this kind are questionable, since they include dimensional factors that are raised to variable powers, and dimensional homogeneity may not be maintained. However, a significant point is that the empirical relations recognize that cutting force f_t is not necessarily related *linearly* to depth of cut, whereas the simple theoretical approaches indicate that cutting force f_t is *directly proportional* to cutting depth ℓ.

Evans (1962) developed a cutting theory for rock (specifically for coal) by considering the normal penetration of a sharp symmetrical wedge into the face of a squared block at a position not far from the corner of the block (Fig. 7). The wedge penetrates the rock and drives a tensile crack along a circular arc from the wedge tip to the free surface, encountering some frictional resistance during penetration. Under certain simplifying assumptions, the penetration resistance, which is taken as analogous to the unit tangential cutting force f_t', is

$$f_t' = \frac{2\sigma_T \ell \sin(\alpha+\psi)}{1-\sin(\alpha+\psi)} \tag{15}$$

where σ_T is the tensile strength of the rock, α is the half-angle of the wedge, and ψ is the "angle of friction" between the wedge and the rock. This initial theoretical development does not give a realistic physical model of a typical shearing tool (it is equivalent to a tool with a strong *negative* relief angle), and Evans went on to consider how oblique penetration might modify the original results. In a later reconsideration of the work, taking into account experimental work by others (Evans and Pomeroy 1973), another simplified expression for a conventional shearing tool having a small relief angle was given as

$$f_t' = \frac{2\sigma_T \ell \sin[1/2(\pi/2-\beta_1)+\psi]}{1-\sin[1/2(\pi/2-\beta_1)+\psi]} \tag{16}$$

* It is worth keeping in mind that f_t and f_n are aribtrarily chosen components of a single resultant force f; they are not separate and independent forces.

where β_1 is the rake angle of the tool. Roxborough (1973) simplified this expression further by assuming small penetration of the tool tip and ignoring ψ. He tested the relationship against experimental cutting data for sandstone and anhydrite, finding qualitative agreement for trends of variation with rake angle and cutting depth, although theoretical values were lower than experimental values.

Evans (1962) also suggested an approach to the problem of stress variation in the vicinity of the wedge tip, postulating that stress varies along the chord of the failure arc in proportion to a power of the distance from the tip, n being the exponent of this power relation. The expression obtained for f'_t was

$$f'_t = \frac{4\sigma_T \ell}{n+2} \frac{\sin(\alpha+\psi)}{1-\sin(\alpha+\psi)} . \tag{17}$$

This equation is almost the same as eq 15, except that the effective tensile strength is reduced by a factor $2/(n+2)$.

Evans (1965) considered the effect of blunting at the tool tip by analyzing the penetration of a wedge having a flat end of width $2b$ (Fig. 8). The expression obtained for f'_t was

$$\frac{f'_t}{2\sigma_T \ell} = \frac{\sin(\alpha+\psi)}{2\sin\gamma\cos(\gamma+\alpha+\psi)} + 2^{(m-1)}\left(\frac{\sigma_c}{\sigma_T}\right)\left(\frac{b}{\ell}\right)^m \left[\frac{1+\sin\gamma\sin(\alpha+\psi)}{\cos(\gamma+\alpha+\psi)}\right] \tag{18}$$

where m is a parameter that has values of approximately 0.5 to 0.7, and σ_c is the compressive strength of the rock. The angle γ is obtained from

$$\frac{\cos(2\gamma+\alpha+\psi)}{1-\cos 2\alpha} = 2^{(m-1)}\left(\frac{\sigma_c}{\sigma_t}\right)\left(\frac{b}{\ell}\right)^m \cos(\alpha+\psi). \tag{19}$$

Nishimatsu (1972) developed another cutting theory for rock by taking a Coulomb-Mohr failure criterion for shearing along a plane, as in the Merchant theory, and by attempting to account for stress concentration factors and stress gradients near the tool tip in much the same way as suggested by Evans. His expressions for the resultant unit cutting force f' and the tangential unit cutting force f'_t are

$$f' = \frac{2}{n+1} \tau_0 \ell \frac{\cos\phi}{1-\sin(\phi-\beta_1+\psi)} \tag{20}$$

$$f'_t = \frac{2}{n+1} \tau_0 \ell \frac{\cos\phi}{1-\sin(\phi-\beta_1+\psi)} \cos(\psi-\beta_1) \tag{21}$$

where n is a stress distribution factor characteristic of the tool (a power law exponent for stress variation with distance), τ_0 is the rock's shear strength for zero normal stress, ϕ is the slope of the linear Mohr envelope, β_1 is rake angle, and ψ is the "angle of friction" for the tool/rock contact, as before. Experimental data for f'_t and f'_n as functions of ℓ were obtained, and straight-line fits of the form $f' = a+b\ell$ were adopted. Values of n and ψ were deduced by somewhat devious procedures, both proving to be functions of the rake angle β_1.

Other developments in rock-cutting theory have addressed the problem of curvature and bluntness at the tool tip.

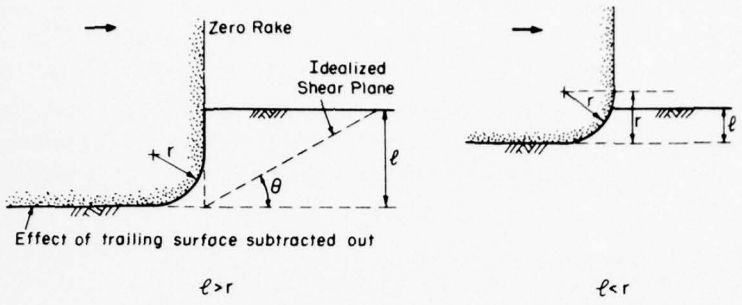

Figure 9. Idealized tool geometry used as a basis for the analysis of Appl and Rowley (1963) and Nalezny (1971).

Appl and Rowley (1963), following on from work by Cheatham (1958), derived theoretical expressions for the cutting stresses on a rounded-edge drag bit with zero rake angle (Fig. 9). For a wide tool cutting to a depth ℓ that exceeds the radius of curvature of the cutting edge:

$$f_n' = (r + \ell \tan\psi)\,\sigma_* \tag{22}$$

$$f_t' = (\ell - r \tan\psi)\,\sigma_* \tag{23}$$

where

$$\sigma_* = \frac{\tau_0/\sin^2\theta}{[1 - r/\ell(\tan\psi + \mu_1)]\,(\cot\theta - \tan\phi) - \tan\psi\,(1 + \tan\phi\cot\theta)} \tag{24}$$

and r = radius of the cutting edge
τ_0 = rock shear strength for zero normal stress
θ = "shear angle" (slope of shear plane)
ψ = angle of friction for tool/rock contact
ϕ = "angle of internal friction" (slope of Mohr envelope)
μ_1 = coefficient of friction for rock on rock.

σ_* is the normal stress acting radially on the rounded cutting edge, and it is assumed to be uniform around the cutting edge.

Appl and Rowley (1963) went on to analyze the cutting stresses for wide rounded-edge tools cutting to shallow depth, with $\ell < r$. For this case it was necessary to consider radial variation of the normal stress σ_* and the interface shear stress ($\sigma_* \tan\psi$), and complicated expressions for f_n' and f_t' resulted:

$$f_n' = \left\{ A_1 \left[\frac{\exp(\pi\tan\phi)}{4\tan^2\phi + 1} \right] (2\tan\phi + \tan\psi) - A_2 \tan\psi \right\}$$

$$- \left\{ A_1 \left[\frac{\exp(2\rho\tan\phi)}{4\tan^2\phi + 1} \right] (2\tan\phi + \tan\psi) - A_2 \tan\psi \right\} \sin\rho$$

$$+ \left\{ A_1 \left[\frac{\exp(2\rho\tan\phi)}{4\tan^2\phi + 1} \right] (1 - 2\rho\tan\phi) - A_2 \right\} \cos\rho \tag{25}$$

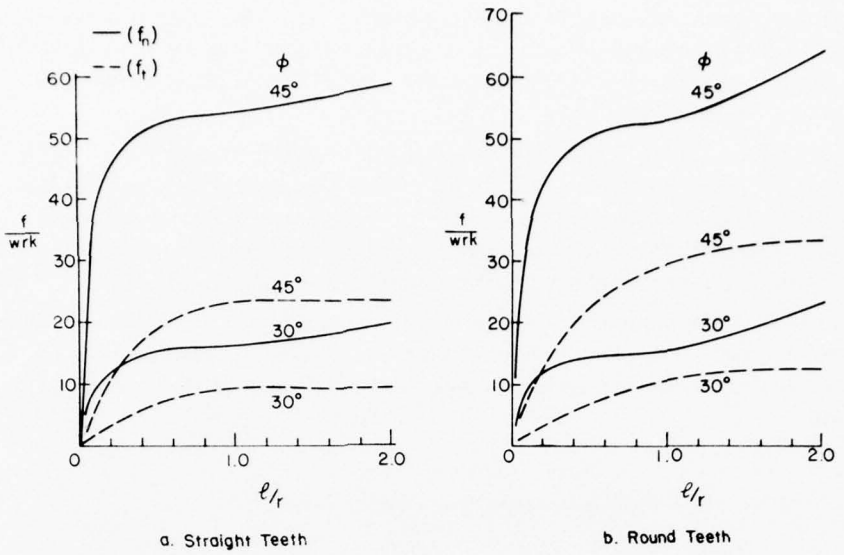

Figure 10. Dimensionless cutting force as a function of ℓ/r according to Nalezny's analysis for (a) "straight" tools (chisel edge) and (b) rounded base tools. Cutting force is divided by tool width w, tip radius r, and rock shear strength k.

$$f_t' = \left\{ A_1 \left[\frac{\exp(\pi \tan\phi)}{4\tan^2\phi + 1} \right] (1 - 2\rho \tan\psi) - A_2 \right\}$$

$$- \left\{ A_1 \left[\frac{\exp(2\rho \tan\phi)}{4\tan^2\phi + 1} \right] (1 - 2\rho \tan\psi) - A_2 \right\} \sin\rho$$

$$- \left\{ A_1 \left[\frac{\exp(2\rho \tan\phi)}{4\tan^2\phi + 1} \right] (\tan\psi + 2\tan\phi) - A_2 \tan\psi \right\} \cos\rho \qquad (26)$$

in which

$$A_1 = \left(\frac{1 + \sin\phi}{2\sin\phi} \right) \qquad (27)$$

$$A_2 = \left(\frac{1 - \sin\phi}{2\sin\phi} \right) \qquad (28)$$

$$\rho = \sin^{-1}(1 - \ell/r). \qquad (29)$$

In a later study on the cutting action of diamond tools, Appl, Rowley and Bridwell (1967) extended the analysis to tangential grooving with a spherical tool surface. The resulting expressions for f_t and f_n are very long and complex, suitable only for evaluation by computer, and it would serve no useful purpose to repeat them here.

The plane strain analysis of Appl and Rowley (1963) for wide tools was repeated later by Nalezny (1971), who also started from Cheatham's punch solution but used a different expression for the normal stress σ_*, and assumed radial variation for both the case of $\ell < r$ and $\ell > r$. The

analysis also covered zero-rake tools having a semicircular face profile on the rake face. The equations in the paper are written incorrectly, but the graphical results appear to be in order. These results, which give normal and tangential cutting forces as functions of chipping depth in dimensionless form, are shown in Figure 10.

Roxborough and Rispin (1973b) noted that wet chalk behaved differently than typical brittle rocks, and for f_t they used a relation that had previously been adapted from the Ernst-Merchant metal-cutting theory by Potts and Shuttleworth (1959), who were concerned with the cutting of weak coal. This relation has already been given as eq 14 during the discussion of metal-cutting theory,* and it has been shown that it can be expressed more simply (eq 12).

The various cutting theories for metals and rocks are useful in bringing disciplined thought to bear on the problem, but so far they have not been directly usable for practical design. The alternative, therefore, is to assemble experimental data that can be used to develop a rational empirical approach.

EXPERIMENTAL DATA ON CUTTING FORCES

Effect of chipping depth on tool forces

For a given tool in a given type of rock, both the tangential cutting force f_t and the normal cutting force f_n increase as the chipping depth ℓ increases (Fig. 11-26). The simplest cutting theories predict that f_t and f_n will be directly proportional to ℓ, and for some materials and some ranges of conditions this is found to be approximately true, especially when ℓ is very small, but also when $\ell \gtrsim w$ (three-dimensional cutting). However, experimental data overall suggest that the more general pattern of behavior is for f_t and f_n to increase nonlinearly with ℓ in two-dimensional cutting ($w >> \ell$), the rate of increase dropping off as ℓ increases according to some kind of irregular parabolic relation; this is reflected in the more sophisticated two-dimensional cutting theories. A simple approximation would make f_t or f_n proportional to some fractional power of ℓ.

The rate of increase of f_n with ℓ often falls off more rapidly than the rate of increase of f_t with ℓ, and in some cases f_n appears to tend to a limiting value while f_t is still increasing. The effect is to vary the value of the ratio f_n/f_t, which represents the direction of the resultant cutting force (Fig. 27-29). When ℓ is very small, f_n and f_t tend to be roughly equal, i.e. the tool appears to scrape along the rock surface with a friction coefficient approximately equal to unity,† and the resultant force is directed at about 45° to the rock surface. As ℓ becomes appreciably larger than the radius of the tool tip, f_n may tend towards a limit while f_t continues to increase, so that f_n/f_t drops to fractional values and the direction of the resultant force moves closer to the tangential direction. With sharp positive-rake tools, f_n/f_t can be as low as 0.3, but with very dull tools or with strong negative rake the value of f_n/f_t is likely to be above 0.8 or so (Fig. 27-30, 50, 67, 71).

Variation of the ratio f_n/f_t is one of the problems in applying some cutting theories, since $f_n/f_t = \tan(\psi - \beta_1)$, and both ψ and β_1 are constants in the theoretical equations.

---

* It appears that a typographical error in the Roxborough and Rispin paper has introduced an incorrect sign in the expression for f_t' (their eq 4).

† Kenny and Johnson (1976) measured the friction coefficient for tungsten carbide rubbing on sandstone. Values based on mean force components were 0.5 to 0.7, while values based on mean peak forces were in the range 0.65 to 0.85.

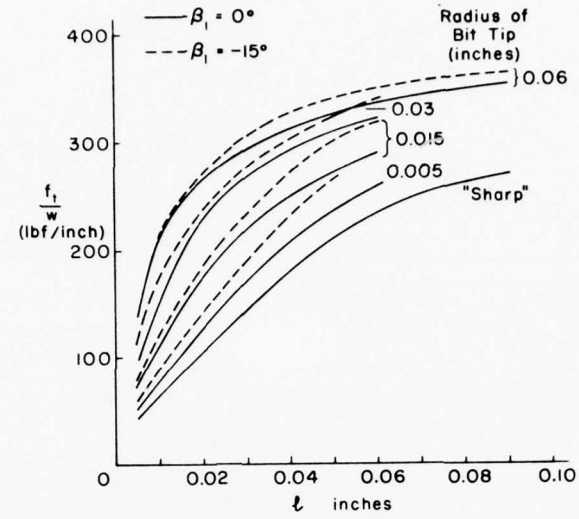

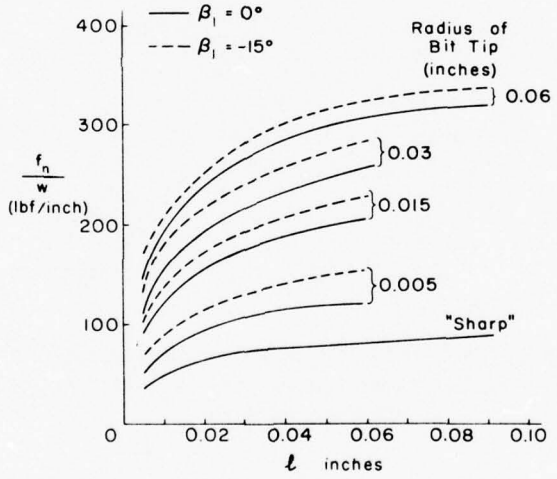

Figure 11. Components of cutting force as functions of chipping depth, with tip radius and rake angle as parameters (Leuders limestone, cutting speed 15 ft/min, relief angle 10°). (After Gray 1963.)

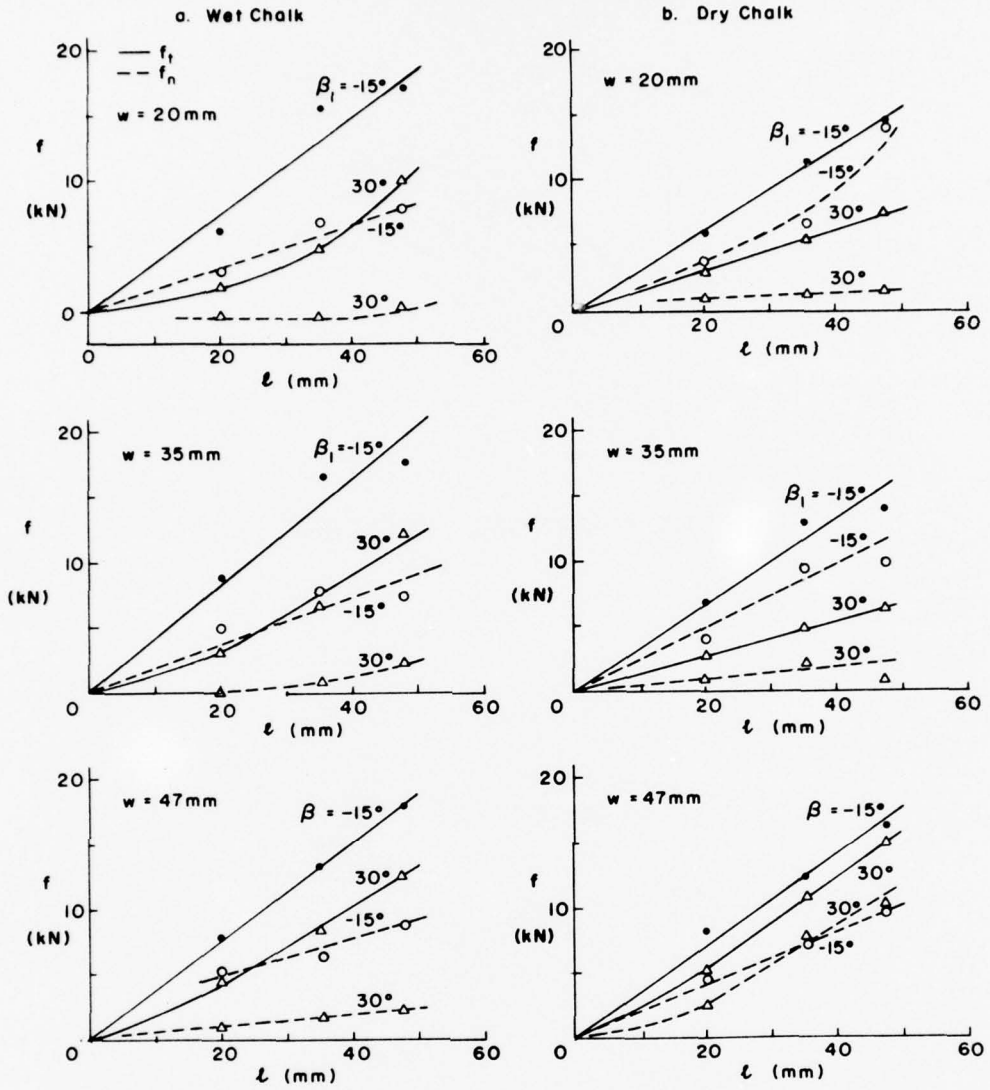

Figure 12. Cutting force as a function of chipping depth for chisel-edge tools in wet chalk and dry chalk. Data are given for two values of rake angle and three values of tool width. (From Roxborough and Rispin 1973a, b.)

The data given in Figures 11-31 are the results of laboratory experiments made under somewhat idealized conditions, and they should be treated with caution. While they may be completely valid for sharp new tools, they are not necessarily valid for the worn condition, which is the most common condition for tools on real cutting and boring machines. This matter is touched on later in the discussion of wear effects. The picture may also be clouded by unspecified edge effects when comparisons are made between results for "wide" and "narrow" tools (the effect of ℓ should be different for two-dimensional and three-dimensional cutting situations).

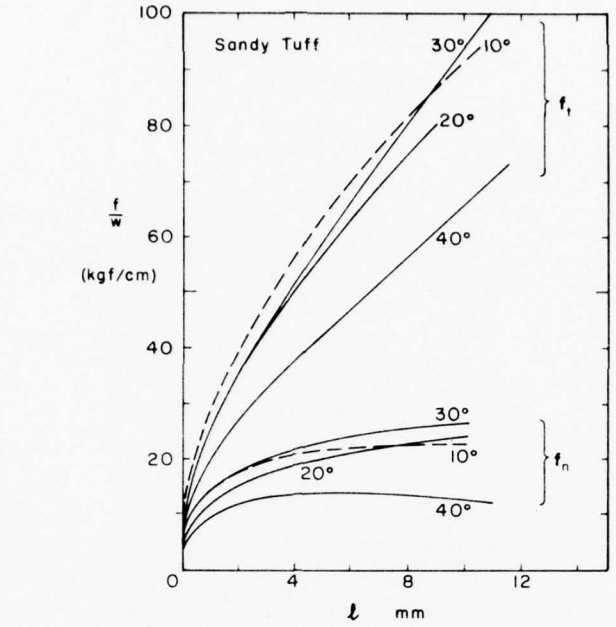

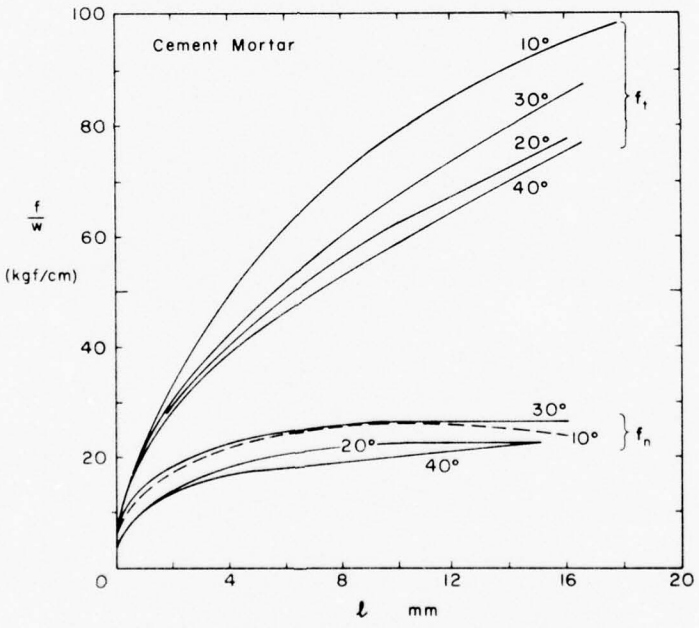

Figure 13. Components of cutting force as functions of chipping depth, with rake angle as parameter. Cutting speed 5.2 m/min (17 ft/min), relief angle 10°, tool width 30 mm (1.2 in.) (Adapted from Nishimatsu (1972) with curves drawn by eye through original data points.)

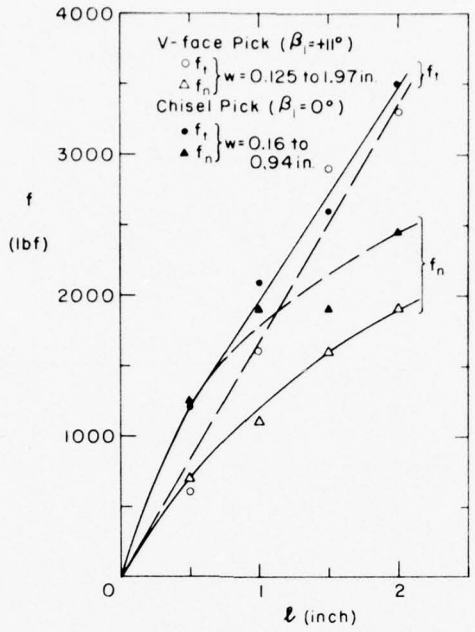

Figure 14. Cutting force as a function of chipping depth for two types of full-scale tools working in Darley Dale sandstone. (Data from Barker 1964.)

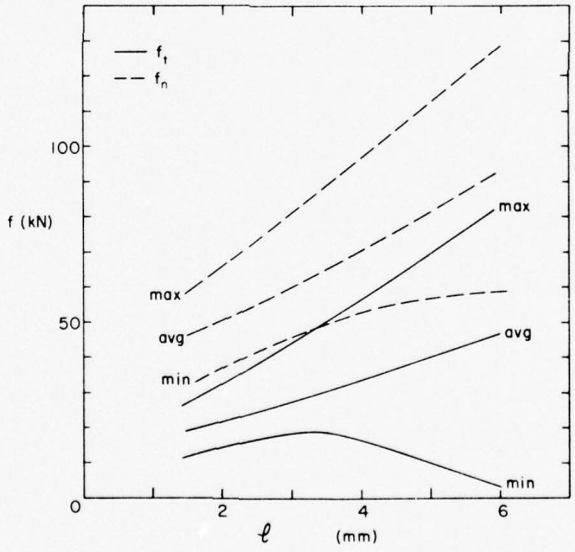

Figure 15. Cutting force as a function of chipping depth in quartzite, showing range of force fluctuations. (From Chamber of Mines of South Africa Research Organization 1971.)

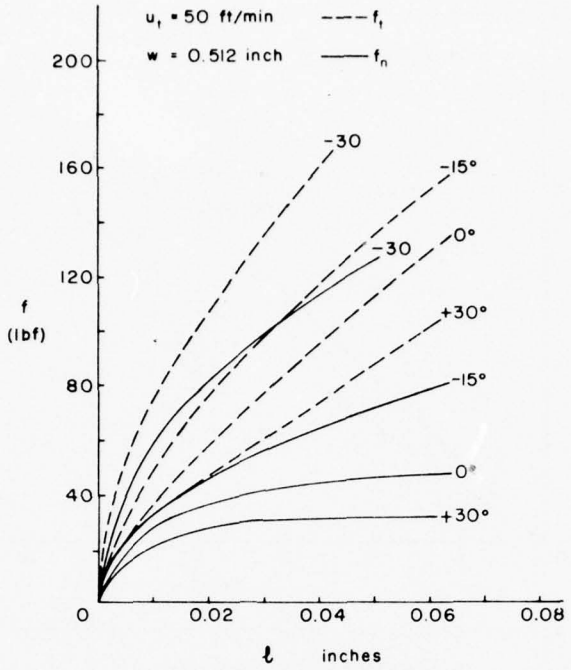

Figure 16. Normal and tangential components of cutting force as functions of chipping depth, with rake angle as parameter, for unworn bits in Leuders limestone (relief angle 10°). (After Gray 1963.)

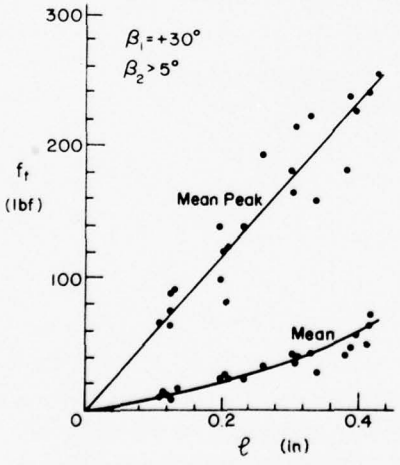

Figure 17. Tangential component of cutting force as a function of chipping depth for a sharp tool working in hard coal (rake angle +30°, relief angle > 5°). (From Evans and Pomeroy 1973.)

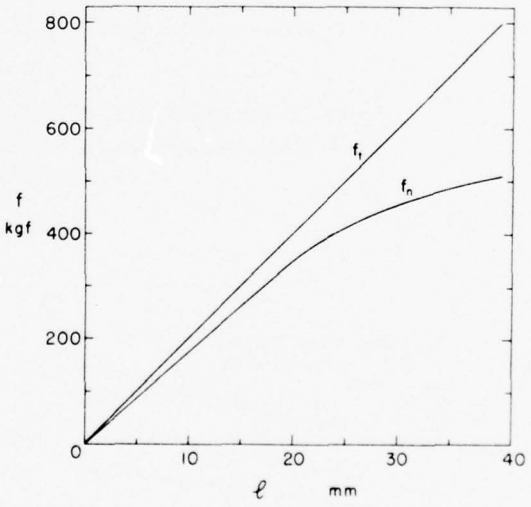

Figure 18. Components of cutting force as function of chipping depth. (From Valantin et al. 1964.)

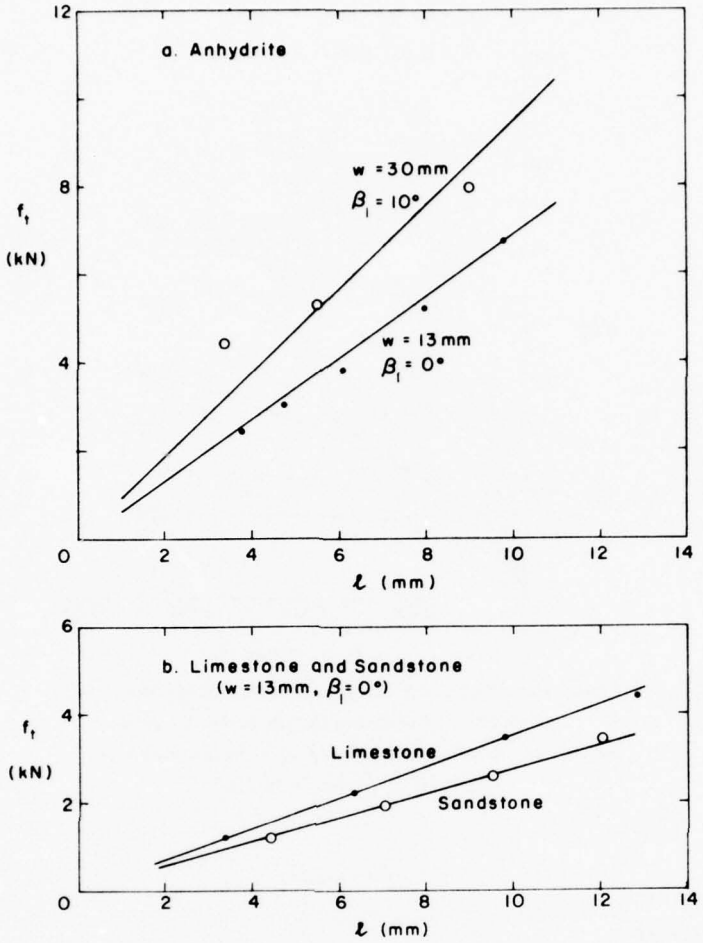

Figure 19. Tangential cutting force as a function of chipping depth for chisel-edge tools in anhydrite, limestone and sandstone. (From Roxborough 1973.)

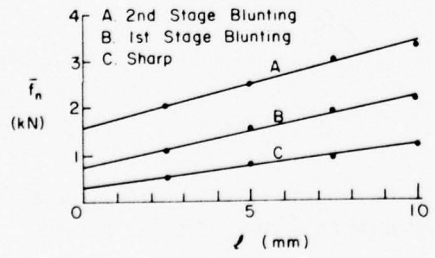

Figure 20. Normal component of tool force as a function of chipping depth for three stages of wear. (After Kenny and Johnson 1976.)

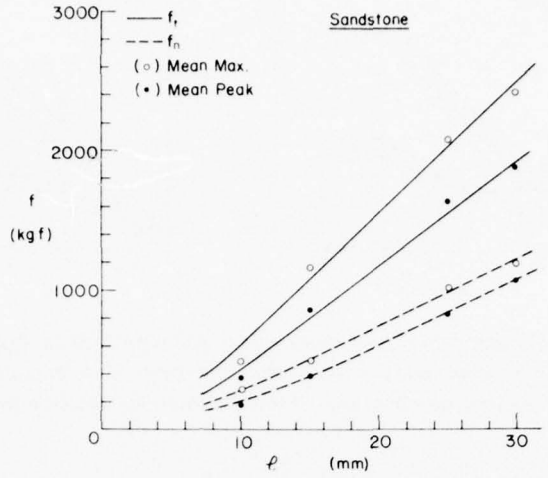

Figure 21. Force components as functions of chipping depth for a tool working in sandstone. (Furumi, personal communication.)

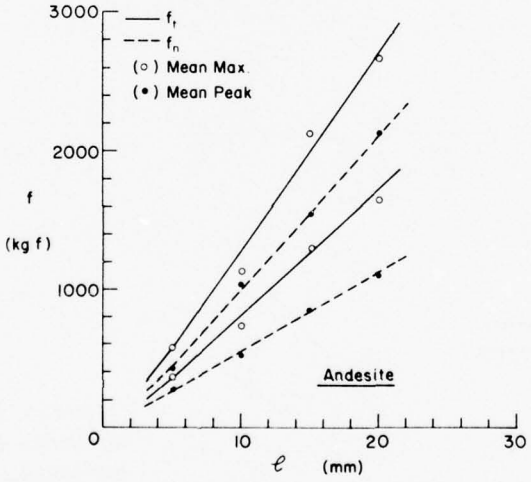

Figure 22. Force components as functions of chipping depth for a tool working in andesite. (Furumi, personal communication.)

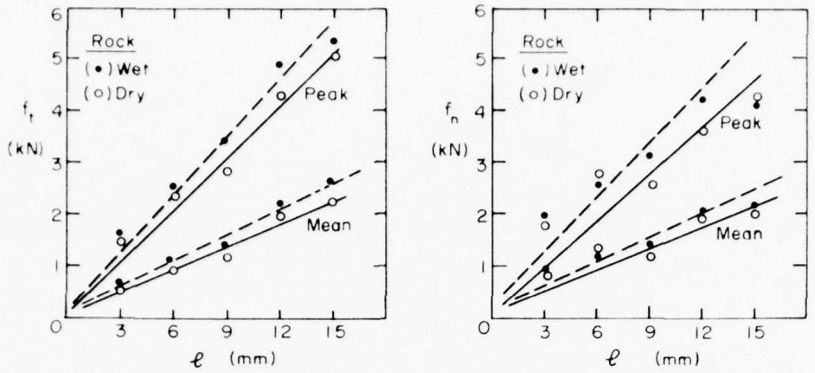

Figure 23. Components of peak cutting force and mean cutting force as functions of chipping depth for wet and dry sandstone. The regression lines appear to have been forced through the origin. (From Roxborough and Phillips 1975.)

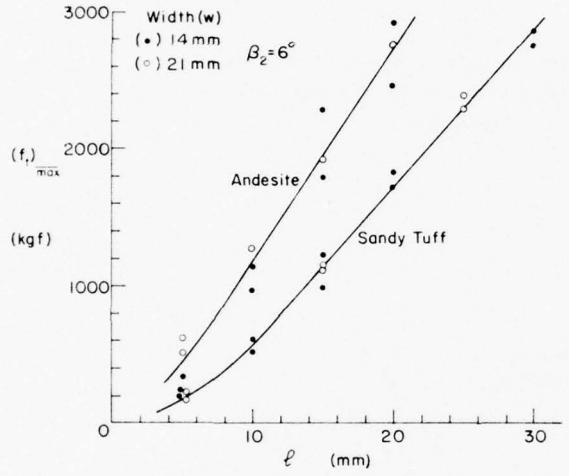

Figure 24. Tangential component of tool force (mean maximum) plotted against chipping depth in andesite and sandy tuff for two different tool widths. (Furumi, personal communication.)

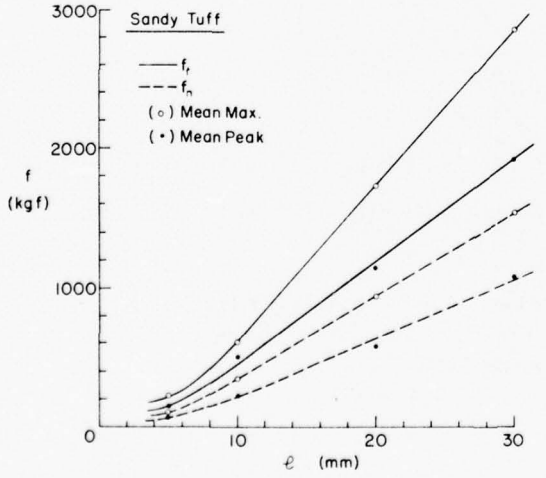

Figure 25. Force components as functions of chipping depth for a tool working in sandy tuff. (Furumi, personal communication.)

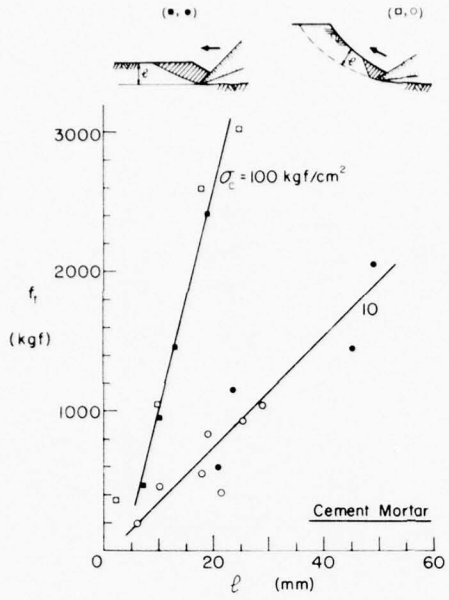

Figure 26. Tangential component of cutting force as a function of chipping depth for a tool cutting cement mortars with different strengths. (Furumi, personal communication.)

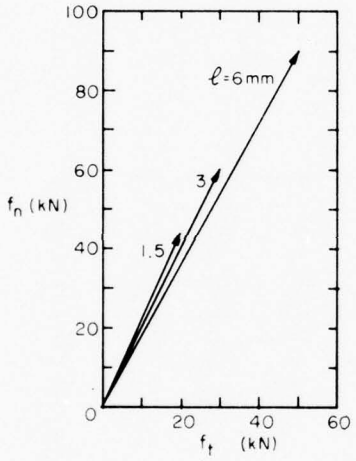

Figure 27. Average values of f_n and f_t for three chipping depths (19-mm-wide tool cutting quartzite at 30 mm/s). (From Chamber of Mines of South Africa Research Organization 1971.)

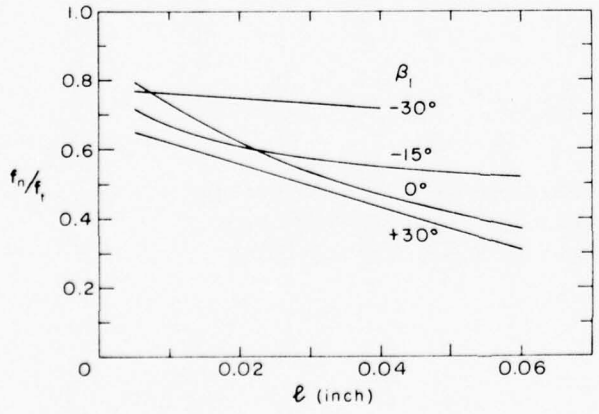

Figure 28. Ratio of force components as a function of chipping depth for a range of rake angles (see Fig. 11). (From smoothed data by Gray 1963.)

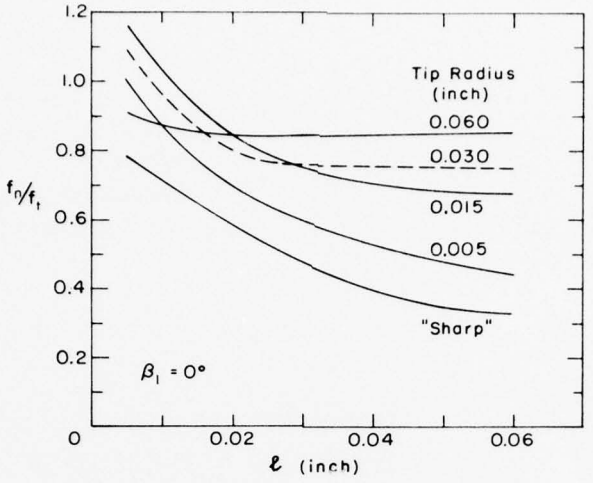

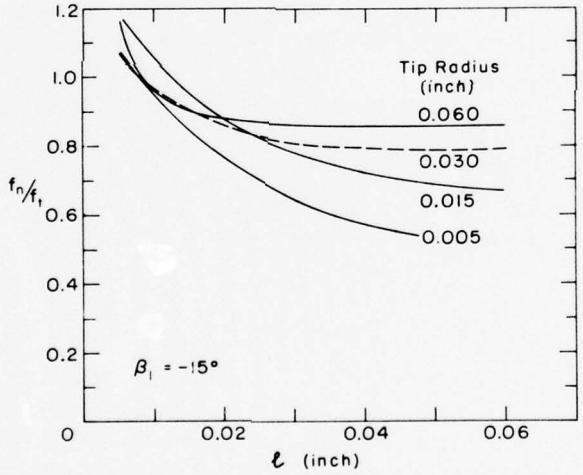

Figure 29. Ratio of force components as a function of chipping depth for a range of tip radii and for two rake angles (see Fig. 11). (From smoothed data by Gray 1963.)

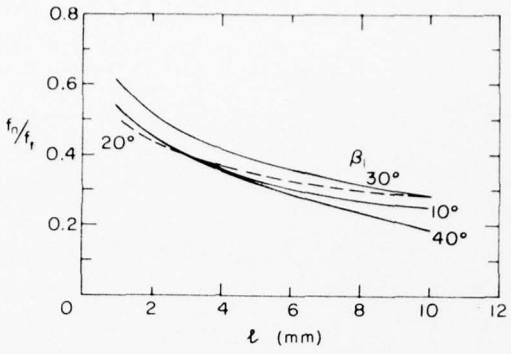

a.

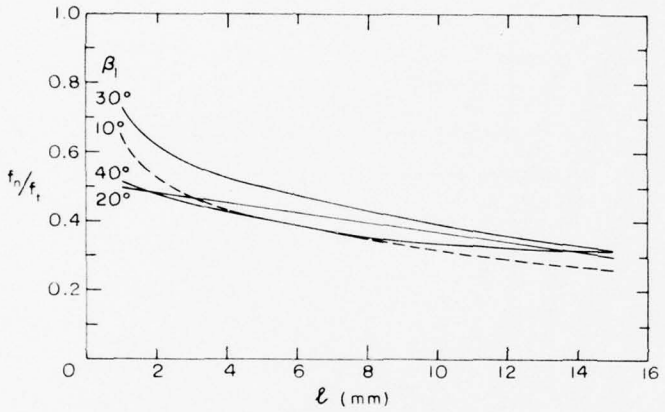

b.

Figure 30. Ratio of force components as a function of chipping depth for a range of rake angles: a) sandy tuff, b) cement mortar. See Fig. 13 for cutting conditions. (Adapted from data by Nishimatsu 1972.)

Effect of rake angle on tool forces

With unworn tools working at large chipping depths, the absolute magnitudes of both f_t and f_n decrease as negative rake angle decreases, and as positive rake angle increases (Fig. 32-40). Another way of looking at this is that cutting forces decrease as the included angle decreases, since the relief angle is usually small, and only varies within narrow limits. The effect has been observed over the range -35° to +60° rake for relatively large chipping depths, but with small chipping depths or with worn tools the rake angle does not have much effect on the cutting forces.

With a rounded tool tip and $\ell < r$, it is obviously the curvature of the tip that determines the effective rake angle. Gray (1963) gave an expression for the effective rake of a rounded (circular arc) cutting edge, taking the angle of the chord of the circular arc as the effective rake angle during

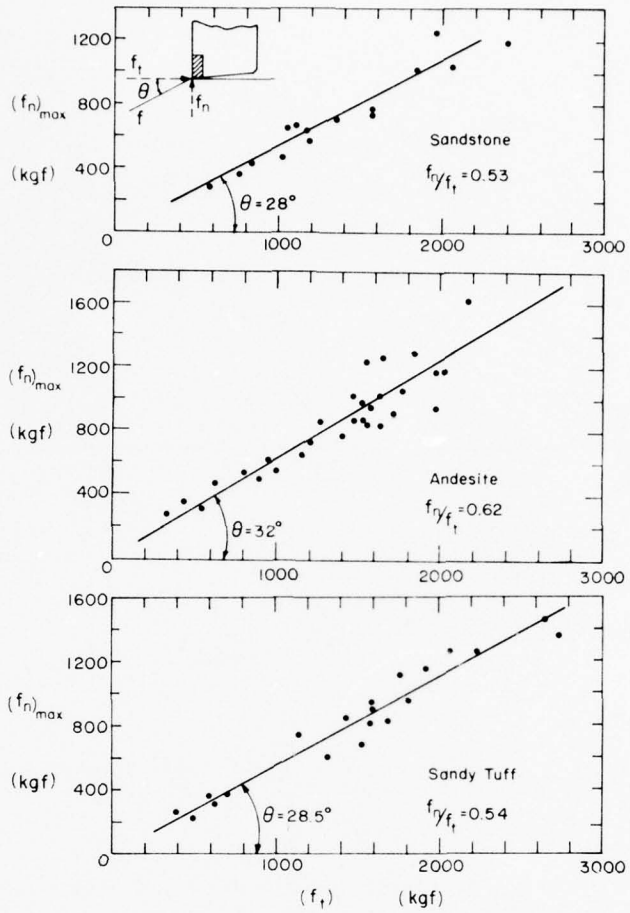

Figure 31. Maximum values of normal component of cutting force plotted against maximum values of tangential component, for tests in sandstone, andesite and sandy tuff. (Furumi, pesonal communication.)

shallow cutting. For a rounded edge cutting with a contact depth of h during chip formation, an alternative expression gives effective rake angle β_1' as

$$\beta_1' = -\cos^{-1}\left(\frac{h}{2r}\right)^{1/2}.$$

In this, h is considered to be less than ℓ under typical cutting conditions.

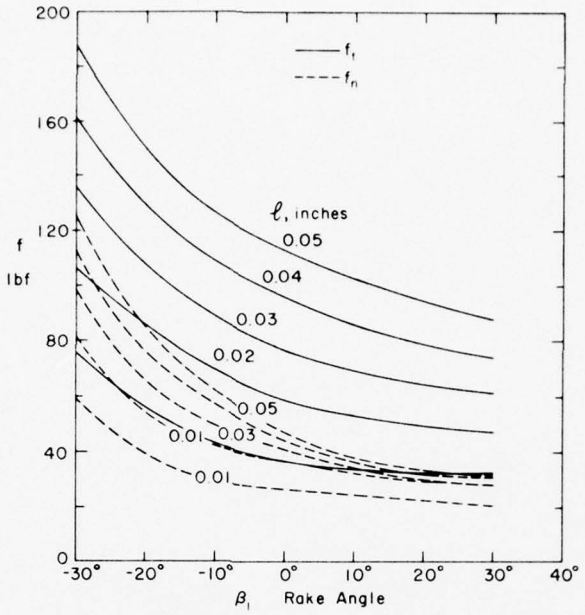

Figure 32. Components of cutting force as functions of rake angle, with chipping depth as parameter. (After Gray 1963.)

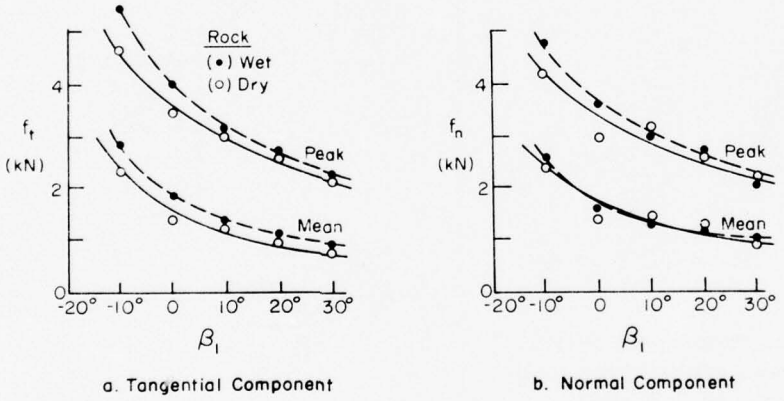

Figure 33. Components of peak cutting force and mean cutting force as functions of rake angle for wet and dry sandstone. (From Roxborough and Phillips 1975.)

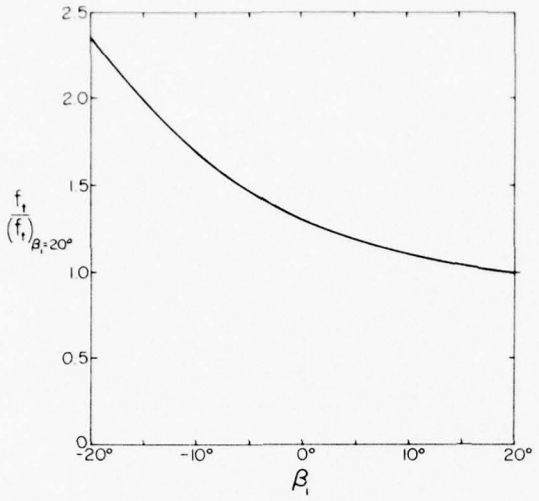

Figure 34. Normalized values of tangential cutting force as a function of rake angle. (After Wagner 1971.)

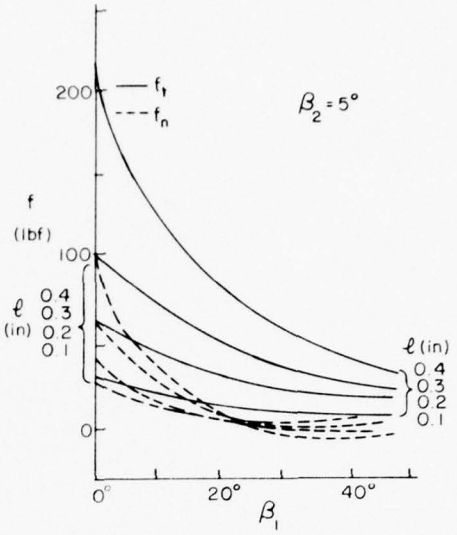

Figure 35. Components of cutting force as functions of rake angle, with chipping depth as parameter, for tools working in coal (β_2 = 5°). (After Evans and Pomeroy 1973.)

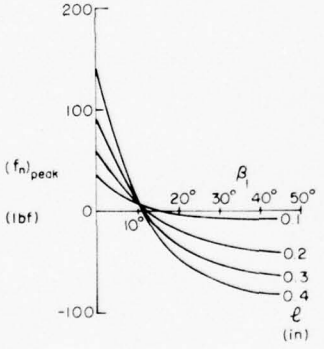

Figure 36. Normal components of peak cutting force as a function of rake angle, with chipping depth as parameter, for sharp blades cutting coal. (Experimental data by Whittaker, as reported by Evans and Pomeroy 1973.)

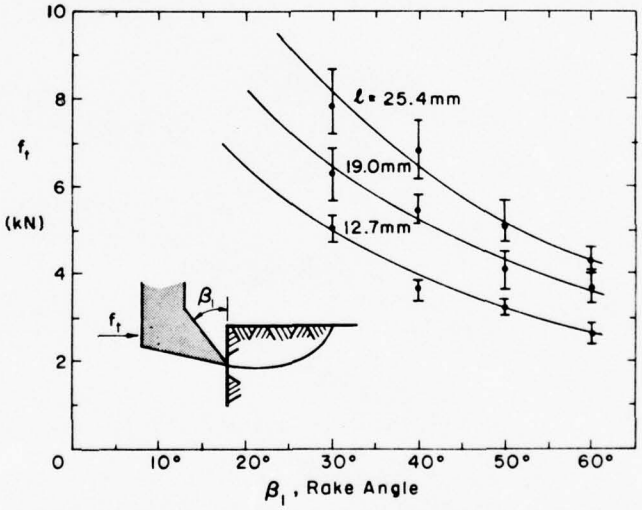

Figure 37. Tangential component of cutting force as a function of rake angle with chipping depth as parameter (sandstone, w = 1 in.). (After Roxborough 1973.)

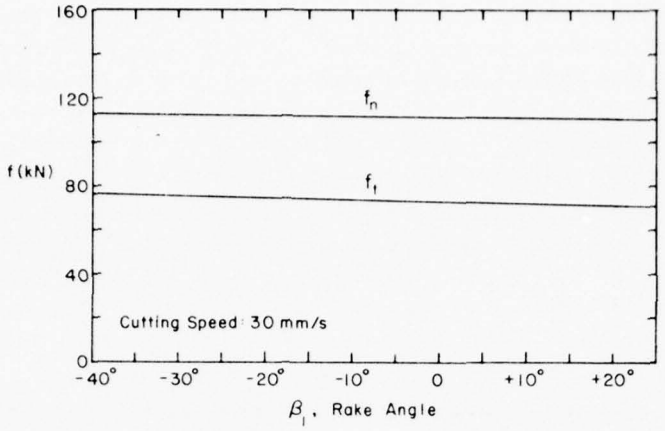

Figure 38. Components of cutting force as functions of rake angle for a worn tool cutting quartzite (width of wear flat = 9 mm, chipping depth = 5 mm, kerf width = 30 mm, cutting speed = 30 mm/s). (From Chamber of Mines of South Africa Research Organization 1971).

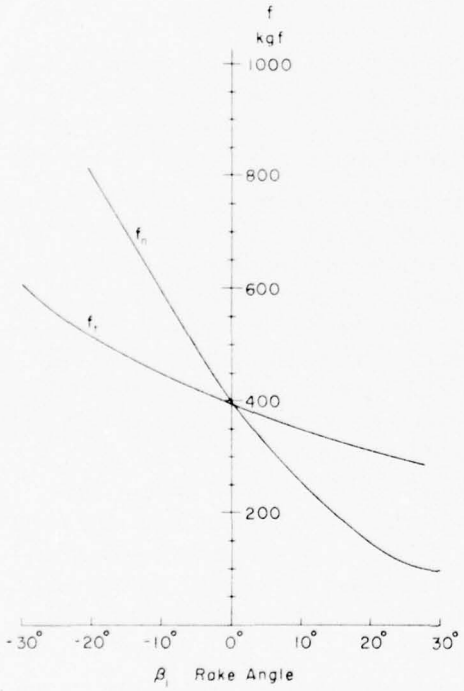

Figure 39. Components of cutting force as functions of rake angle for deep chipping in weak rock. (After Valantin et al. 1964.)

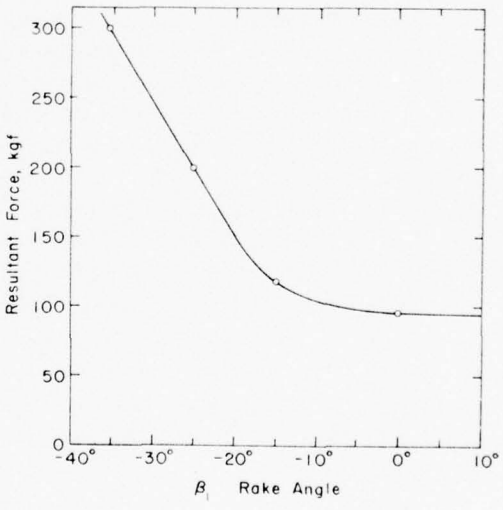

Figure 40. Resultant cutting force as a function of rake angle in strong rock. (After Valantin et al. 1964.)

When a tool is cutting deeply, it is no surprise to find that cutting forces decrease as rake angle increases, especially for the tangential component f_t. The effect of rake on the normal component f_n may be a little more difficult to appreciate intuitively, although in the cutting of softer and more ductile materials it is easy to imagine that a negative rake might tend to make the tool ride up out of the work, thus increasing hold-down forces, while a tool with strong positive rake might tend to pull itself down into the work, causing f_n to decrease or even assume negative values.*

In deep cutting the relative magnitudes of f_t and f_n might be expected to vary, but the available experimental data do not reveal strong systematic trends for variation of f_n/f_t with β_1. Referring back to theory (cf. eq 1 and 2), $f_n/f_t = \tan(\psi - \beta_1)$, and if ψ were a true constant, which clearly it is not, then f_n/f_t would be expected to decrease with increasing rake angle. There are data to support this expectation (e.g. Fig. 32, 39), but there are also other results that either fail to show much effect or contradict the expectation.

If the tool has developed a significant wear flat on the relief face (flank), then rake angle may not have much effect on either f_n or f_t. This is probably because the wear flat greatly increases f_t by adding a large frictional drag. This effect is illustrated by the analysis of Appl and Rowley (1963), which includes flank forces.

The beneficial effects of increasing rake angle, which to some extent are offset by increased vulnerability to breakup and wear, tend to reach a limit at large values of positive rake. Present indications are that rake angles of +20° to +30° are probably sufficient to reap most of the benefit of lowered cutting forces.

Effect of relief angle on cutting forces

In the discussion of kinematic factors (Mellor 1975, 1976a, 1976b), the relief angle necessary to clear the shoulder of a rotary tool was calculated. However, even when a cutting tool is planing along a flat surface, where the required "kinematic" relief angle is close to zero, it is found that there are definite dynamic advantages to be gained from a finite relief angle.

Gray (1963) showed that both f_t and f_n for his experiments were sensibly constant for relief angles between 4° and 10°, but that a sharp increase in both components occurred when the relief angle dropped below about 3° (Fig. 41). These tests were made on flat surfaces. A similar result was obtained by Valantin et al. (1964) in a somewhat different experiment; resultant cutting force was constant for relief angle above 5°, and there was a sharp increase as the relief angle dropped to lower values (Fig. 42). Evans and Pomeroy (1973) report much the same effect for coal-cutting (Fig. 43), both f_t and f_n staying constant for $\beta_2 > 5°$, and rising sharply with smaller relief angles. As far as can be ascertained from the available experimental data, the limiting value for an effective "dynamic" relief angle does not appear to be sensitive to chipping depth.

From these results it seems that a relief angle of about 5° is required to meet dynamic needs. Thus, in designing or setting a tool, 5° should be added to the required kinematic relief angle to obtain a minimum value for the primary relief angle (keeping in mind the distinction between apparent and effective tool angles when the cutters are set on a machine; see Parts 1-3). The final value of relief angle might have to be adjusted further as a result of wear considerations, which are introduced later in this report.

Looking at the bullet bits in Figure 1b, it can be seen that the large tool in the center of the top row needs to be mounted at an angle of 50° or more to the tangential direction, since the half-angle of the tip is 45°. It can also be seen that the bit/block combination in the top right corner gives zero relief angle.

---

* In wood cutting with rake angles of 20° to 30°, f_n tends to decrease as ℓ increases, eventually becoming negative. Wood cutting data also indicate that rake angle affects the magnitude of the exponent in a power relation between f and ℓ; as β_1 decreases, the exponent increases towards unity.

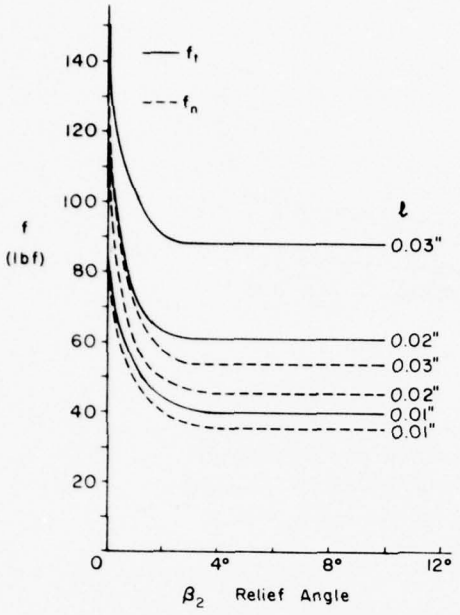

Figure 41. Components of cutting force as functions of relief angle with chipping depth as parameter. (After Gray 1963.)

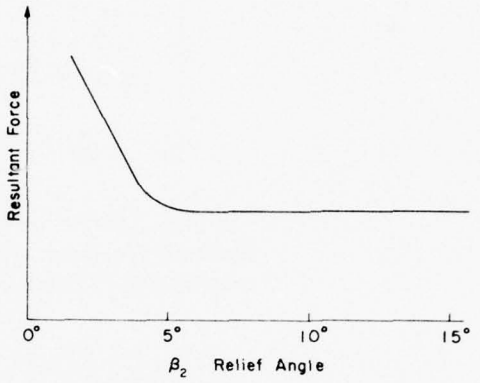

Figure 42. General trend of resultant cutting force as a function of relief angle. (From Valantin et al. 1964).

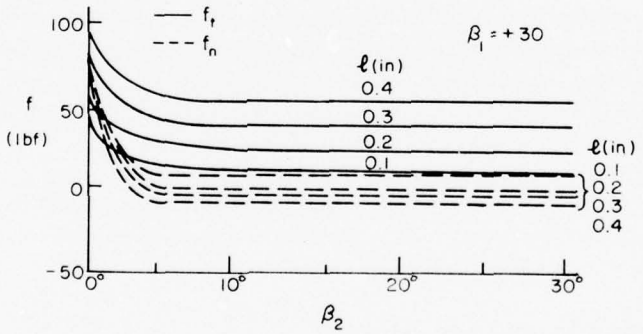

Figure 43. Components of cutting force as functions of relief angle, with chipping depth as parameters, for a sharp tool cutting hard coal (rake angle = +30°). (After Evans and Pomeroy 1973.)

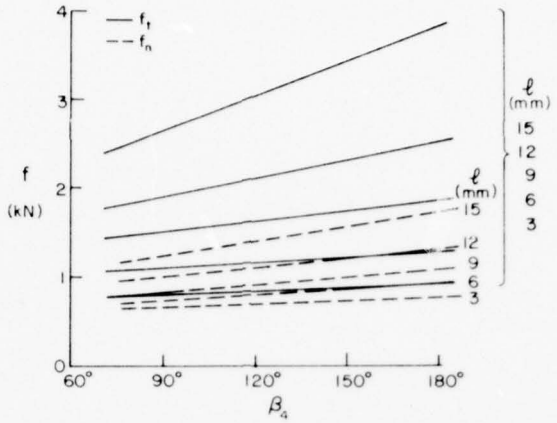

Figure 44. Effect of symmetrical side rakes (V-face pick). Components of mean cutting force as functions of β_4, with chipping depth ℓ as parameter. (Roxborough and Phillips 1975.)

Effect of side rake on tool forces

Most practical rock-cutting tools are symmetrical in plan, so that side rake angles are usually equally disposed about the center line, as on a V-face pick. With such tools, it is found that both f_n and f_t decrease as the equal side rake angles β_4 increase (Fig. 44). The relationships between f_n and β_4, and between f_t and β_4, are approximately linear over the range that is of practical interest (so that f_n/f_t does not vary significantly with β_4).

An asymmetrical tool with one-way side rake will develop a transverse component of force f_s, and there has been speculation that this might be beneficial in facilitating breakout to an adjacent parallel kerf. Roxborough and Phillips (1975) investigated the effect of one-way side rake on cutting forces for unrelieved cutting (no adjacent kerfs) and for relieved cutting (parallel kerfs at varying distances to either side). In neither case was there any significant effect on f_n or f_t, but in both cases the side force f_s increased with increase of side rake β_4 (Fig. 45, 46). In the unrelieved situation, f_s should be zero at zero side rake, but in the relieved situation it appears that a tool with zero side rake will actually experience a finite side force that tends to drive the tool towards the relieving cut. Looked at another way, this means that a chisel-edge tool working parallel to a single relieving kerf could be stabilized by giving it a positive side rake of a few degrees (positive being the direction that tends to plow material towards the relieving kerf).

Effect of base angle or face profile on tool forces

Both tangential cutting force f_t and normal cutting force f_n decrease nonlinearly as the base angle β_6 of a V-base tool increases. A similar effect can be expected as the radius of curvature decreases for a round-base tool. Experimental results by Roxborough and Phillips (1975) show f_n and f_t decreasing as β_6 increases (Fig. 47), but tending towards a lower limit for values of β_6 in the range 45° to 60°. The changes in f_n and f_t corresponded to changes in the area of the kerf cross section, which reduced as β_6 increased up to the point where the half-angle of the V-base became less than the overbreak angle of the rock, i.e. there was not much change in f_n and f_t for $\beta_6 > (\pi/2 - \phi)$. This effect is mentioned again in the discussion of specific energy.

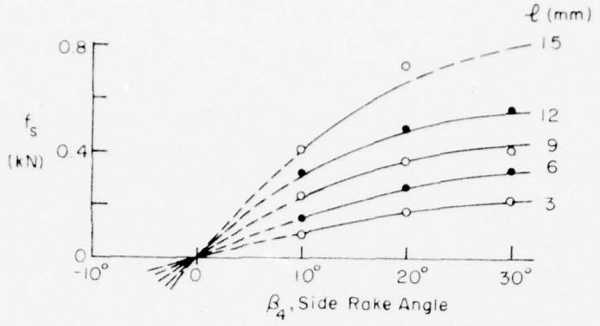

Figure 45. Effect of one-way side rake in unrelieved cutting. Transverse force component f_s as a function of β_4, with chipping depth ℓ as parameter. (Roxborough and Phillips 1975.)

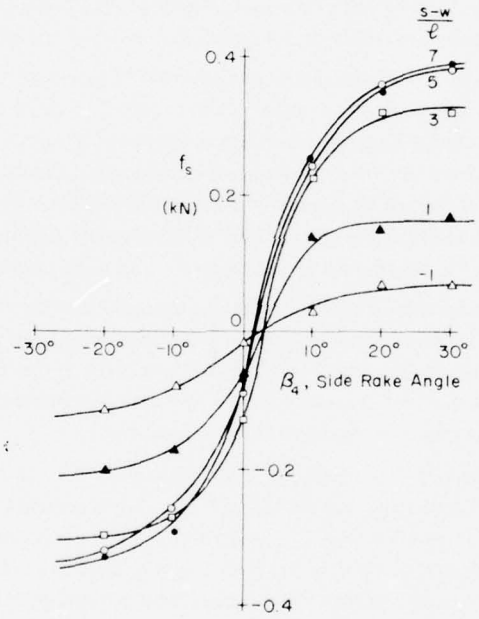

Figure 46. Effect of one-way side rake when cutting parallel to an existing kerf. Transverse force component f_s as a function of β_4, for β_4 angled towards and away from the relieving kerf. The parameter is distance from the relieving kerf. (Roxborough and Phillips 1975.)

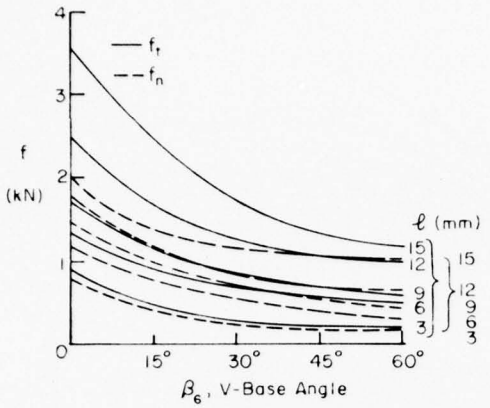

Figure 47. Force components as functions of base angle β_6, with chipping depth ℓ as parameter. (Roxborough and Phillips 1975.)

Effect of rounding at the cutting edge

When the cutting edge of the tool tip is not perfectly sharp, but instead has a finite radius, the cutting forces may vary with the tip radius. The edge radius of a wedge-shaped tool determines the force level needed to initiate indentation of the rock, and it sets the lower limit of penetration below which tool geometry (rake and relief) has no significant effect on the cutting process.

In Figure 48 the smoothed experimental data of Gray (1963) have been replotted to show components of cutting force as functions of tip radius. Both f_t and f_n increase nonlinearly with increase of tip radius r, apparently tending towards a limit when r becomes of comparable magnitude to the chipping depth ℓ. The variation of f with r is strongest in the range where tip radius r is small compared with chipping depth ℓ. Figure 49 gives similar data from Roxborough and Rispin (1973a), but in these cases tip radii never reach values comparable to the values of chipping depth ℓ. Figures 50 and 51 show the ratio f_n/f_t increasing with tip radius r, and Figure 52 implies a similar effect.

Gray used tip radius r to normalize values of chipping depth ℓ, plotting f' against dimensionless chipping depth ℓ/r (Fig. 53). This did not produce any obvious simplification of the plots, although it indicated that the maximum curvature of each graph might occur in the range $0.5 < \ell/r < 1.0$. Normalizing f' with respect to r for the data of Figure 53 does not remove the effect of the parameter r, i.e. the data do not collapse to form curves independent of r.

The theoretical approaches of Appl and Rowley (1963) and of Nalezny (1971) deal with the effects of rounding directly, and show that tip radius r is a rational parameter for normalizing chipping depth ℓ. The numerical results of Nalezny indicate that there is strong variation of f_t and f_n at dimensionless chipping depths of $\ell/r < 1$, but both f_t and f_n tend towards limiting values with $\ell/r > 1$. This is more or less in agreement with the experimental findings of Gray, but most experimental results show f_t continuing to increase with ℓ at large values of ℓ/r. In other words, tip radius r continues to affect the tangential tool force even when chipping depth is large relative to tip radius.

Evans and Pomeroy (1973) found that data for penetration of coal by wedges gave a linear relation on a log-log plot, leading them to a simple parabolic relation between penetration force and tip radius, i.e. force was proportional to $r^{1/2}$.

Both Gray (1963) and Roxborough and Rispin (1973a) used increasing tip radius to simulate tool wear. This may be somewhat unrealistic for drag bits working in hard, abrasive material, since most of the wear tends to take place on the relief face, or flank, forming a flat as shown in Figures 2c and 65.

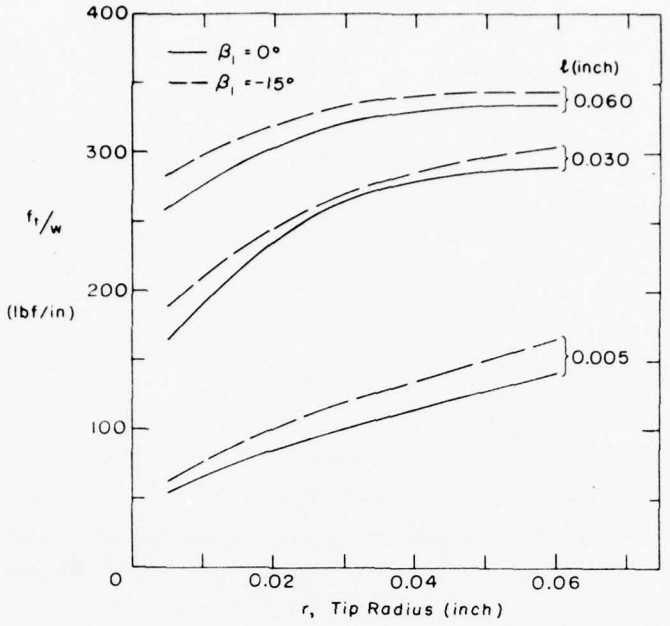

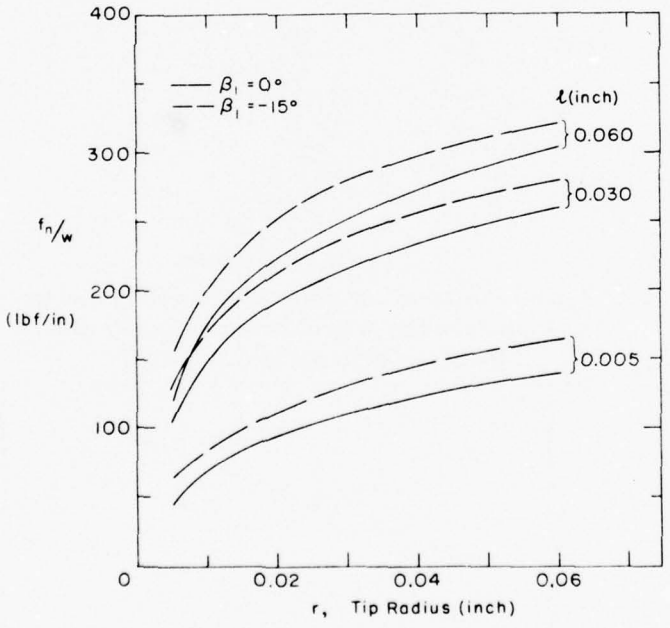

Figure 48. Components of cutting force as functions of tip radius, with chipping depth and rake angle as parameters. (From smoothed data by Gray (1963) – see Fig. 11.)

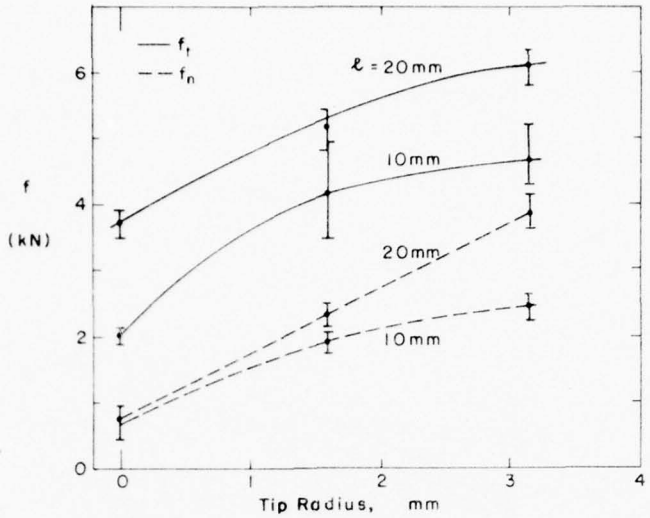

Figure 49. Components of cutting force as functions of tip radius for two values of chipping depth in dry chalk. (From Roxborough and Rispin 1973a.)

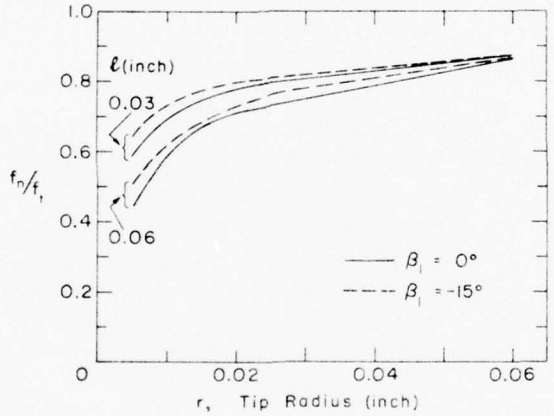

Figure 50. Ratio of force components as a function of tip radius, with chipping depth and rake angle as parameters. (From smoothed data by Gray 1963.)

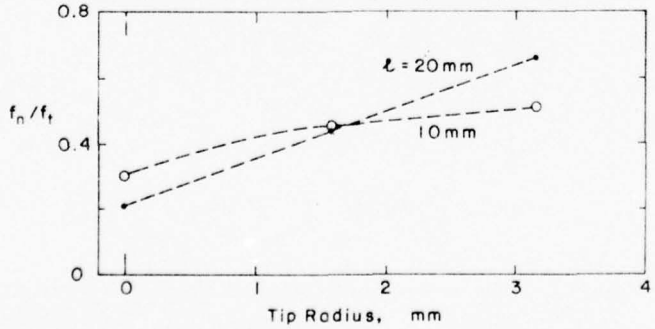

Figure 51. Ratio of force components as a function of tip radius for two values of chipping depth in dry chalk. (From Roxborough and Rispin 1973a.)

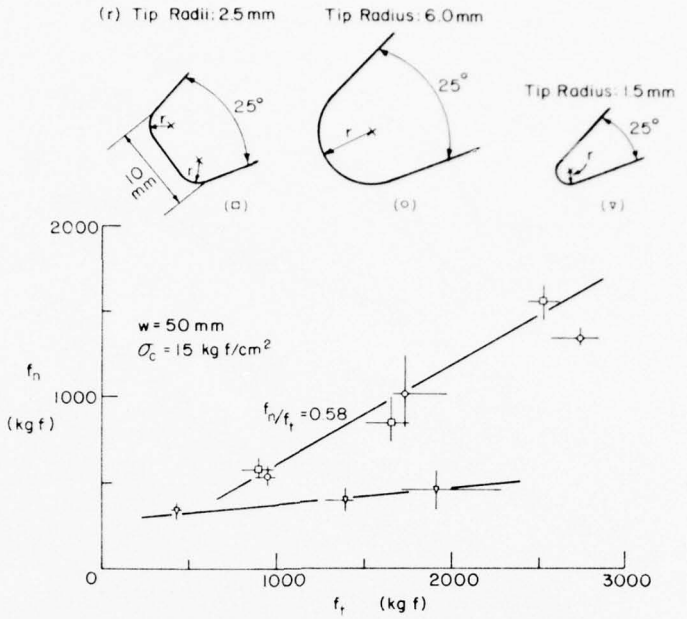

Figure 52. Relation of normal to tangential force components for different values of tip radius. (Furumi, personal communication.)

Effect of tool width on cutting forces

In some of the foregoing graphs, cutting forces for chisel-edge tools are given as force per unit tool width, following the practice of the original investigators. This is often convenient for analysis and design, and it is a reasonably valid procedure where wide tools are concerned. However, it implies simple proportionality between cutting force and tool width, and this is not strictly correct, since the tool has to overcome both frontal resistance and edge resistance.

The obvious expectation is that chisel-edge tools cutting at constant depth in a given material would experience force proportional to width, plus a constant increment of force representing side breaks at the edges of the tools. This expectation is borne out by the experiments of Roxborough and Rispin (1973a, b) and of Roxborough and Phillips (1975), results of which are illustrated in Figures 54 and 55. In these graphs, the slope of the line gives the proportionality constant relating direct resistance and tool width, while the force intercept for zero tool width represents the edge forces. The edge force is, of course, a function of the chipping depth ℓ, and the proportionality constant should also increase with w.

Pointed tools (such as V-face picks, bullet bits, or pyramid-tip bits) might be expected to develop cutting forces approximately equal to the "zero-width" forces of chisel edge tools, provided that tip radii, rake angles and relief angles are comparable, and that side angles of the pointed tool provide clearance from the overbreak.

Tool compliance and force fluctuations

When brittle materials are being cut, discrete chips are formed, and consequently the cutting forces fluctuate in magnitude. The amplitude of these force fluctuations depends to some extent on the compliance of the cutting tool.

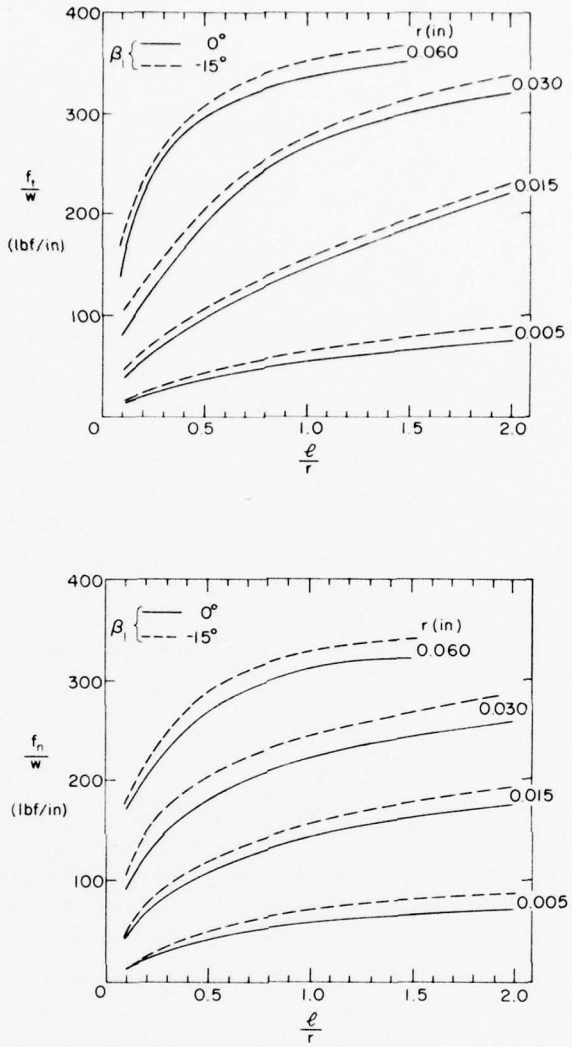

Figure 53. f'_t and f'_n as a function of ℓ/r for four different values of r and two different values of β_1. (From smoothed data by Gray, 1963.)

Although effects of tool compliance do not appear to have been investigated systematically for drag bits, some general principles can be deduced. If a tool is perfectly rigid (i.e. it does not deflect under load), then the force on the tool will drop abruptly each time the rock fails locally and undergoes large displacement, since the tool speed is likely to be two orders of magnitude lower than the speed of crack propagation in the rock. By contrast, if the tool has large elastic compliance (i.e. it has a low modulus, allowing large deflection under load), then it is capable of springing forward and maintaining the force level as the rock yields. However, in a real machine the tool compliance is unlikely to be great enough to allow the tip to maintain full loaded contact at large chipping depths, since the chip-forming crack is likely to be long compared with the elastic deflection of the tool.

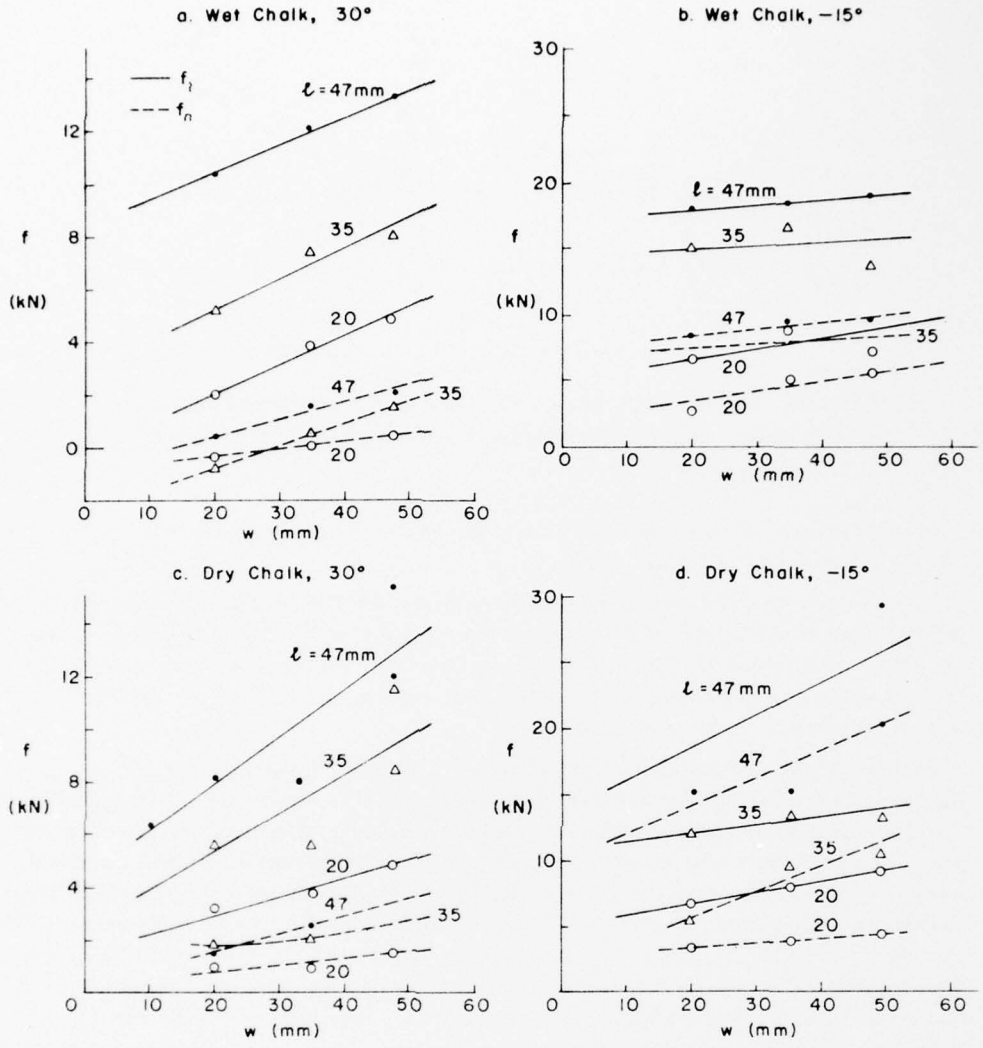

Figure 54. Components of cutting force as functions of tool width for chisel-edge tools working in wet and dry chalk, with rake angles of +30° and -15°. (Roxborough and Rispin 1973a, b).

In principle, compliance may have the potential for damping out force fluctuations, but in practice the response time of a compliant tool is likely to be too slow for high-speed fracture to be followed. A robust tool will presumably allow considerable force fluctuations, but it is likely to be resistant to deflection. A highly elastic tool may tend to damp force fluctuations, but it would be more prone to fatigue failure because of its large oscillations.

An interesting case of very high compliance is represented in the rotary flail principle, which has been applied to the cutting of rock and pavement materials (Furby 1970). In this type of machine the fixed drag bit is replaced by a pivoted tine whose cutting forces are controlled by the rotation speed of the drum. The tine is capable of undergoing large displacements, with a restoring force

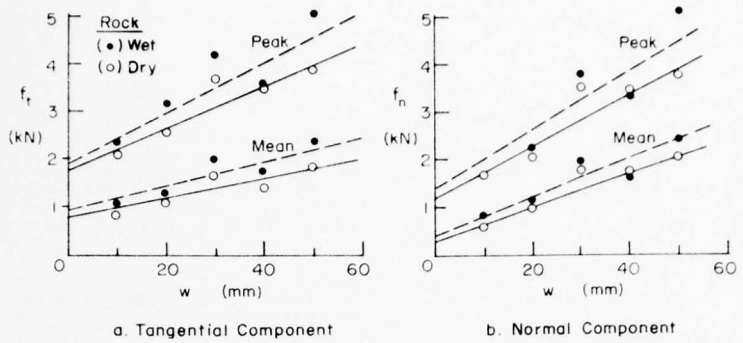

Figure 55. Components of peak tool force and mean tool force as functions of tool width in wet and dry sandstone. (Roxborough and Phillips 1975.)

continuously applied by radial accelerations, and the tangential tool speed is likely to be an order of magnitude higher than for a fixed tool.

Calibrated records giving data on the amplitude and frequency of force fluctuations are not often published, except as brief examples, but there is some information on relative magnitudes of mean and peak force components. Terminology tends to vary somewhat, but *mean force* is usually obtained by *integration of the area under* the trace, while *mean peak force* is the average of an arbitrary number of arbitrarily chosen peak values.

Fairhurst (1955) gave records for soft limestone that show amplitude decreasing as mean and peak force levels decrease, with total amplitude roughly equal to the mean force level. Specimen test records published by Roxborough (1969) show both f_n and f_t dropping almost to zero at some points, presumably after chip release, so that total amplitude (range from maximum to minimum) was almost equal to peak force. By contrast, Wagner (1971) gave a record for quartzite that showed maximum amplitude for f_n fluctuations an order of magnitude smaller than the mean force $\bar{f}_n$, with maximum amplitude for f_t fluctuations about half the mean force $\bar{f}_t$. Evans and Pomeroy (1973) show some typical records for coal-cutting experiments, also showing that force fluctuations for f_n have much smaller amplitude than force fluctuations for f_t. They also give data (see Fig. 17) that show peak values of f_t about 5 times higher than mean values. In tests where large picks were used to cut sandstone on a massive test rig, Barker (1964) found that the ratio of peak force to mean force for two different pick designs had average values of 6.2 and 7.7 for f_t, and 4.7 and 6.2 for f_n. Roxborough (1973), discussing cutting tests in sandstone, limestone and anhydrite, gave values for the peak to mean ratio of f_t that ranged from 1.8 to 2.8, and suggested 2 as a typical value that would also be representative for coal cutting. Data from a major series of experiments in wet and dry sandstone by Roxborough and Phillips (1975) confirmed that a peak to mean ratio of 2, or perhaps slightly higher, was representative for both f_t and f_n (see Fig. 23, 33, 55).

In considering force fluctuations, data records should perhaps be regarded with caution, since the compliance of the dynamometer used in the experiments can affect the results. The results which show f_t fluctuating much more than f_n imply that the ratio f_n/f_t fluctuates, or that the direction of the resultant cutting force is continually fluctuating. They contrast with other results that give in-phase fluctuations of f_n and f_t, and relative constancy of f_n/f_t. Such differences of behavior could arise from dynamometer characteristics, or they could represent differences of compliance in different directions for the tool or its mount.

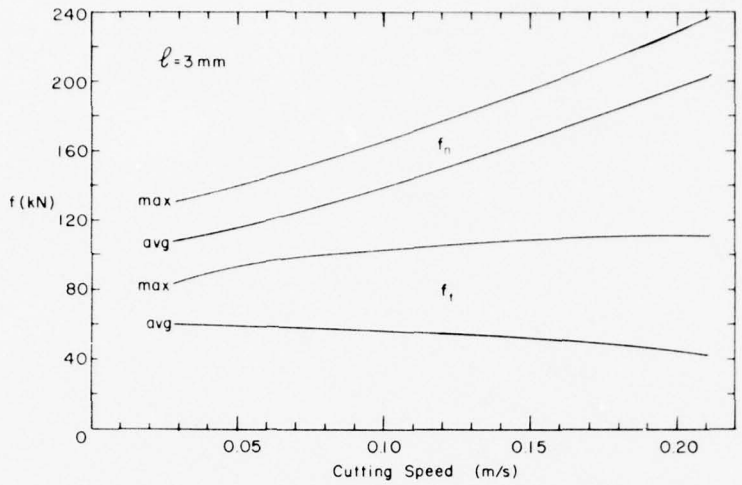

Figure 56. Components of cutting force as functions of cutting speed. (From Chamber of Mines of South Africa Research Organization, 1971.)

The frequency of force fluctuations ought to be determined by chip length and tool speed u; if the length of major chips is of the same order of magnitude as the chipping depth ℓ, the corresponding frequency for major peaks would be of the order of u/ℓ.

The significance of mean force or peak force in machine design is related to the part of the system under consideration. For design of the tools or their mountings, peak forces have to be resisted, but on a multi-cutter machine the power requirements and overall machine forces are more likely to be related to mean forces.

Effect of tool speed on cutting forces

Most investigators agree that the tangential cutting force f_t is unaffected by cutting speed over the usual range of variation found on rock-cutting machines. This insensitivity to speed has been noted for the range 1 to 1000 ft/min (0.005 to 5 m/s) (Gray 1963, Evans and Pomeroy 1973, Roxborough 1973, Roxborough and Phillips 1975, Valantin et al. 1964, Chamber of Mines of South Africa Research Organization 1971, Cook et al. 1968). For the normal component of cutting force f_n, Gray (1963) found some increase of maximum values for negative rake tools when speed increased from 15 to 150 ft/min (0.075 to 0.75 m/s), but speculated that this might be a vibration effect rather than a reflection of strain-rate sensitivity in rock strength. Roxborough's (1973) data for anhydrite also showed a 25% increase in the mean value of f_n when speed increased from 30 to 112 ft/min (0.15 to 0.57 m/s). However, in tests on sandstone by Roxborough and Phillips (1975) there was no significant change in either the mean or peak values of f_n when speed was raised from 30 to 90 ft/min (0.15 to 0.45 m/s). Low speed tests by the Mining Research Laboratory of the South African Chamber of Mines (Fig. 56) showed a significant increase of average and maximum values of f_n when speed increased from 6 to 41 ft/min (0.03 to 0.21 m/s). Results by Cook et al. (1968) show f_n increasing significantly with speed in the range 20 to 130 ft/min (0.10 to 0.66 m/s), as can be seen in Figures 57 and 58.

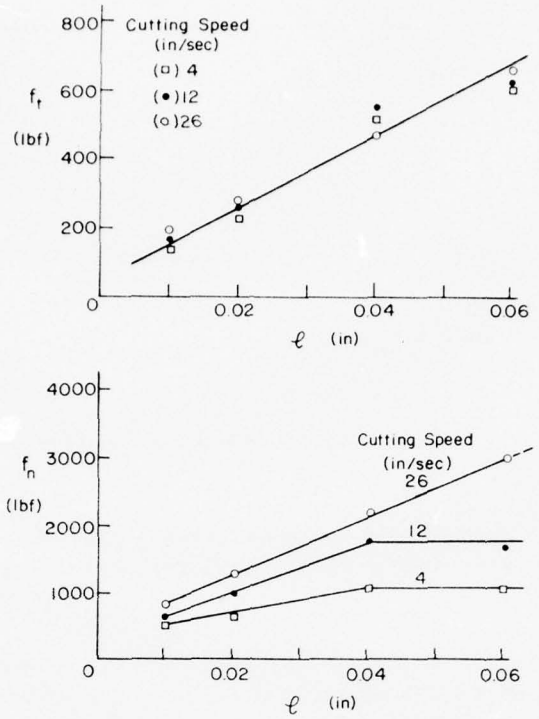

Figure 57. Components of cutting force (mean peak) plotted against chipping depth for three different cutting speeds in shaly quartzite. (Cook et al. 1968.)

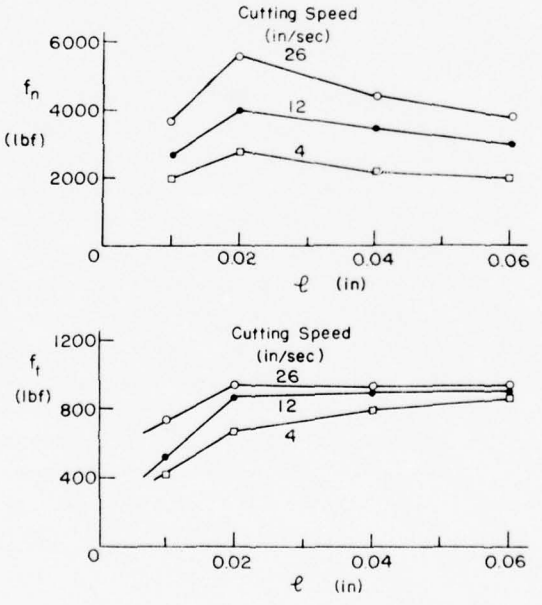

Figure 58. Components of cutting force (mean peak) plotted against chipping depth for three different speeds in hard pebbly quartzite. (Cook et al. 1968.)

The insensitivity of f_t to tool speed suggests that apparent rock strength does not vary much within the speed ranges that have been investigated. It also indicates that inertial forces related to acceleration of cuttings up to velocity u are small compared with cutting forces. The apparent speed-dependence of f_n that has been found in some experiments could be related to the dynamic response characteristics of the tool or the dynamometer, but even so this dependence could appear in a working machine. The implication of the effect is that f_n/f_t could increase with cutting speed, i.e. the direction of the resultant cutting force could incline nearer to the normal direction.

Effect of rock properties on cutting forces

The effect of rock properties on cutting forces has not been fully established by experimental work. The simpler theories of metal-cutting and rock-cutting predict direct proportionality between cutting force and a single strength parameter, such as shear strength or tensile strength. The more elaborate rock-cutting theories also make cutting force proportional to shear strength or tensile strength, but they introduce an additional property, such as the "angle of internal friction" or the ratio of compressive strength to tensile strength.

Roxborough and Phillips (1975) made strength and cutting tests on sandstone specimens which all came from the same geological formation, but had strengths varying by about a factor of 5. The mean tangential cutting force f_t was compared with uniaxial compressive strength, uniaxial tensile strength, Shore rebound, and resistance to cone indentation, and a linear correlation was obtained in each case. The best correlation was with uniaxial compressive strength (correlation coefficient 0.92); the straight line relation, of the form $f_t = a\sigma_c + b$, had a force intercept b that was very small, and for practical purposes the data could probably be represented adequately by direct proportionality. However, it was found that wetting of the rock gave an anomalous effect, in that strength decreased and cutting force increased with respect to values for the dry state. This last effect was noted for both sandstone and chalk.

In studies of wedges penetrating coal, Evans and Pomeroy (1973) found that results for different specimens could be unified by normalizing the penetration stress with respect to uniaxial compressive strength. They also found a linear correlation between the mean peak value of f_t and the tensile strength for coal (but the regression line implies existence of appreciable cutting force with zero strength).

Some investigators have considered the effect of confining stresses on cutting forces. Appl, Rowley and Bridwell (1967) gave a theoretical treatment for cutting with spherical diamond tools and took into account the effect of confining stress. Their numerical results show cutting forces increasing steadily with confining stress; at 15,000 lbf/in.^{2}, both f_t and f_n were higher than the zero confinement values by almost a factor of 4. Evans and Pomeroy (1973) made measurements in laterally confined specimens of various types of coal, and found f_t for deep cuts increasing with the confining pressure up to about 500 lbf/in.^{2} Above 500 lbf/in.^{2}, f_t decreased with increasing pressure for some types of coal. At small cutting depth (0.1 in.) the confining stress did not appear to have much effect. Roxborough and Phillips (1975) measured f_t and f_n for a range of lateral confining stresses up to 20 MN/m^2 (2900 lbf/in.^{2}), but found no significant change for chipping depths from 3 to 9 mm (0.12 to 0.35 in.).

Tool interaction and kerf spacing

Tool forces will obviously vary to some extent with the transverse spacing of adjacent kerfs, or cutting tracks. When the kerfs are wide apart, each tool will operate independently, and tool

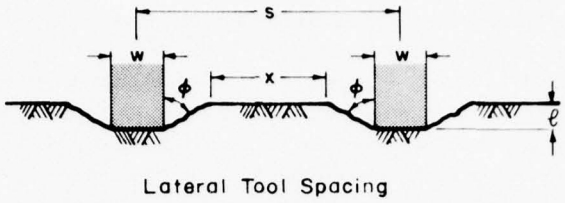

Figure 59. Designation of dimensions for discussion of tool spacing.

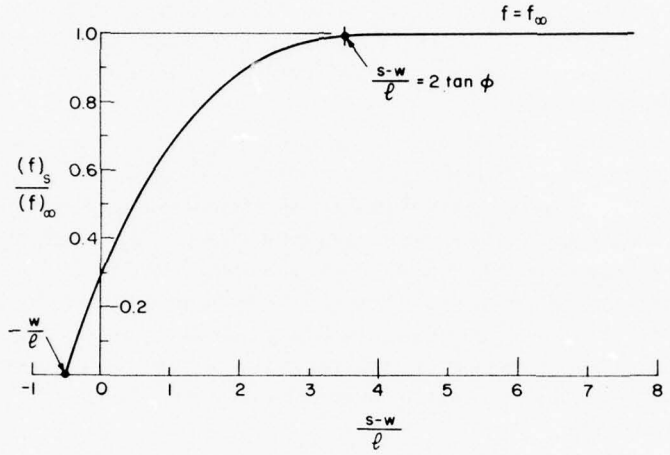

Figure 60. Side force as a function of tool spacing for relieved cutting.

forces will be the same as for a single tool making unrelieved cuts. At the other extreme, when there is complete overlap of kerfs, a tool following in the wake of a preceding tool will experience zero force if there is no provision for deepening the kerf. Between these extremes, tool forces will vary with the degree of overlap of adjacent kerfs, decreasing as spacing decreases.

Transverse spacing of tools has already been discussed from a geometrical viewpoint (Mellor 1975, 1976a), but it remains to be seen how tool forces vary with spacing. Referring to Figure 59, it was previously pointed out that the limit of interaction is the situation where $x = 0$, i.e. where $(s-w)/\ell = 2\tan\phi$, where ϕ is the overbreak angle. For spacings wider than this, tool forces should be independent of spacing, while at smaller spacings the tool forces should decrease, reaching zero at $s = 0$. Thus the general form of the relationship can be deduced, as in Figure 60, where the ratio of force $(f)_s$ at spacing s to the force $(f)_\infty$ at infinite spacing is plotted against $(s-w)/\ell$. With overbreak angles in the range 50° to 70°, the range of values for $2\tan\phi$ is approximately 2.5 to 5.5, and these values would be the limits for tool interaction. If there was no overbreak at all, tool interaction would not occur until $s = w$, or $(s-w)/\ell = 0$.

According to work by Valantin et al. (1964), the upper limit of spacing for tool interaction was $(s-w)/\ell = 1$. Evans (1972) gave data obtained by Pomeroy and Robinson, and these results indicate that interaction was just beginning to occur at values of $(s-w)/\ell$ ranging from 1.5 to 4.1. Data by

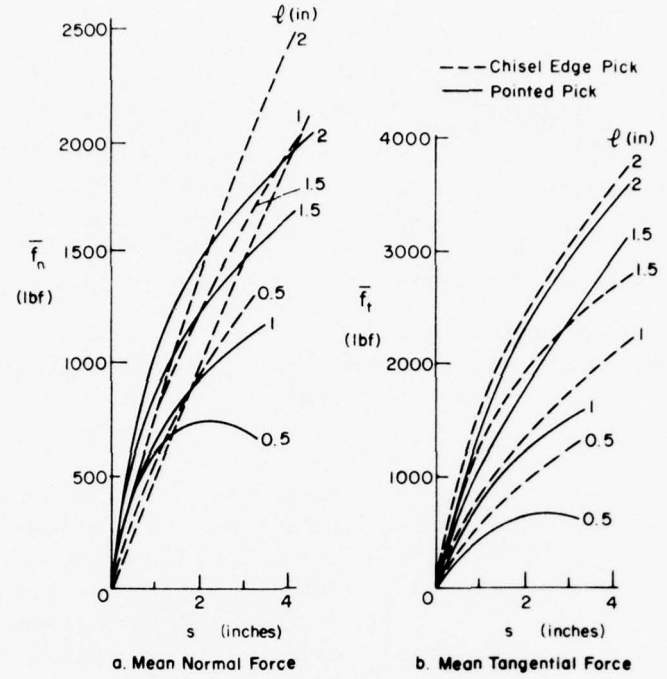

Figure 61. Components of cutting force as functions of transverse spacing for two types of picks cutting sandstone. The parameter is chipping depth ℓ. (After Barker 1964.)

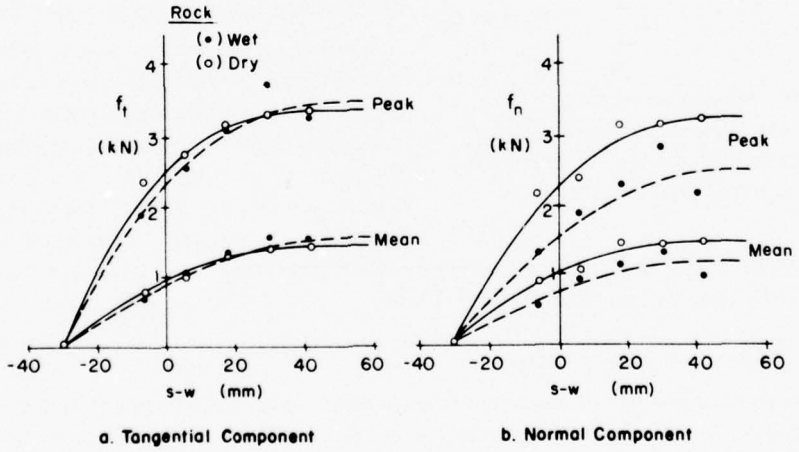

Figure 62. Components of peak cutting force and mean cutting force as functions of space between adjacent parallel tool tracks (wet and dry sandstone). (Roxborough and Phillips 1975.)

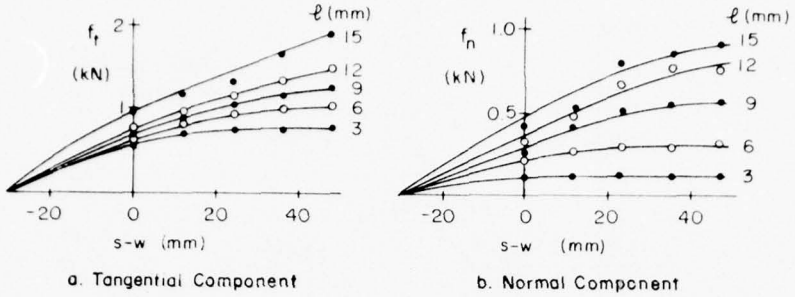

Figure 63. Components of cutting force as functions of spacing between adjacent parallel tool tracks, with chipping depth as parameter. (Roxborough and Phillips 1975.)

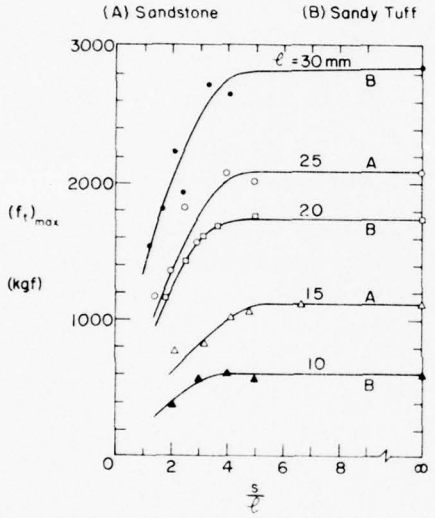

Figure 64. Tangential component of cutting force as a function of spacing for two rock types: sandstone and sandy tuff. (Furumi, personal communication.)

Barker (1964) show f_t and f_n varying strongly with spacing (Fig. 61); the only curves reaching a maximum value did so at $(s-w)/\ell = 3.75$. Roxborough (1973) found that the limit of interaction occurred at approximately 2 $\tan\phi$ in his experiments, where ϕ values for anhydrite, limestone and sandstone were 52°, 70° and 62° respectively. A similar result (Fig. 62, 63) was obtained in further work on sandstone by Roxborough and Phillips (1975). Data by Furumi (personal communication – Fig. 64) indicate the limit of interaction occurring at s/ℓ values of approximately 4 to 5, with w/ℓ values probably of the order of 1.

Effect of multiple pass cutting on tool forces

If a deep kerf, or groove, is cut progressively by repeated tool passes along the same track, the cutting forces f_t and f_n become higher at each pass, even though the chipping depth is the same for each pass. Eventually the cutting forces reach a limit and thereafter remain the same for each successive pass. Limiting values might be reached when the kerf depth exceeds the kerf width. Data for groove deepening experiments are given by Roxborough and Phillips (1975) and by Evans and Pomeroy (1973).

Effect of tool wear on cutting forces

Although discussion of tool wear tends to occur almost as an afterthought, it could well be the most important aspect of the cutting process from a practical point of view. The results of both theoretical and experimental studies for sharp tools can be modified almost beyond recognition when wear is accounted for, and the amount of wear needed to bring about this transformation can occur very early in the life of a typical tool.

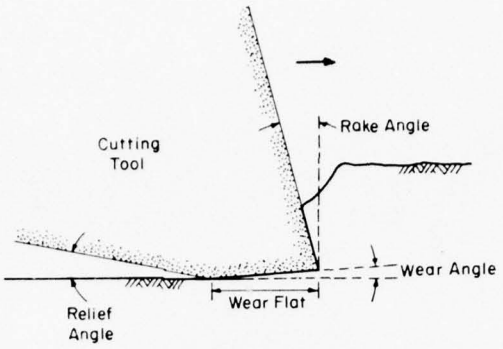

Figure 65. Development of typical wear flat, showing "wear angle."

In the usual mode of frictional or abrasive wear, a flat develops under the tip of the tool on the relief face, or flank. The wear flat, or "wear land," is almost parallel to the tangential direction, but in general it inclines slightly in the opposite direction to the relief face (Fig. 65). This "wear angle" is typically a few degrees, and it is said to be smallest with the hardest and strongest tool materials. Other types of wear patterns can occur, especially on softer tools and in weaker ground materials; wear can take place on both the relief and rake surfaces, producing general rounding or blunting of the tool tip. Heavy wear can lead to breakage and detachment of hard tip materials (Fig. 66).

As the classic wear flat develops, both f_n and f_t have to increase in order to maintain constant chipping depth ℓ. In general, cutting force f for chisel-edge tools increases nonlinearly with the width of the wear flat (Fig. 67, 68); the relation may be representable by a simple function of the form $f = ax^n$, where n is a fractional power. In some cases data might also be represented approximately by a straight line, possibly one that has an intercept on the force axis (Fig. 69, 70, 71). In the case of a chisel-edge tool of constant width, the *area* of the wear flat is proportional to the *width* of the wear flat.

The normal component of cutting force f_n always increases more rapidly than the tangential component f_t, and the ratio f_n/f_t attains values greater than unity after only small amounts of wear (Fig. 72, 73). Under experimental conditions, it appears that development of wear flats less than 1 mm wide is sufficient to make $f_n/f_t > 1$.

Figure 74 shows the increase of f_t with the breadth of a flat that is normal to the rake face (cf. the blunt wedge of Evans' theory – Fig. 8). The trend is similar to that observed for the classic wear flat.

The width or area of the wear flat, and hence the force components, must obviously increase with the distance L traveled by the tool. Figure 75 gives a direct example of variation of f_t with L, while Figure 76 illustrates how f_n/f_t can increase with L. In experimental studies it is more usual to relate tool forces with wear flat dimension, treating the dependence of wear dimensions on other variables separately, as discussed below.

Figure 66. Progressive development of wear in a rock-cutting drag bit. (Photo courtesy of D. Fourmaintraux, Laboratoire Central des Ponts et Chaussées, Paris.)

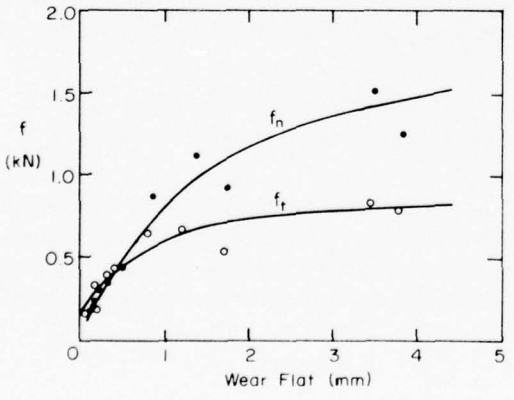

Figure 67. Components of cutting force as functions of wear flat length for a chisel edge tool. (Roxborough and Phillips 1975.)

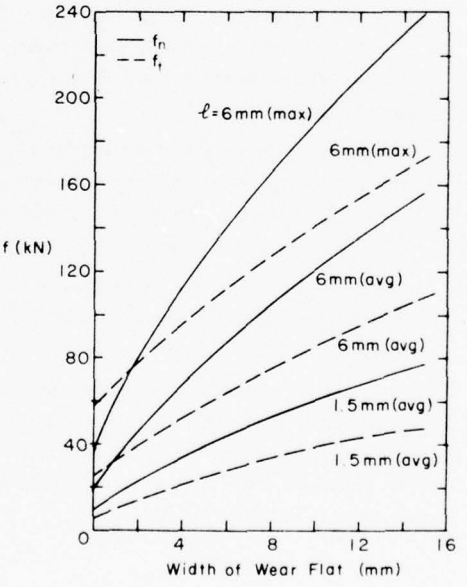

Figure 68. Components of cutting force as functions of wear flat length, with chipping depth as parameter. (From Chamber of Mines of South Africa Research Organization 1971.)

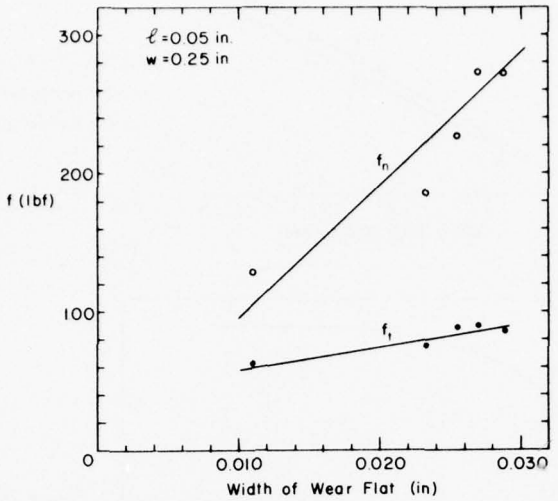

Figure 69. Components of cutting force as functions of wear flat length for a chisel edge tool. (Fairhurst 1955.)

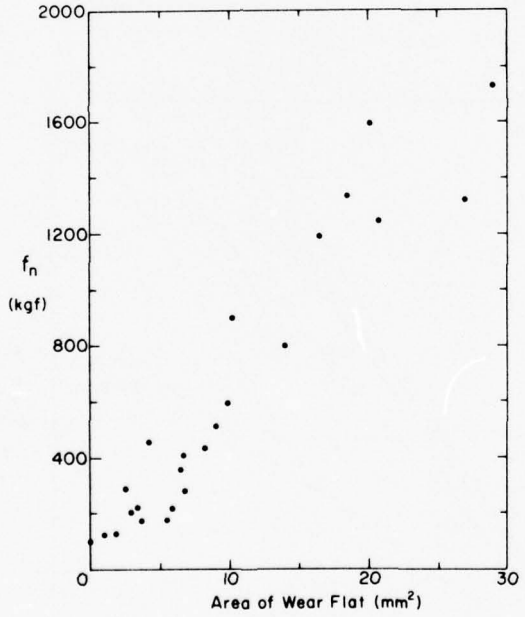

Figure 70. Normal component of cutting force plotted against area of wear flat. (Valantin et al. 1964.)

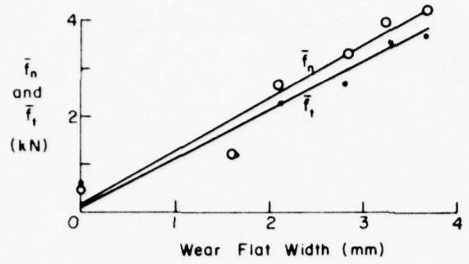

Figure 71. Increase of mean force components with wear flat width. (After Kenny and Johnson 1976.)

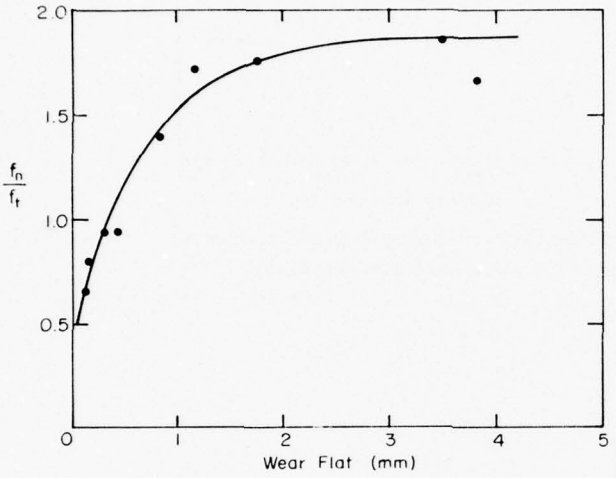

Figure 72. Ratio f_n/f_t as a function of wear flat length. (Roxborough and Phillips 1975.)

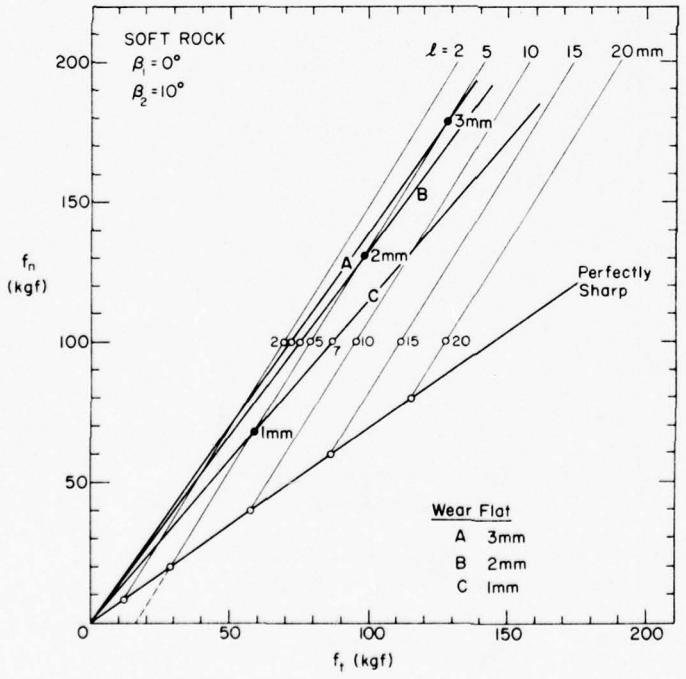

Figure 73. Plot of f_n against f_t showing effects of chipping depth ℓ and wear flat length. (Valantin et al. 1964.)

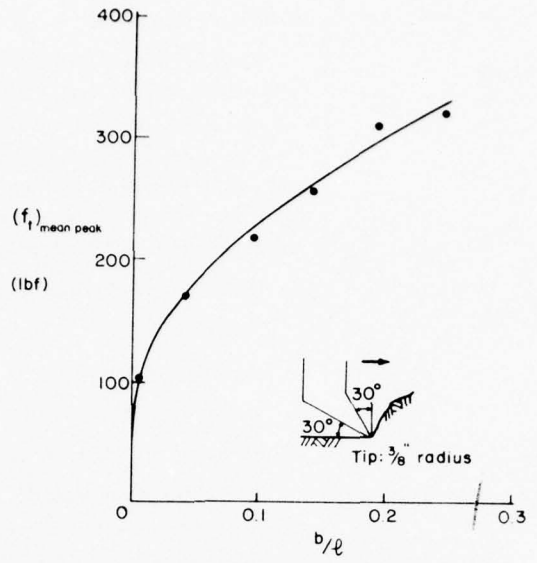

Figure 74. Tangential component of mean peak cutting force as a function of wear flat width for a flat that is normal to the tool's rake face. (Evans and Pomeroy 1973.)

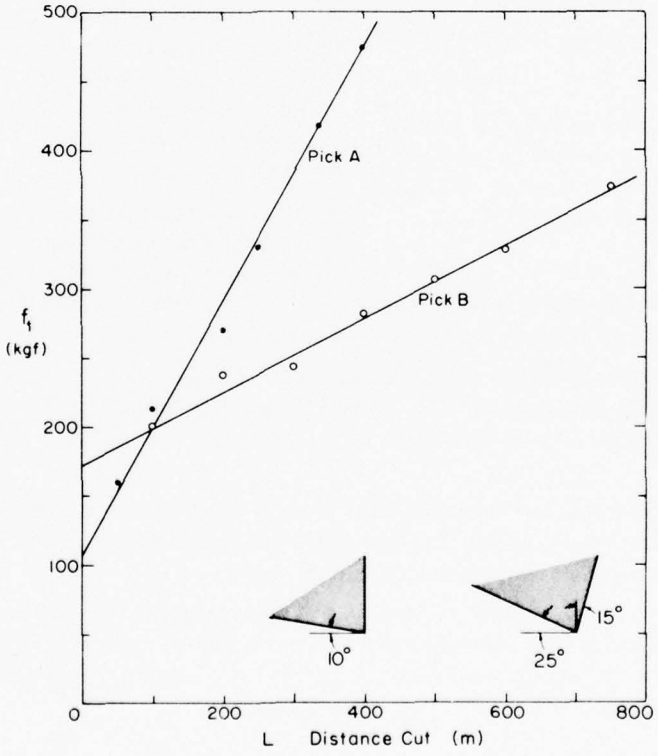

Figure 75. Tangential component of cutting force as a function of distance traveled for a chisel-edge tool in two different orientations (β_3 constant; β_1, β_2 changed). (Valantin et al. 1964.)

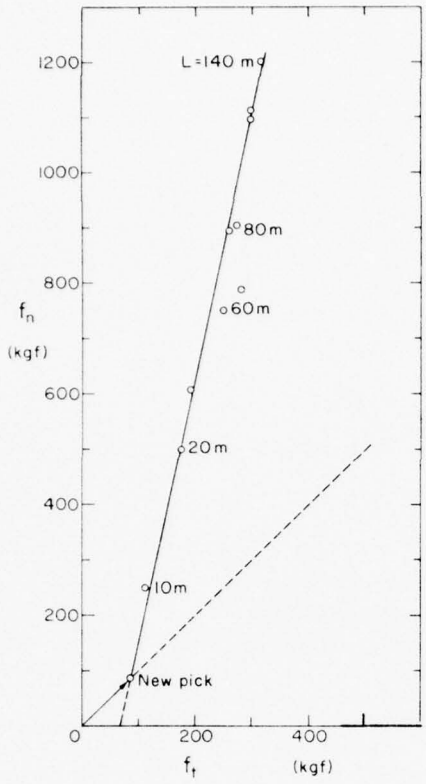

Figure 76. f_n plotted against f_t for various travel distances. This shows the increase in the ratio f_n/f_t as wear progresses. (Valantin et al. 1964.)

Development of wear

There is no standard method of measuring and reporting tool wear, and it has been given in terms of weight loss, width of wear flat, area of wear flat, and decrease of gauge length Δh. For a chisel-edge tool of uniform cross section, which is the typical geometry for experimental work, these different measures can be interrelated as follows:*

Width of wear flat = $\Delta h\ (\cot\beta_2 - \tan\beta_1)$

Area of wear flat = $w\,\Delta h\ (\cot\beta_2 - \tan\beta_1)$

Volume loss = $\frac{1}{2}w(\Delta h)^2\ (\cot\beta_2 - \tan\beta_1)$

Weight loss = $\frac{1}{2}w(\Delta h)^2\ (\cot\beta_2 - \tan\beta_1)\gamma_T$

where γ_T is unit weight of the tool material.

The width of the wear flat on a chisel-edge tool increases nonlinearly with distance traveled L, approximately as L^m, where m is a fractional power (Fig. 77-82). After an initial stage of rapid wear, the weight loss, or volume loss, increases almost linearly with L (Fig. 79, 82, 83, 84, 85), and since weight loss for a chisel edge is proportional to the square of the wear flat width, there is an implication that the power m is approximately ½, or perhaps somewhat lower. This is in agreement with the wedge penetration results of Evans and Pomeroy (1973), which showed penetration force proportional to the square root of wear land width.

Figures 86 and 87 show a remarkable effect that should be of great practical significance: the volume loss, or weight loss, from the cutting edge actually *decreases* significantly with *increase* of chipping depth ℓ. This implies that the ratio of wear volume to volume of cut rock decreases even more dramatically as ℓ increases.

A detailed study of tool wear was made by Kenny and Johnson (1976). In brief, they found that the volumetric wear rate at the cutting edge was a) independent of β_1 and β_2, and of wear flat width, b) proportional to L (after the initial stage), and to w, c) inversely related to ℓ and to tool hardness.

Wear rates can be expected to increase with tool speed when other factors remain unchanged, since the hardness of the tool material decreases with increasing temperature, and increased cutting speed almost invariably raises the temperature of the tool tip.

A great deal of nonsense has been talked about "self-sharpening tools." It is an incredible fact that many rock-cutting tools, especially bullet bits, are set with an apparent relief angle of zero, which means negative relief for finite feed rate. The best that a rigidly mounted tool can do is grind itself so as to maintain zero "kinematic" relief angle.

---

* Wear flat area is related geometrically to Δh for a variety of tool types by Linenko (1972).

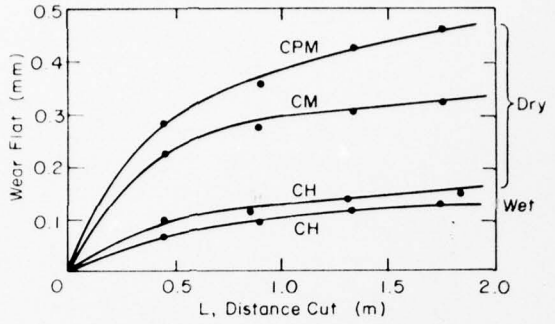

a. Enlargement of plot for first 2 m.

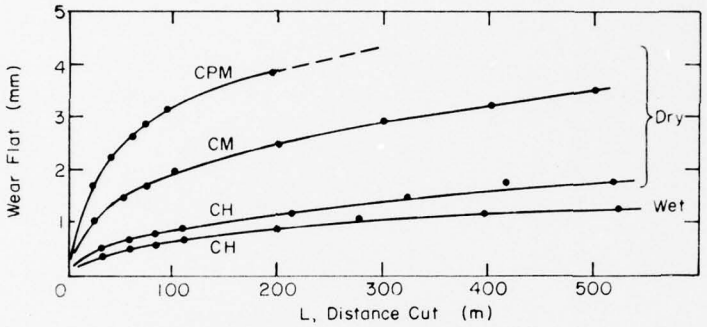

b. Complete plot covering several hundred meters of travel.

Figure 77. Wear flat length as a function of distance traveled by the tool, for three different grades of tungsten carbide working in sandstone (CPM-3.5 μm grain size, 15% cobalt; CM-3.5 μm grain size, 10% cobalt; CH-3.5 μm grain size, 7% cobalt. (Roxborough and Phillips 1975.)

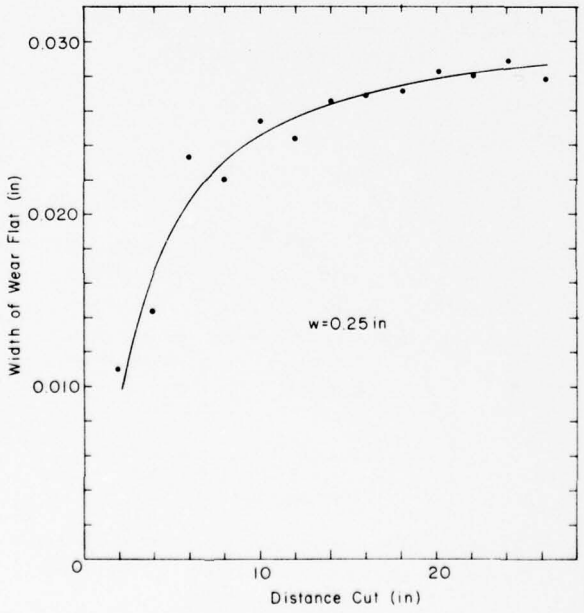

Figure 78. Wear flat length as a function of distance traveled by the tool. (Fairhurst 1955.)

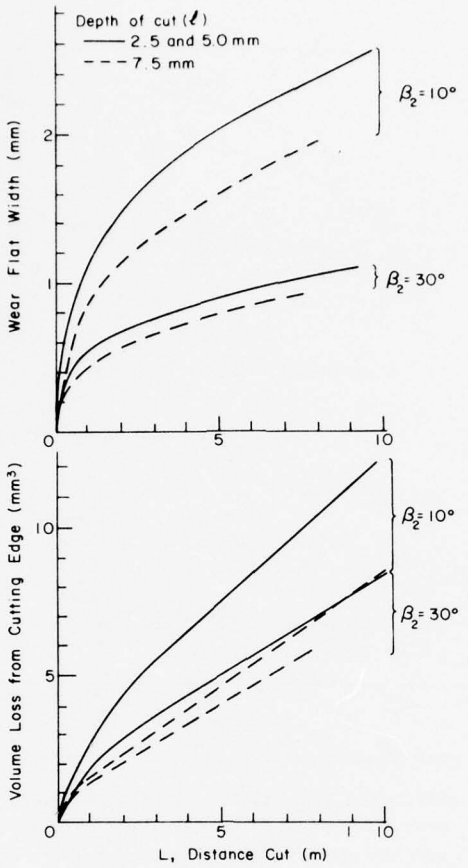

Figure 79. Development of wear with distance traveled by a tool steel cutter ($\beta_1 = 30°$). (After Kenny and Johnson 1976.)

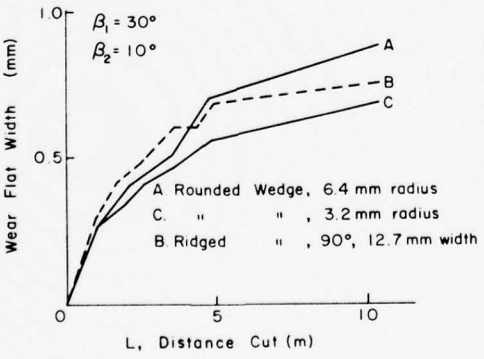

Figure 80. Wear flat width as a function of distance traveled for three types of tool tips. (After Kenny and Johnson 1976.)

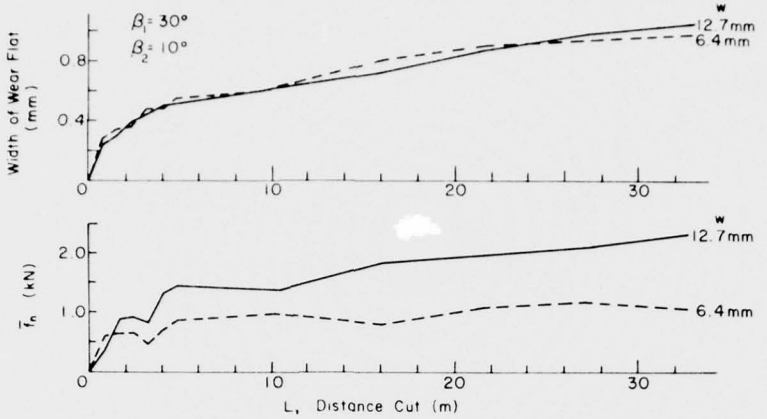

Figure 81. Wear flat length and normal component of cutting force as functions of distance traveled for two tool widths. Note that wear flat length is independent of tool width w, while f_n is a function of w (or of wear flat area). (After Kenny and Johnson 1976.)

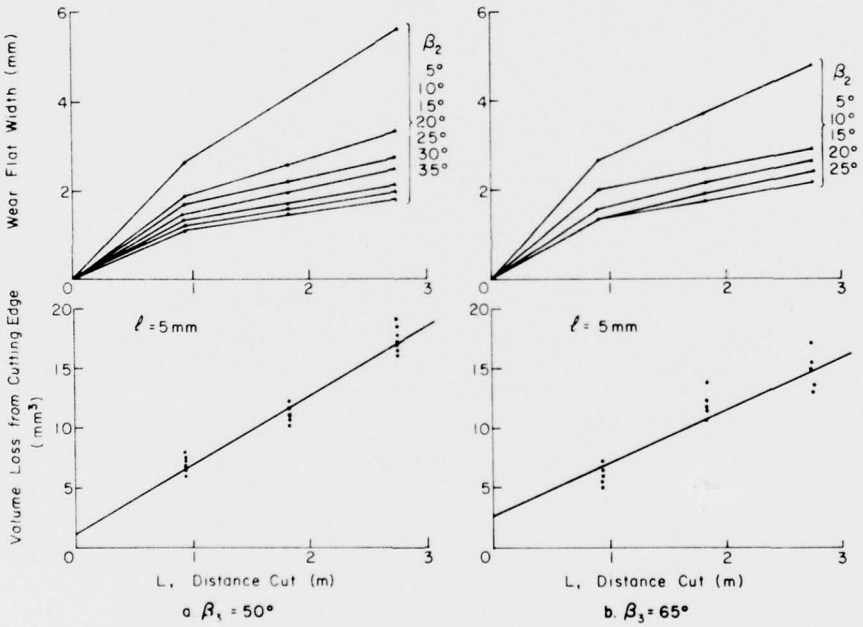

Figure 82. Wear flat width and volume loss as functions of distance traveled for various tool angles. (After Kenny and Johnson 1976.)

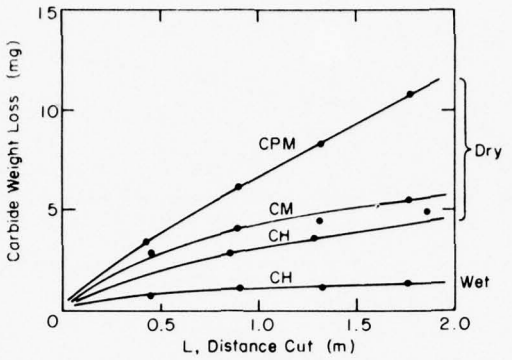

a. Enlargement of plot for first 2 m.

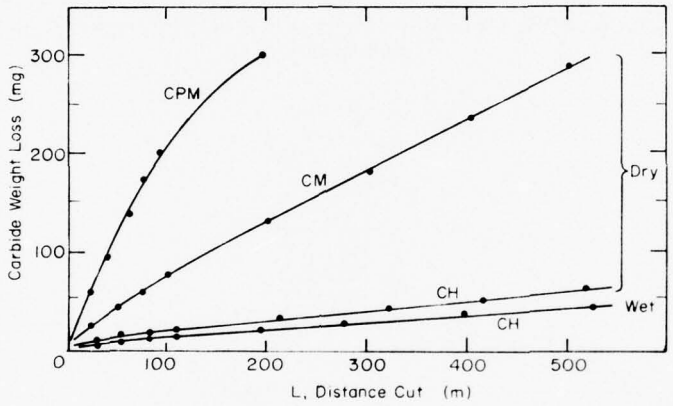

b. Complete plot for tool travel of several hundred meters.

Figure 83. Weight loss from tungsten carbide tips as a function of distance traveled by the tools (see Fig. 77 for meaning of carbide grade codes). (Roxborough and Phillips 1975.)

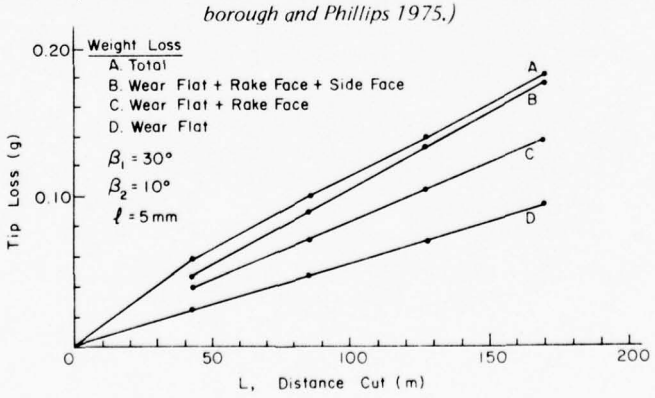

Figure 84. Distribution of wear on a carbide tool cutting rock. (After Kenny and Johnson 1976.)

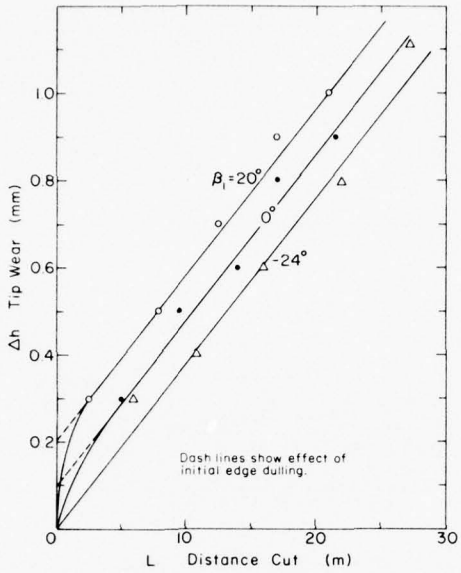

Figure 85. Tip wear (measured in the normal direction) as a function of distance traveled, for three different rake angles. (Valantin et al. 1964.)

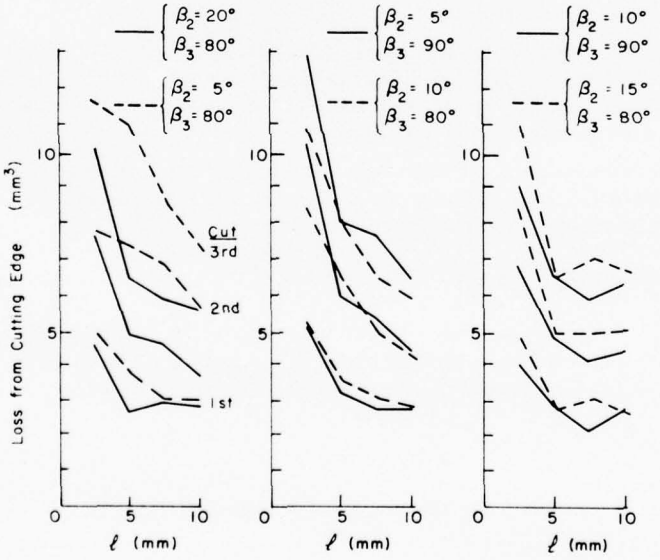

Figure 86. Volume loss from cutting edge as a function of chipping depth for various tool angles and different stages of wear. (After Kenny and Johnson 1976.)

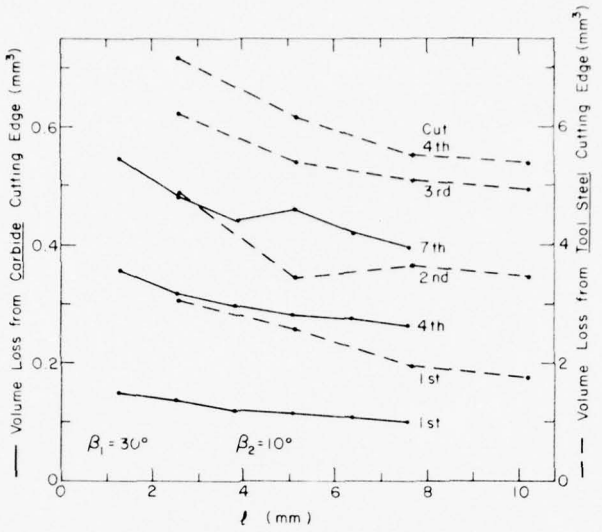

Figure 87. Volume loss from cutting edge as a function of chipping depth for carbide (full line, left scale) and tool steel (dashed line, right scale). (After Kenny and Johnson 1976.)

ENERGETICS OF CUTTING

Energetics of parallel-motion tools

Since problems involving tool forces on rock-cutting machines can be so complicated, it is often convenient to bypass the complexities and the unknowns by considering the overall energetics of the cutting process. This approach is particularly useful for making estimates of average tool forces from simple field measurements of machine performance, as well as for assessing power requirements.

The energy W expended by a cutting tool in any given operation is, in simple terms, the cutting force multiplied by the distance through which the force moves. More precisely, it is the product of force and displacement integrated through the operation:

$$W = \int f_x dx + \int f_y dy + \int f_z dz \tag{30}$$

where f_x, f_y, f_z are the varying time-dependent force components in orthogonal directions x, y, z. In the case of a simple parallel motion tool cutting to constant depth ℓ, the work done only involves moving the mean tangential component of cutting force $\bar{f}_t$ through a distance L, and it is simply

$$W = \bar{f}_t L \tag{31}$$

where $\bar{f}_t$ is a mean value taken over numerous individual chipping sequences.

The results of the work done by the tool can be expressed in terms of the mass or volume of material that has been cut. In the case of a parallel-motion tool that moves a distance L at constant chipping depth ℓ, the mass M and volume V are

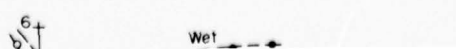

$$V = \ell L \bar{w}_k = M/\rho \tag{32}$$

where $\bar{w}_k$ is the mean kerf width and ρ is the in-place density of the material that has been cut.

Some of the work done by the tool is expended in imparting kinetic energy to the cuttings, but even at the highest tool speeds used in rock cutting this is an insignificantly small proportion of the total energy input.

In order to characterize the effectiveness of different cutting processes in a given material, or alternatively to characterize the behavior of various materials under the action of a particular cutting process, the work done by the tool can be related to the cutting production. The energy expended by the tool in producing unit mass or unit volume of cutting defines a specific energy E_s:

$$E_s = W/M$$

or

$$E_s = W/V. \tag{33}$$

Although production is often measured in terms of mass, definition of specific energy in terms of energy per unit volume is preferable for most analytical purposes, especially as it has the dimensions of a stress. The reciprocal of specific energy is sometimes used as an index of energetic efficiency; the term used for this quantity is "energy effectiveness." For a simple parallel motion tool that moves a distance L at constant depth ℓ:

$$E_s = \frac{W}{V} = \frac{W}{\ell L \bar{w}_k} = \frac{\bar{f}_t L}{\rho L \bar{w}_k} = \frac{\bar{f}_t}{\ell \bar{w}_k}. \tag{34}$$

Specific energy E_s can also be defined in terms of the time derivatives of energy and volume, i.e. in terms of the *rates* at which energy is consumed and cuttings are produced:

$$E_s = \frac{dW/dt}{dV/dt} = \frac{\dot{W}}{\dot{V}} = \frac{P}{\dot{V}} \tag{35}$$

where P is power consumption. For many practical purposes this alternative is preferable, since the tool's rate of energy consumption can be measured by the power supplied, and volumetric cutting rate is given by tool velocity and kerf cross section. For a parallel-motion tool cutting a constant depth ℓ:

$$E_s = \frac{P}{\dot{V}} = \frac{P}{\ell u \bar{w}_k} = \frac{\bar{f}_t u}{\ell u \bar{w}_k} = \frac{\bar{f}_t}{\ell \bar{w}_k}. \tag{36}$$

When E_s is expressed as W/V or $P/\dot{V}$ it has the dimensions of stress, and from eq 34 and 36 it can be seen that for a parallel motion tool this could be interpreted physically as mean tangential tool force divided by the kerf cross section which lies normal to that force.* When geometrically

---

* In analytical work on metal-cutting machine tools, E_s for orthogonal cutting is sometimes referred to as the "specific cutting pressure."

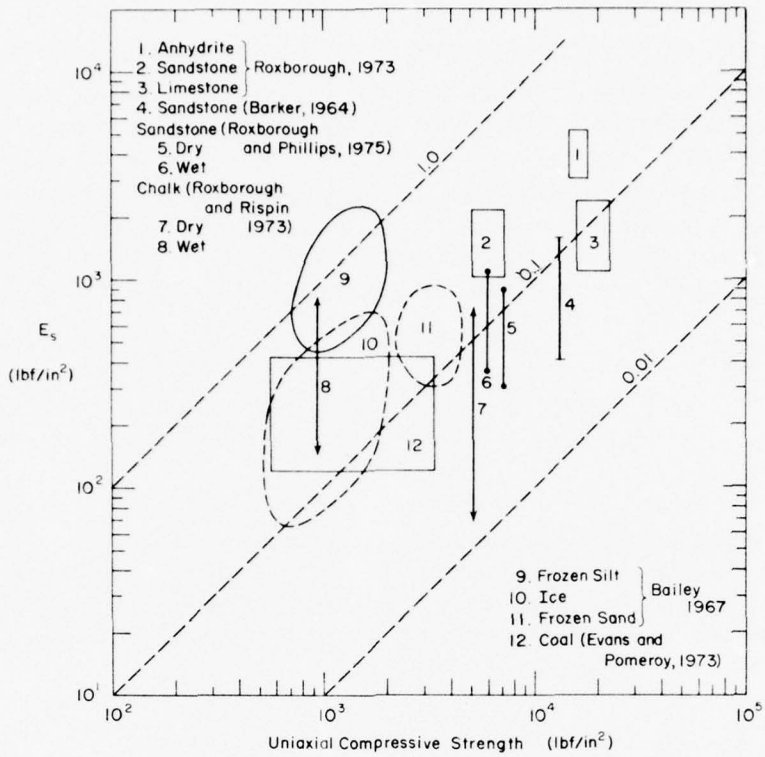

Figure 88. Specific energy for drag bit cutting plotted against uniaxial compressive strength. The lines drawn across the plot denote fixed values of the ratio E_s/σ_c.

similar chips are being sheared or split ahead of the tool tip, it would seem that the stress represented by E_s could be directly proportional to the shear stress or tensile stress required to form chips. Whatever the physical significance of E_s in terms of stress, there has been a longstanding empirical practice of normalizing E_s with respect to the uniaxial compressive strength of the material σ_c in order to obtain a dimensionless performance index for a particular type of tool or cutting process. In view of the foregoing comments, this is not too unreasonable, since the uniaxial compression test is a standard procedure that applies normal force to a cross section so as to fragment the specimen by forming internal tensile cracks and finally shearing across surfaces that are not parallel to the applied force. A more formal justification of this normalizing procedure has been given elsewhere (Mellor 1972).

Figure 88 gives some ranges of values of specific energy that have been obtained in laboratory experiments with drag bits. The ranges for each type of rock, frozen soil or ice represent results for different types of tools and varying operating conditions. However, being plotted against uniaxial compressive strength they do give order of magnitude indications of the dimensionless index E_s/σ_c. For friable brittle materials that are acted on by effectively applied tools, it appears that E_s/σ_c is of the order of 0.1 or less. There is some indication that for tougher or more ductile materials, E_s/σ_c may be somewhat higher, say between 0.1 and 1.0. (The effect of rock properties on E_s is discussed further in a subsequent section – see p. 71.)

If the specific energy of a drag bit in a certain rock is known or can be estimated, and if it is assumed that E_s is not strongly dependent on cutting speed, then the mean tangential cutting force $\bar{f}_t$ can be estimated from the power consumption and the tool's "excavation rate" $\dot{V}$, in accordance with eq 33.

It might be noted in passing that tool speed and tangential tool force are inversely proportional when power is constant so that, for a given machine operating at constant power, the mean tool force decreases as the tool speed increases. For machines overall, there is a corresponding tendency for tool force to decrease with tool speed, since available power tends to stay within narrower limits than does tool speed when all types of devices are considered.

The mean kerf width $\bar{w}$ that occurs in eq 32, 34 and 36 can be expressed in terms of actual tool width w, chipping depth ℓ, and overbreak angle ϕ, as can be seen from Figure 59:

$$\bar{w} = w + \ell \tan\phi. \tag{37}$$

Substituting for $\bar{w}$ in eq 36 then gives

$$E_s = \frac{\bar{f}_t}{\ell(w + \ell \tan\phi)} \tag{38}$$

in which $\tan\phi$ might be in the range 1 to 3 for typical rocks and typical cutting conditions. Actually, the idea that ϕ is invariant with ℓ seems questionable.

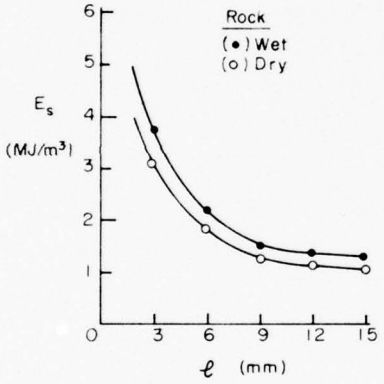

Figure 89. Specific energy as a function of chipping depth for wet and dry sandstone. (Roxborough and Phillips 1975.)

Variation of specific energy with chipping depth for a single tool

Experimental data usually show the specific energy E_s for a single tool decreasing as chipping depth increases, but tending to some lower limit (Fig. 89-94). However, some data for "deep" cutting suggest that specific energy reaches a minimum value and then begins to increase again as chipping depth is further increased (Fig. 93).

In assessing these trends, it is interesting to recall that

$$E_s = \frac{\bar{f}_t}{\ell^2 (w/\ell + \tan\phi)} \tag{39}$$

and that the empirical relationship between $\bar{f}_t$ and ℓ is representable approximately by

$$\bar{f}_t = k\ell^n \tag{40}$$

where k is a proportionality constant and $n \leq 1$. Thus

$$E_s = \frac{k}{\ell^{2-n}(w/\ell + \tan\phi)}. \tag{41}$$

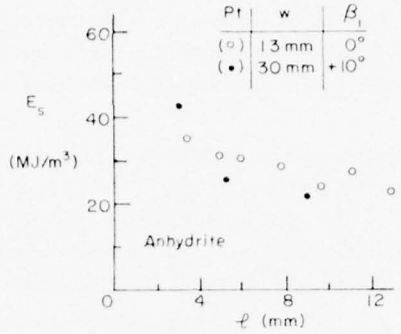

a. Two different tools in anhydrite.

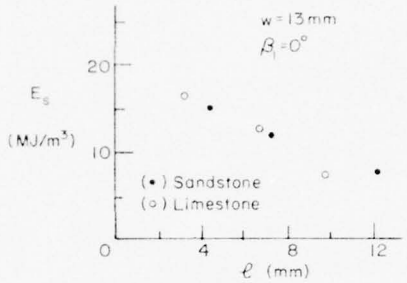

b. Similar tool in limestone and sandstone.

Figure 90. Specific energy plotted against chipping depth. (Roxborough 1973.)

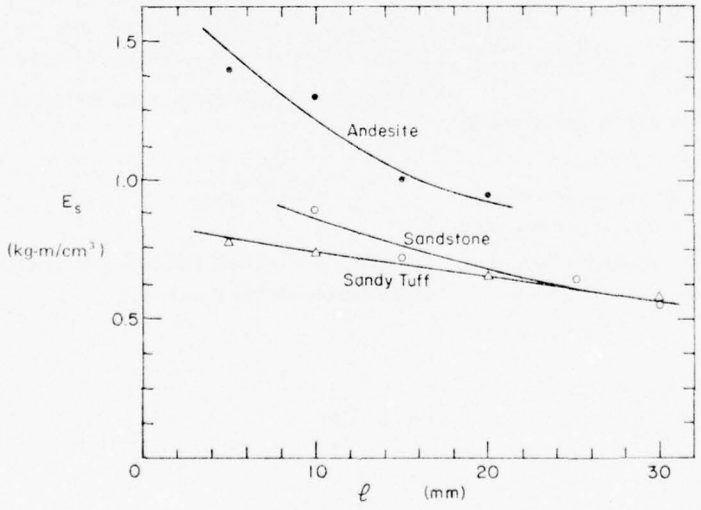

Figure 91. Specific energy as a function of chipping depth for three rock types. (Furumi, personal communication.)

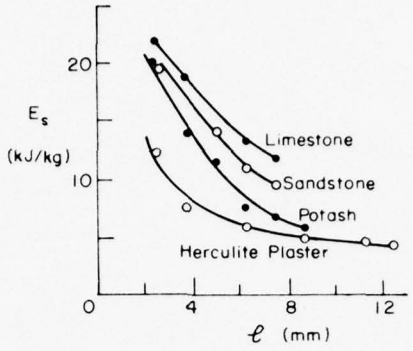

Figure 92. Specific energy as a function of chipping depth for four different materials. (Whittaker and Szwilski 1973.)

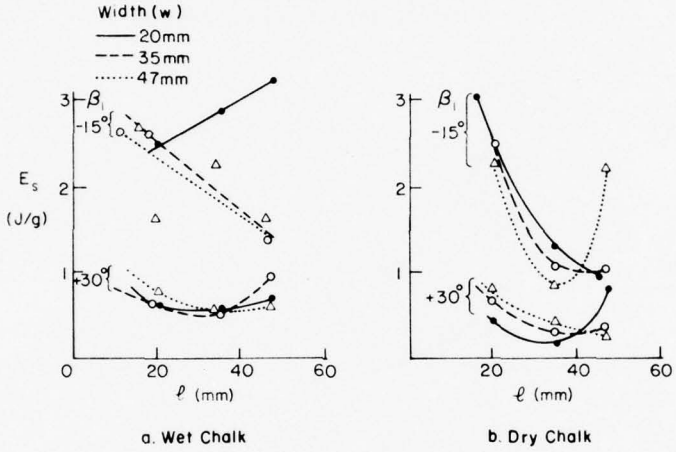

Figure 93. Specific energy as a function of chipping depth for six different tools working in wet and dry chalk. (Roxborough and Rispin 1973a, b.)

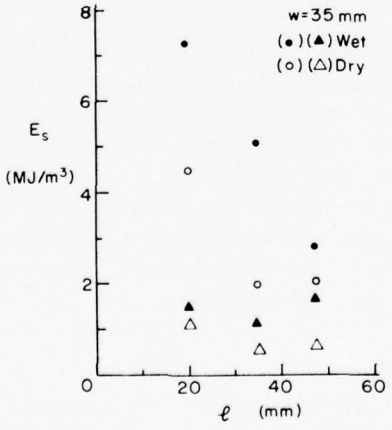

Figure 94. Specific energy plotted against chipping depth for two different tools in wet and dry chalk. (Roxborough and Rispin 1973a.)

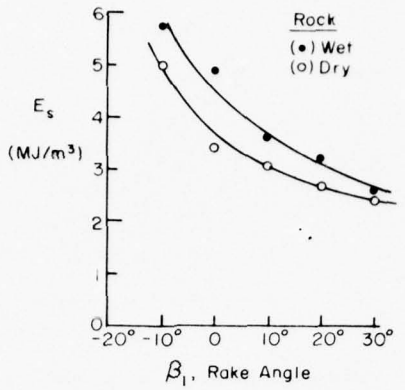

Figure 95. Specific energy as a function of rake angle for chisel edge tools in wet and dry sandstone. (Roxborough and Phillips 1975.)

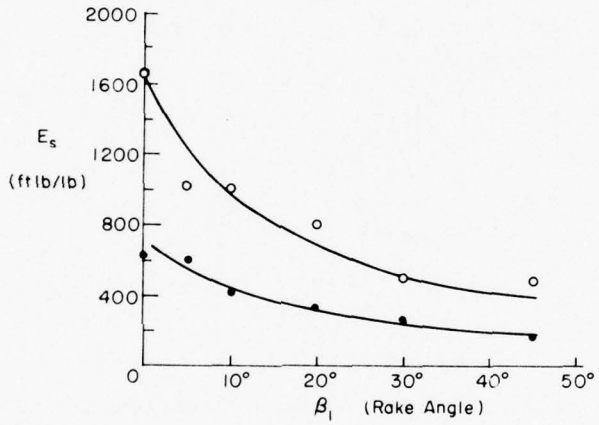

Figure 96. Specific energy as a function of rake angle for two types of coal. (Evans and Pomeroy 1973.)

With $w/\ell >> \tan\phi$, this implies that E_s is approximately proportional to ℓ^{n-1}, while with $w/\ell << \tan\phi$, E_s is approximately proportional to ℓ^{n-2}, assuming in both cases that ϕ is invariant with ℓ. The first case represents two-dimensional cutting, for which n is probably fractional, while the second case represents "deep," or three-dimensional, cutting for which n seems to be close to unity. In both cases there is an approximation to inverse proportionality between E_s and ℓ. The observed minimum in E_s for some deep cutting experiments could be explained by a decrease in the effective value of ϕ as ℓ increases. The latter might well occur, judging by the results of Roxborough and Phillips (1975) for kerf deepening experiments, in which ℓ was increased by multiple tool passes, making the effective value of ϕ decrease with increase of ℓ.

Effect of rake angle on specific energy

The rake angle of a tool affects the cutting force, but it does not directly affect the volume of material cut out by the tool. Hence, specific energy ought to vary with rake angle in exactly the

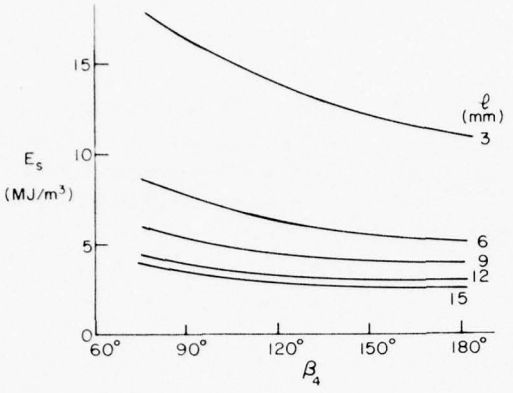

Figure 97. Variation of specific energy with side rakes for a symmetrical (V-face) tool, with chipping depth as parameter. Unrelieved cutting in sandstone. (Roxborough and Phillips 1975.)

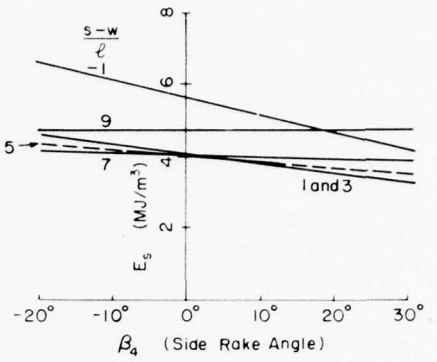

Figure 98. Specific energy as a function of side rake for a tool with one-way side rake. The graphs show the effect of distance from a parallel relieving kerf. (Roxborough and Phillips 1975.)

same way as the mean tangential cutting force $\overline{f}_t$ varies. In other words, for an unworn tool cutting deeply ($\ell > r$), specific energy ought to decrease as the rake angle increases, tending to a lower limit as the rake angle reaches +20° to +30° (see p. 32).

Figures 95 and 96 give direct examples of the variation of E_s with rake angle β_1.

Effect of relief angle on specific energy

The relief angle of the tool affects the mean tangential cutting force $\overline{f}_t$, but not the volume of material that is cut. Thus specific energy E_s ought to vary with relief angle β_2 in exactly the same way as $\overline{f}_t$ varies with β_2. This means that E_s should be constant for values of the "dynamic relief angle greater than about 5°, but it can be expected to increase sharply after the dynamic relief angle drops below 5° or so. It should be recalled that "dynamic" relief angle is the difference between actual tool relief angle and the "kinematic" relief angle needed to prevent scraping of the tool flank (i.e. the maximum angle given by the tool trajectory).

Effect of side rake on specific energy

With symmetrical side rakes, as on a V-face pick, the mean tangential cutting force $\overline{f}_t$ decreases linearly with increase of the side rake angles β_4 (see Fig. 44). However, according to experiments on sandstone by Roxborough and Phillips (1975), the kerf cross section, or mean kerf width $\overline{w}$, also decreases with increase of the side rakes β_4, and the net effect for unrelieved cutting is that specific energy E_s increases with increasing values of β_4 (Fig. 97).

With one-way side rake and unrelieved cutting there is no significant variation of E_s with β_4 over the practical range of β_4. However, when the tool is traveling parallel to an existing kerf, there is a small but significant decrease in E_s as β_4 increases. The variation of E_s with β_4 becomes more pronounced as the spacing between the tool and the relieving kerf decreases (Fig. 98). The absolute values of E_s for positive side rake (i.e. plowing towards the relief) are lowest for offsets in the range $1 < (s-w)/\ell < 3$.

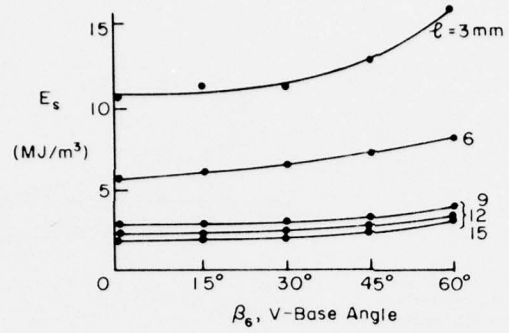

Figure 99. Specific energy as a function of base angle with chipping depth as parameter. (Roxborough and Phillips 1975.)

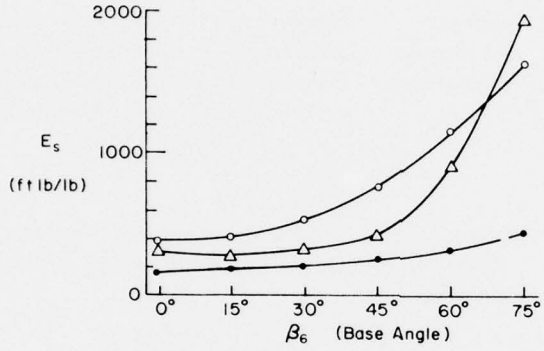

Figure 100. Specific energy as a function of base angle for three types of coal. (Evans and Pomeroy 1973.)

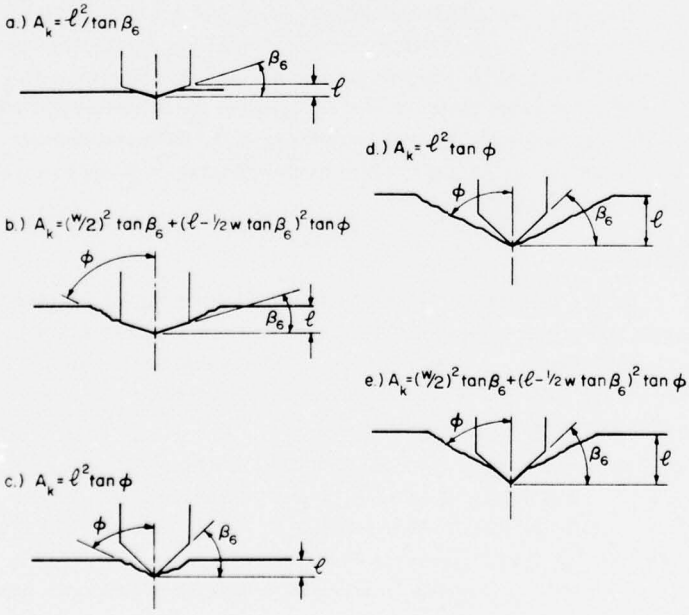

Figure 101. Idealized kerf cross sections, showing area for different base angles and different chipping depths. (After Roxborough and Phillips 1975.)

Effect of base angle or face profile on specific energy

As the base angle β_6 of a symmetrical cutting tool increases, the specific energy increases (Fig. 99, 100). Although the mean tangential cutting force $\bar{f}_t$ decreases with increase of β_6 (see Fig. 47), the kerf cross section decreases, and the net effect is an increase of E_s.

It is not altogether clear why specific energy does not tend to a steady value when the half-angle of the V-base drops below the overbreak angle ϕ (i.e. when $\beta_6 > \pi/2 - \phi$), since $\bar{f}_t$ stabilizes in this range and the area of the kerf cross section A_k should also stabilize if ϕ is a constant. As a matter of interest, the kerf area A_k is given by the following relations for various cutting situations (Fig. 101), following Roxborough and Phillips (1975):

a. Blunt-base tool chipping to shallow depth

$$\beta_6 < (\pi/2 - \phi); \qquad \ell < \tfrac{1}{2} w \tan\beta_6$$

$$A_k = \ell^2 / \tan\beta_6$$

b. Blunt-base tool chipping deeply

$$\beta_6 < (\pi/2 - \phi); \qquad \ell > \tfrac{1}{2} w \tan\beta_6$$

$$A_k = (w/2)^2 \tan\beta_6 + (\ell - \tfrac{1}{2} w \tan\beta_6)^2 \tan\phi$$

c. Sharp V-base tool chipping to shallow depth

$$\beta_6 > (\pi/2 - \phi); \qquad \ell < \tfrac{1}{2} w \tan\beta_6$$

$$A_k = \ell^2 \tan\phi$$

d. Sharp V-base tool chipping deeply

$$\beta_6 > (\pi/2 - \phi); \qquad \ell > \tfrac{1}{2} w \tan\beta_6$$

$$A_k = \ell^2 \tan\phi.$$

If A_k continues to decrease with increase of β_6 when $\beta_6 > (\pi/2 - \phi)$, then there is an implication that the tool tip is partly embedded as shown in Figure 101e.

Available data for variation of E_s with the radius of curvature of the face profile show a somewhat different trend (Fig. 102). These results from coal-cutting experiments suggest that E_s may have a minimum value with a base radius of approximately 0.07 in.

Effect of tip radius on specific energy

Tool tip radius r is another parameter that affects only the tool force, so that specific energy ought to vary with tip radius in the same way as $\bar{f}_t$ varies with r. Thus E_s may be expected to increase non-linearly with r, tending progressively towards a limit when r becomes greater than the chipping depth ℓ (see p. 36). Figure 103 gives a direct example of the variation of E_s with r, although in this case r never approaches the same magnitude as ℓ (cf. Fig. 49, which gives the corresponding relation between $\bar{f}_t$ and r).

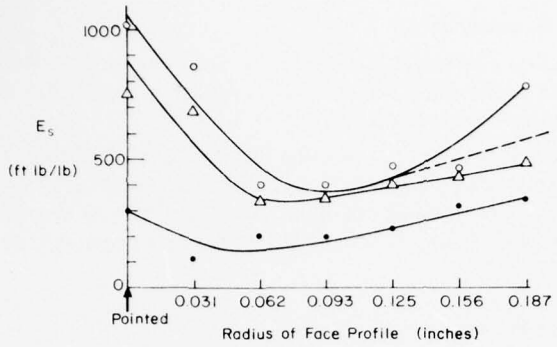

Figure 102. Specific energy as a function of base radius for three types of coal. (Evans and Pomeroy 1973.)

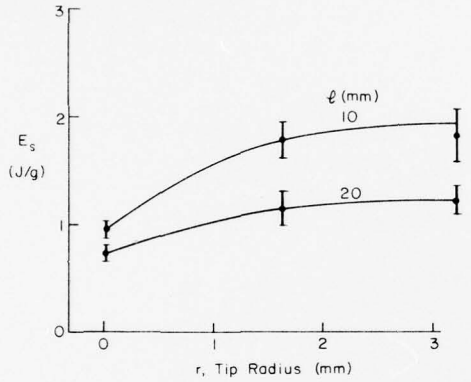

Figure 103. Specific energy as a function of tool tip radius for two chipping depths in chalk. (Roxborough and Rispin 1973a.)

Effect of tool width on specific energy

Tool width affects both the mean tangential cutting force $\bar{f}_t$ and the excavated cross section. Tool force varies linearly with tool width w, the relationship being of the form

$$\bar{f}_t = a_0 + a_1 w = f_0(\ell) + f_1(\ell) w \tag{42}$$

where a_0 and a_1 are depth-dependent constants. The effective kerf width $\bar{w}$ is often taken as

$$\bar{w} = w + \ell \tan\phi \tag{43}$$

assuming that ϕ is invariant with ℓ over the range of interest. If these relations are accepted, the specific energy E_s can be expressed as

$$E_s = \frac{f_0(\ell) + f_1(\ell) w}{\ell(w + \ell \tan\phi)}. \tag{44}$$

With constant chipping depth ℓ, and with overbreak angle ϕ either constant or some function of ℓ, the relationship for E_s is of the form

$$E_s = \frac{a_0 + a_1 w}{b_0 + b_1 w} \tag{45}$$

where b_0 and b_1 are constants. Thus E_s could increase with w, decrease with w, or remain almost independent of w, depending on the relative values of the constants a_0, a_1, b_0, b_1. Figure 104 gives an example of experimental data that show E_s varying only slightly with w. This is not too surprising, since f_t is likely to vary in direct response to changes in $\bar{w}$, i.e. f_t may be directly proportional to $\bar{w}$.

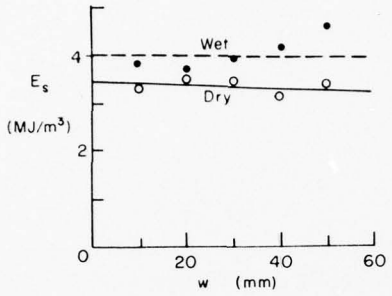

Figure 104. Specific energy plotted against tool width (wet and dry sandstone). (Roxborough and Phillips 1975.)

Effect of tool speed on specific energy

As far as is currently known, tool speed u does not significantly alter the effective kerf width when the cutting process involves only brittle fracture. Furthermore, it appears that tool speed has no significant effect on the mean tangential cutting force $\bar{f}_t$ over the range of speeds applicable to rock-cutting machines (see p. 43). Thus there is no reason to expect that the specific energy E_s will vary with tool speed as long as there is no question of ductile yielding, or of ductile/brittle transition, in the cutting process. The kinetic energy imparted to the cutting does increase with u^2 for wide tools, but this appears to be insignificant in typical rock-cutting conditions.*

Variation of specific energy with rock properties

The mean tangential cutting force $\bar{f}_t$ increases almost linearly with rock strength; to a first approximation, $\bar{f}_t$ is directly proportional to uniaxial compressive strength σ_c, which is often the only known strength parameter. However, according to theory there might be a better overall correlation with tensile strength. If this is so, the expression for $\bar{f}_t$ could be written as

$$\bar{f}_t = k\,\sigma_c/R \tag{46}$$

where k is a proportionality constant and R is the ratio of uniaxial compressive strength to uniaxial tensile strength.

The mean kerf width $\bar{w}$ also depends on rock properties, in that the overbreak angle ϕ for any given depth of cut is a variable:

$$\bar{w} = w + \ell \tan\phi. \tag{47}$$

For very brittle or friable materials, ϕ is expected to be relatively large at moderate chipping depth, whereas for ductile materials ϕ is likely to be small.

---

* The situation is very different with wood-cutting machines, which can have tool speeds above 20,000 ft/min (> 100 m/s).

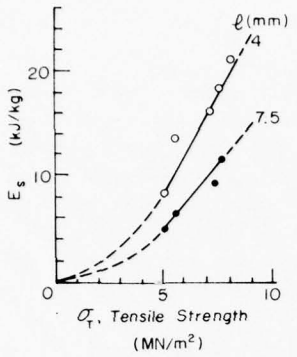

Figure 105. Specific energy as a function of tensile strength. (Whittaker and Szwilski 1973.)

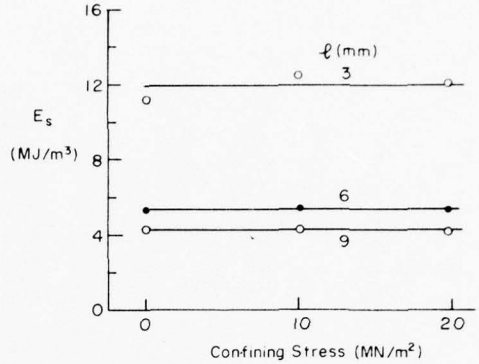

Figure 106. Specific energy plotted against lateral confining stress for three values of chipping depth in sandstone. (Roxborough and Phillips 1975.)

The net effect of rock properties on specific energy can perhaps be deduced from the relation

$$E_s = \frac{\bar{f}_t}{\bar{w}} = \frac{k\sigma_c/R}{\ell(w+\ell\tan\phi)} \quad . \tag{48}$$

Applying the foregoing arguments to this relation, E_s can be expected to increase as R decreases and as ϕ decreases. Otherwise, E_s will be directly proportional to compressive strength. The data summarized in Figure 88 are consistent with this supposition (the rather skimpy data of Figure 105 are not quite in agreement).

When the rock to be cut is at considerable depth, as in a tunnel, a mine, or a borehole, the confining stress might be expected to increase the cutting forces, and hence the specific energy, since the relevant cutting theories usually assume failure in accordance with the Coulomb-Mohr criterion. This has been discussed earlier (see p. 45). However, Roxborough and Phillips (1975) have shown experimentally (Fig. 106) that the effect of confinement on E_s is insignificant in sandstone subjected to confining stresses up to 20 MN/m^2 (2900 lbf/in.^{2}).

Effect of kerf spacing on specific energy

When tools are spaced so that adjacent parallel kerfs are very wide apart, there is no interaction between tools, and specific energy E_s does not vary with spacing. As adjacent kerfs are set closer together, a stage is reached at which a tool obtains relief from an existing kerf. As this critical limit of interaction is passed and kerf spacing decreases, specific energy decreases to a minimum and thereafter rises again to high values as the tool moves out into the existing kerf. The highest values of E_s occur just as the tool moves into the center of the existing kerf, where it is running exactly in the track of a preceding tool.

Previous discussions of kinematics and of tool forces have brought out the point that tools can be expected to begin interacting when the overbreaks of adjacent kerfs just begin to touch, i.e. when x in Figure 59 drops to zero. This means that the critical lateral spacing between tools would be given by $(s-w)/\ell = 2\tan\phi$, where s is center-to-center spacing of adjacent kerfs, w is tool width, and ϕ is the overbreak angle of the rock. With overbreak angles in the range 50° to 70°, the critical spacing between tools would be in the range $2.5 < (s-w)/\ell < 5.5$ according to theoretical prediction.

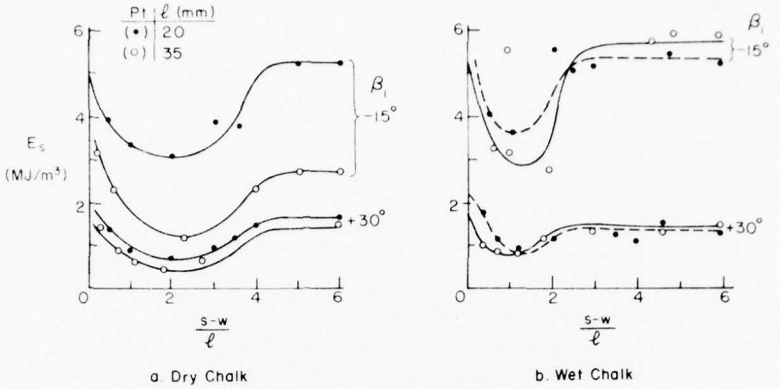

Figure 107. Variations of specific energy with dimensionless kerf spacing in wet and dry chalk. (Roxborough and Rispin 1973a, b.)

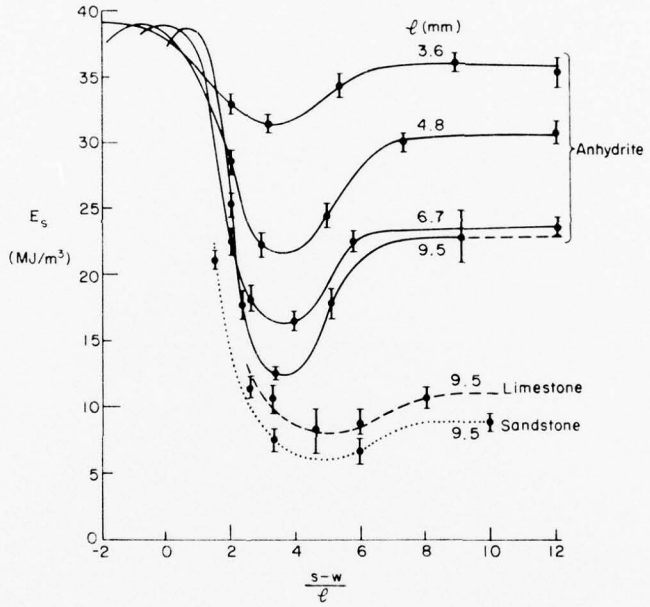

Figure 108. Specific energy as a function of dimensionless kerf spacing for anhydrite, limestone and sandstone. (Roxborough 1973.)

Direct experimental evidence on critical spacing is in reasonably good agreement with such a prediction. Roxborough and Rispin (1973a, b) found that critical values of $(s-w)/\ell$ were approximately 3 in wet chalk (predicted value 2.9) and between 4 and 5 in dry chalk (predicted value 5). Experimental results are shown in Figure 107. Roxborough (1973) showed a critical spacing of about 4 for anhydrite (Fig. 108), which was higher than the predicted value of 2.6. His experimental data for limestone showed critical spacing of about 6 (predicted value 5.5), and for sandstone about 5 (predicted value 3.8). For coal, Evans and Pomeroy (1973) found interaction starting at a spacing of $(s-w)/\ell \approx 3$.

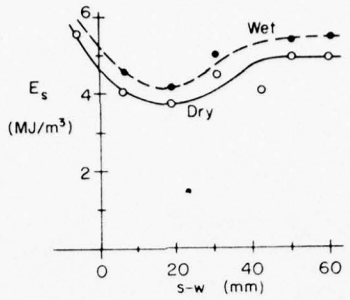

Figure 109. Specific energy as a function of kerf spacing in wet and dry sandstone. (Roxborough and Phillips 1975.)

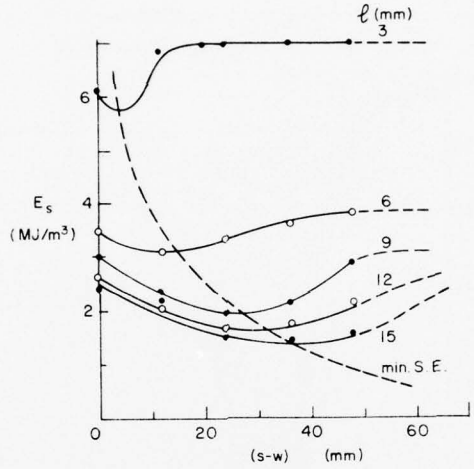

a. Dimensional plot.

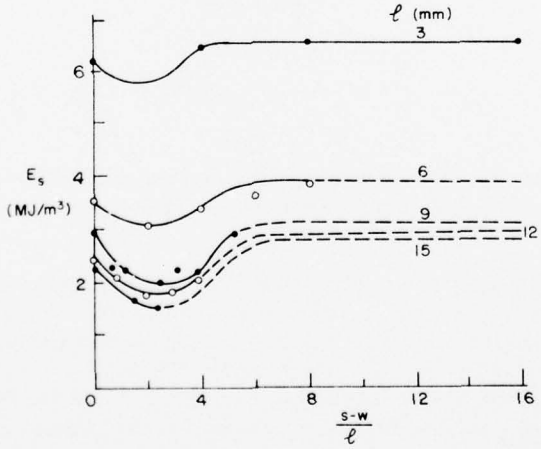

b. Dimensionless spacing.

Figure 110. Specific energy as a function of kerf spacing, with chipping depth as parameter. (Roxborough and Phillips 1975.)

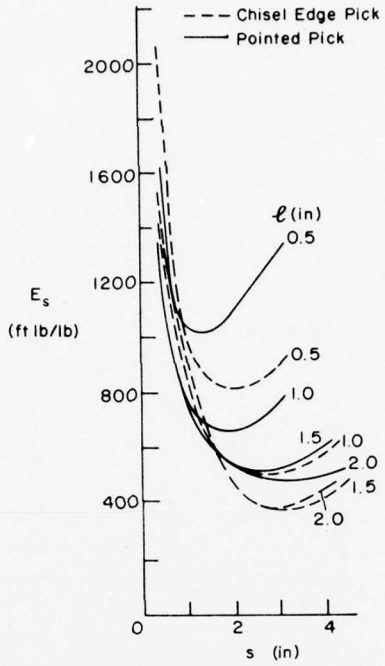

a. Dimensional plot.

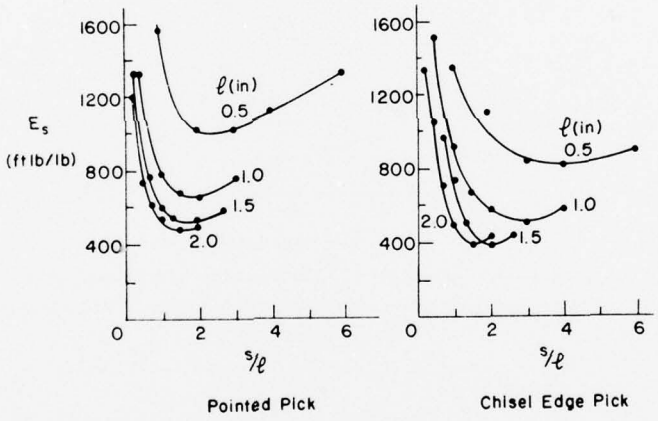

b. Dimensionless spacing.

Figure 111. Specific energy as a function of kerf spacing for two types of tools cutting sandstone. (After Barker 1964.)

In a previous discussion on the geometric aspects of tool spacing (Mellor 1976a) it was suggested that optimum spacing in brittle materials might be found near the positions which give complete overlap of the side breaks, i.e. when $(s-w)/\ell \approx \tan\phi$. In the Roxborough and Rispin study mentioned above (Fig. 107), the optimum spacings found experimentally were 1 to 1.5 for wet chalk ($\tan\phi$ = 1.43), and 2 to 2.5 for dry chalk ($\tan\phi$ = 2.48). In the Roxborough work (Fig. 108), specific energy was a minimum at spacings of approximately 1.5 in anhydrite ($\tan\phi$ = 1.28), 3 in limestone ($\tan\phi$ = 2.75), and 3 for sandstone ($\tan\phi$ = 1.88). Roxborough and Phillips (1975) tested a sandstone in both wet and dry conditions (Fig. 109, 110) and found that optimum spacing lay between 2 and 2.5

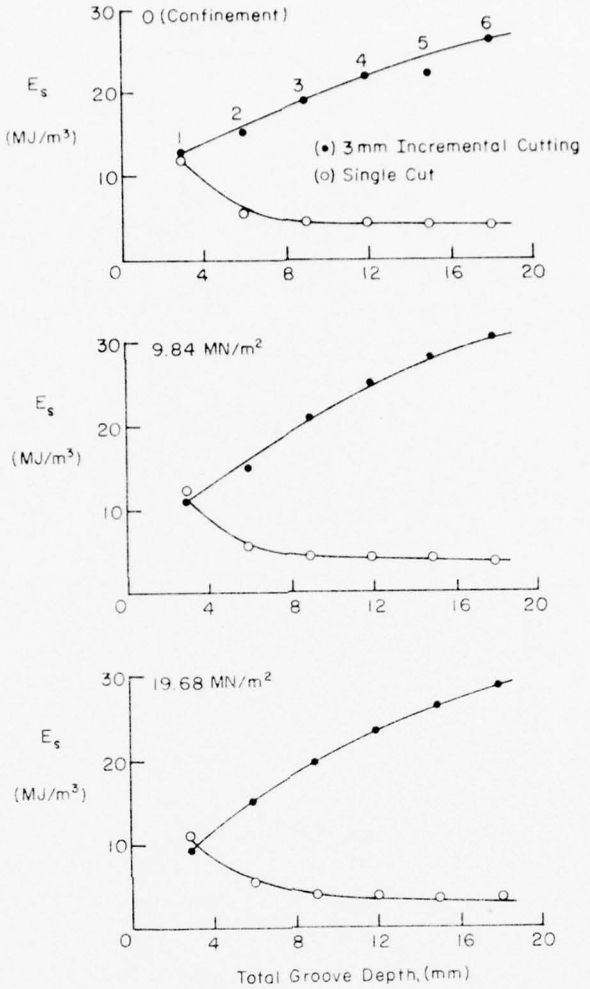

Figure 112. Effect of multiple pass groove deepening on specific energy for three levels of confining stress. (Roxborough and Phillips 1975.)

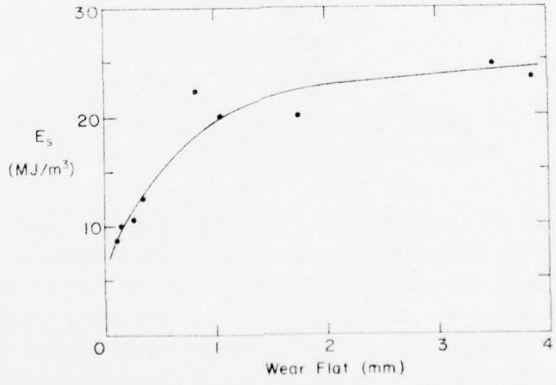

Figure 113. Variation of specific energy with wear flat length. (Roxborough and Phillips 1975.)

($\tan\phi \approx 1.73$ for the dry material). Barker's (1964) test results for large picks indicate that optimum values of $(s-w)/\ell$ were in the range 1 to 1.7 for a chisel edge pick and in the range 1.5 to 2 for a "pointed" pick (Fig. 111).

It is important to note that these spacings are dimensionless numbers obtained by dividing the actual distance between tool edges $(s-w)$ by the chipping depth ℓ. When tools are fixed to a multiple-tool machine, their spacing will be optimum for only one value of ℓ in any given material.

Effect of multiple pass cutting on specific energy

When a single isolated kerf is progressively deepened by multiple passes of a cutting tool, the cutting force f_t at first increases with each pass, even though the chipping depth is constant for each pass. At the same time, the area of the kerf cross section swept out by the tool at first decreases with each pass, since the overbreak is gradually suppressed. These two effects combine to produce a large increase in specific energy for each successive pass in the early stages. Specific energy eventually stabilizes at a steady value, perhaps after the kerf depth has become greater than the kerf width.

Figure 112 shows some results of kerf deepening experiments by Roxborough and Phillips (1975). The cumulative specific energy needed to reach a certain depth by multi-pass cutting is compared with the specific energy needed to reach that depth with a single cut. It can be seen that the multiple pass procedure is extremely inefficient. This could be of great practical importance in the design of a machine.

Effect of tool wear on specific energy

Development of a typical wear flat that is almost parallel to the tangential direction results in increase of the mean tangential cutting force $\overline{f}_t$, but there is no significant effect on the cross section of the kerf for a chisel-edge tool. The increase of $\overline{f}_t$ with wear flat width x is of the form $\overline{f}_t = kx^n$, where n is a fractional power. Thus specific energy E_s is also expected to increase in proportion to x^n as wear develops. The direct experimental results of Roxborough and Phillips (1975) support this idea (Fig. 113).

With a V-base tool or a rounded-base tool, the area of the wear flat increases with the square of a linear dimension for the wear flat. It is therefore possible that $\overline{f}_t$ might increase more rapidly with x, possibly in a way that makes $\overline{f}_t$ proportional to x^{2n}. If this were so, then E_s would also be proportional to x^{2n}.

GENERAL SUMMARY

In reviewing the available information on rock-cutting tools it is not always easy to reconcile findings from different sources, especially where some variables are left uncontrolled or are ignored. However, once the information has been compiled and digested, a reasonably coherent picture emerges. The following summary is intended to bring out general patterns of behavior, without dwelling too much on complications and apparent anomalies.

Theory. Theoretical studies bring a disciplined approach to the problem, and provide guidance for the interpretation of experimental data. There are still major shortcomings in rock cutting theories, so that experimental studies remain essential. Comparisons with theories for metal cutting and wood cutting are instructive.

Chipping depth. Both f_t and f_n increase with ℓ. With "wide" cutters ($w >> \ell$), force is approximately proportional to some fractional power of ℓ. When ℓ is of comparable magnitude to w the

cutting is three-dimensional, and under these circumstances it appears that f_n and f_t may be approximately proportional to ℓ. When force is increasing nonlinearly with ℓ, f_t increases more rapidly than f_n and therefore the ratio f_n/f_t decreases with increase of ℓ. When f_n and f_t are both approximately proportional to ℓ, the ratio f_n/f_t is insensitive to changes in ℓ.

While f_t is increasing with ℓ, the area of the kerf cross section is also increasing, and the net result is that specific energy E_s decreases nonlinearly with increase of ℓ and it tends to a lower limit with wide cutters. In some cases E_s appears to pass through a minimum and then increase again as ℓ continues to increase, perhaps because overbreak becomes less effective.

Rake angle. β_1 only affects performance when ℓ is significantly greater than tool tip radius r. It does not have much influence when tools are badly worn. Both f_t and f_n decrease nonlinearly as β_1 increases, i.e. as the included angle β_3 decreases. f_n and f_t come close to reaching a limiting low value when β_1 reaches $+20^\circ$ to $+30^\circ$. There does not appear to be a strong or consistent variation of the ratio f_n/f_t when β_1 varies.

β_1 has virtually no effect on kerf width, and therefore the specific energy E_s decreases with increase of β_1 in exactly the same way as $\bar{f}_t$ decreases with β_1.

Relief angle. β_2 has no perceptible effect on f_n and f_t for values greater than 5° when the tool is unworn. When β_2 drops below 3°–5°, there are sharp increases in both f_n and f_t. These comments apply to "dynamic" values of β_2, which have to be added to the "kinematic" values that are required to provide flank clearance in accordance with the penetration trajectory.

E_s ought to vary with β_2 in the same way as $\bar{f}_t$ varies with β_2.

Side rake. With symmetrical side rakes, both f_n and f_t decrease approximately linearly as β_4 increases, and the ratio f_n/f_t does not vary significantly with β_4. With one-way side rake a transverse force component f_s is developed, but β_4 has no significant effect on f_n and f_t for either relieved or unrelieved cutting. f_s increases nonlinearly with β_4 in both relieved and unrelieved situations, tending towards a limit in the range $\beta_4 > 20^\circ$.

With symmetrical side rakes, mean kerf width $\bar{w}$ decreases approximately linearly with increase of β_4. With one-way side rake, E_s does not vary with β_4 in unrelieved cutting, but there is a slight decrease in E_s as β_4 increases when the tool is plowing towards an existing kerf.

Base angle. f_n and f_t decrease nonlinearly as β_6 increases, tending to reach a lower limit when $\beta_6 > (\pi/2-\phi)$.

The cross-sectional area of the kerf also decreases nonlinearly as β_6 increases, and the net effect on specific energy is increase of E_s with increase of β_6.

Tool tip radius. Both f_n and f_t increase nonlinearly with increase of r, possibly in proportion to $r^{1/2}$. Curvature of the graphical relation appears greatest in the range $0.5 < \ell/r < 1.0$, and linear approximations may be acceptable for the ranges $r << \ell$ and $r >> \ell$. The latter condition represents very shallow cutting, where operation is very inefficient and tool angles are largely irrelevant. r can be used as a normalizing parameter for chipping depth ℓ.

Since r affects f_t but not the area of the kerf cross section, E_s ought to vary with r in the same way as $\bar{f}_t$ varies with r.

Tool width. For a chisel-edge tool, f_n and f_t increase linearly with w. In a graphical relation, the force intercept, which represents edge effects, increases with increase of ℓ, and the proportionality constant should also increase with ℓ.

The effective kerf width $\bar{w}$ is equal to tool width w plus a depth-dependent constant: $\bar{w} = w + \ell\tan\phi$. For any given value of ℓ, E_s could either increase or decrease with w, but it is likely to be rather insensitive to changes in w.

Force fluctuations. Force levels fluctuate during the cutting of brittle materials in response to repetitive formation of discrete chips. The amplitude of force fluctuations is related to the mean force and to the compliance of the tool and its mounting. Test records, which in some cases may be influenced by the compliance of the dynamometer, indicate that the ratio of mean peak force to mean force might be typically in the range 2 to 6 for f_t, but for f_n the variation appears to be much less in some cases. If the amplitude of force fluctuations is different for f_t and f_n, or if fluctuations for the two components are not in phase, then the direction of the resultant cutting force is fluctuating.

Tool speed. f_t is not significantly affected by tool speed u in the range 1 to 1000 ft/min (0.005 to 5 m/s) for typical rocks. In some experiments f_n has been found to increase with u; if this effect is real, it implies that the direction of the resultant cutting force moves closer to the normal direction as u increases. In ductile material, both f_t and f_n might be expected to vary with u.

E_s is not likely to vary with u when cutting involves brittle fracture, but it could do so in ductile material, or when ductile/brittle transitions are caused by change of u.

Rock properties. Cutting forces increase, approximately linearly, with increase of rock strength. Lateral confining stresses are expected to cause an increase in cutting forces, but some experiments indicate that confinement does not have much influence on either f_t or f_n. Tool forces are usually correlated with uniaxial compressive strength, although correlation with tensile strength might be more appropriate. For materials that are anomalous with respect to the ratio of compressive strength to tensile strength (R), it might be useful to account for this difference by a suitable factor.

Mean kerf width is to some extent dependent on rock properties, in that the overbreak angle ϕ varies with material type. For typical brittle rocks, a linear correlation between specific energy and compressive strength σ_c can be expected, but decrease of R or ϕ (perhaps indicative of increasing ductility) would increase E_s for any given value of σ_c.

Kerf spacing. Tools that cut parallel kerfs operate independently of each other when the space between them is sufficient to separate the overbreaks, i.e. when $(s-w)/\ell > 2\tan\phi$. As kerf spacing decreases from this critical value, f_n and f_t decrease, falling to zero when a tool tracks exactly behind a preceding tool.

Specific energy E_s decreases as kerf spacing decreases from the critical value, passes through a minimum at the optimum spacing, and then rises to relatively high values as the tool moves out into the track cut by a preceding tool. Optimum spacing is given approximately by $(s-w)/\ell \approx \tan\phi$. For tools fixed to a machine, lateral spacing can be optimum for only one value of ℓ in a given rock.

Multiple pass cutting. Progressive deepening of a kerf by repeated passes of a tool along the same track results in increase of f_n and f_t with each successive pass, until a limit is reached after the depth of the kerf exceeds its width.

The incremental area of the kerf cross section at first decreases with each successive pass, due to progressive suppression of overbreak. This effect combines with the effect of increasing tool force to produce large increases of specific energy E_s, a limit being reached after the depth of the kerf exceeds the width. The cumulative specific energy for cutting to a certain depth by multiple passes is much higher than E_s for a single cut to the same depth.

Tool wear. Development of a wear flat beneath the tip of a tool leads to increase of f_n and f_t with increase of the wear flat dimensions (assuming ℓ is maintained constant). f_n increases more rapidly than f_t, so that the ratio f_n/f_t increases with increase of wear flat dimensions. For a chisel-edge tool, on which the area of a wear flat is proportional to the length of the wear flat x, force components increase approximately in proportion to a fractional power of x. Also, x is approximately

proportional to a fractional power of the total cutting distance L traveled by the tool. A wear flat that is normal to the rake face of a tool causes similar increases of force with wear flat dimensions.

Volume loss, or weight loss, from a chisel-edge tool is approximately proportional to travel distance L after a brief initial period of very rapid loss. Wear rate decreases with increase of chipping depth ℓ, and with increase of tool hardness.

Specific energy E_s can be expected to increase in proportion with the increase of $\bar{f}_t$ as wear develops.

LITERATURE CITED

Appl, F.C. and D.S. Rowley (1963) Drilling stresses on drag bit cutting edges. *Proceedings of 5th Symposium on Rock Mechanics.* Pergamon/Macmillan, p. 119-136.

Appl, F.C., D.S. Rowley and H.C. Bridwell (1967) Theoretical analysis of cutting and wear of surface set diamond cutting tools. Christensen Diamond Products Company, Salt Lake City, 216 p.

Bailey, J.J. (1967) A laboratory study of the specific energy of disengagement of frozen soils. Conducted by Creare, Inc. for USA CRREL. USA CRREL Internal Report 99 (unpublished).

Barker, J.S. (1964) A laboratory investigation of rock cutting using large picks. *International Journal of Rock Mechanics and Mining Sciences*, vol. 1, no. 4, p. 519-534.

Chamber of Mines of South Africa Research Organization (1971) Ninth Annual Research Review. P.R.D. Series no. 158.

Cheatham, J.B. (1958) An analytical study of rock penetration by a single tooth bit. 8th Drilling and Blasting Symposium, Univ. Minnesota.

Cook, N.G.W., N.C. Joughin and G.A. Wiebols (1968) Rock-cutting and its potentialities as a new method of mining. *Journal of the South African Institute of Mining and Metallurgy*, May, p. 435-454.

Ernst, H. (1938) Physics of metal-cutting. In *Machining of metals.* American Society for Metals, Cleveland, Ohio.

Ernst, H. (1951) Fundamental aspects of metal cutting and cutting fluid action. *Annals of New York Academy of Science*, vol. 53, p. 936.

Evans, I. (1962) A theory of the basic mechanics of coal ploughing. *Proceedings of International Symposium on Mining Research*, vol. 2, Pergamon, p. 761-798.

Evans, I. (1965) The force required to cut coal with blunt wedges. *International Journal of Rock Mechanics and Mining Sciences*, vol. 2, p. 1-12.

Evans, I. (1972) Line spacing of picks for effective cutting. *International Journal of Rock Mechanics and Mining Sciences*, vol. 9, p. 355-361.

Evans, I. and C.D. Pomeroy (1973) The strength, fracture and workability of coal. Published by the authors and available from National Coal Board, Mining Research and Development Establishment, Stanhope Bretby, Burton-on-Trent, England, 277 p.

Fairhurst, C. (1955) Some possibilities and limitations of rotary drilling in hard rock. *Transactions of the Institute of Mining Engineers*, vol. 115, p. 85-103.

Fourmaintraux, D. (1972) Machines foreuses pour tunnels et galeries. Rapport de Recherche no. 20, Laboratoire des Ponts et Chaussées, Ministère de l'Aménagement du Territoire de l'Equipement, du Logement et du Tourisme, 70 p.

Furby, J. (1970) Experiments in rock cutting by impact methods. *Tunnels and Tunneling*, November, p. 360-365.

Furumi, K., Personal communication on rock cutting experiments at Komatsu Ltd.

Gray, K.E. (1963) Fixed blade planing of rocks in the brittle stress state. Ph.D. Thesis, University of Texas, Austin, 240 p.

Hughes, H.M. (1972) Some aspects of rock machining. *International Journal of Rock Mechanics and Mining Sciences*, vol. 9, p. 205-211.

Kenny, P. and S.N. Johnson (1976a) The effect of wear on the performance of mineral-cutting tools. *Colliery Guardian.*

Kenny, P. and S.N. Johnson (1976b) An investigation of the abrasive wear of mineral-cutting tools. *Wear*, vol. 36, p. 337-361.

Koch, P. (1964) *Wood machining processes.* New York: Ronald Press, 530 p.

Lee, E.H. and B.W. Shaffer (1951) The theory of plasticity applied to a problem of machining. *Journal of Applied Mechanics*, vol. 18, p. 405.

Linenko, Yu. P. (1972) Analytical investigation of the wear resistance of a rock-cutting tool. *Fiziko-Tekhnicheskie Problemy Razrabotki Iskopaemykh*, no. 2, p. 56-61. (English translation in *Soviet Mining Research*, 1973, p. 165-169, Plenum.)

Mellor, M. (1972) Normalization of specific energy values. *International Journal of Rock Mechanics and Mining Sciences*, vol. 9, p. 661-663.

Mellor, M. (1975) Mechanics of cutting and boring, Part I: Kinematics of transverse rotation machines. CRREL Special Report 226.

Mellor, M. (1976a) Mechanics of cutting and boring, Part II: Kinematics of axial rotation machines. CRREL Report 76-16.

Mellor, M. (1976b) Mechanics of cutting and boring, Part III: Kinematics of continuous belt machines. CRREL Report 76-17.

Merchant, M.E. (1945) Mechanics of the metal-cutting process. I – Orthogonal cutting and type 2 chip. *Journal of Applied Physics*, vol. 16, no. 5, p. 267.

Nalezny, C.L. (1971) Cutting rock or frozen soil with a circular saw. *Journal of Terramechanics*, vol. 8, no. 1, p. 23-40.

Nishimatsu, Y. (1972) The mechanics of rock cutting. *International Journal of Rock Mechanics and Mining Sciences*, vol. 9, p. 261-270.

Potts, E.L.J. and P. Shuttleworth (1959) A study of ploughability of coal with special reference to the effects of blade shape, direction of planing to the cleat, planing speed and the influence of water infusion. *Transactions of the Institute of Mining Engineers*, vol. 117, no. 8, p. 519-553.

Roxborough, F.F. (1969) Rock cutting research. *Tunnels and Tunneling*, vol. 1, no. 3, p. 125.

Roxborough, F.F. (1973) Cutting rock with picks. *Mining Engineer*, June, p. 445-455.

Roxborough, F.F. (1976a) The influence of pick shape and some operational factors on the performance of hard rock excavation machines. *Proceedings, Institute of Engineers* (Australia).

Roxborough, F.F. (1976b) Rock excavation by machine – A comparative study of picks and discs. *Second Australian Tunnelling Conference, Proceedings.*

Roxborough, F.F. and H.R. Phillips (1974) Experimental studies on the excavation of rock using picks. *Proceedings of 3rd Congress, International Society of Rock Mechanics*, Denver, vol. IIB, p. 1407-1412.

Roxborough, F.F. and H.R. Phillips (1975) The mechanical properties and cutting characteristics of the Bunter sandstone. Report by Department of Mining Engineering, University of Newcastle upon Tyne for Transport and Road Research Laboratory, Department of the Environment, England.

Roxborough, F.F. and A. Rispin (1972) The mechanical cutting characteristics of the Lower Chalk. Report by Department of Mining Engineering, University of Newcastle upon Tyne for Transport and Road Research Laboratory, Department of the Environment, England.

Roxborough, F.F. and A. Rispin (1973a) The mechanical cutting characteristics of the Lower Chalk. *Tunnels and Tunneling*, Jan/Feb.

Roxborough, F.F. and A. Rispin (1973b) A laboratory investigation into the application of picks for mechanized tunnel boring in the Lower Chalk. *Mining Engineer*, Oct, p. 1-13.

Valantin, A., P. Belugou and P. Guillon (1964) Étude des pics des machines d'abattage. *Revue de l'Industrie Minérale*, Oct, p. 815-848.

Wagner, H. (1971) Der Mechanismus der Spanentstehung beim Zerspanen von Gesteinen. *Rock Mechanics*, vol. 3, no. 3, p. 159-174.

Whittaker, B.N. and A.B. Szwilski (1973) Rock cutting by impact action. *International Journal of Rock Mechanics and Mining Sciences*, vol. 10, p. 659-671.

Zelenin, A.N. (1959) Rezanie Gruntov. Izdat. Akad. Nauk, SSSR, Moscow.

Zelenin, A.N. (1968) Fundamentals of ground excavation by mechanical means. Mashinstroenie, Moscow (text in Russian).

APPENDIX A. ADDITIONAL DATA FOR ICE

Some additional results from ice cutting experiments were located after this report was prepared for publication. Machining tests were made with a lathe and a milling machine at the National Research Council of Canada, and results were given in an internal report of the Division of Mechanical Engineering (*Cutting of ice and its specific resistance* by T.M. Mazur, LTR-LT-53, October 1974). The ice was cut by a "wide" tool, and results were given as specific cutting resistance plotted against cutting cross section on logarithmic scales.

Specific cutting resistance is equivalent to specific energy for this type of operation, as noted on page 61. Cutting cross section for a wide tool of constant width is proportional to chipping depth ℓ. Mean tangential tool force $\overline{f}_t$ is equal to E_s multiplied by tool width and chipping depth, as indicated by eq 36, and $\overline{f}_t'$ is equal to $E_s\ell$. The results have been transformed accordingly, and they are summarized in Figures A1 and A2.

E_s was apparently insensitive to temperature and cutting speed for temperatures of ~5 to −10°C and speeds of about 300 to 700 ft/min. It decreased by a factor of 50 as chipping depth increased from 0.008 to 0.8 mm.

$\overline{f}_t'$ did not show much systematic variation with ℓ for chipping depths less than 0.04 mm. Even at the upper end of the range, $\overline{f}_t'$ only increased with about the 1/3 power of ℓ.

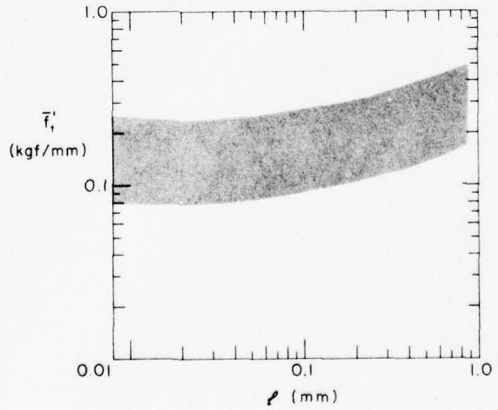

Figure A1. $\overline{f}_t'$ as a function of ℓ, as deduced from machining tests on ice. (Original data from Mazur, 1974.)

AD-A040 760 COLD REGIONS RESEARCH AND ENGINEERING LAB HANOVER N H F/G 13/9
MECHANICS OF CUTTING AND BORING. PART 4. DYNAMICS AND ENERGETIC--ETC(U)
APR 77 M MELLOR

UNCLASSIFIED CRREL-77-7 NL

2 OF 2
AD
A040760

END
DATE FILMED
7-77

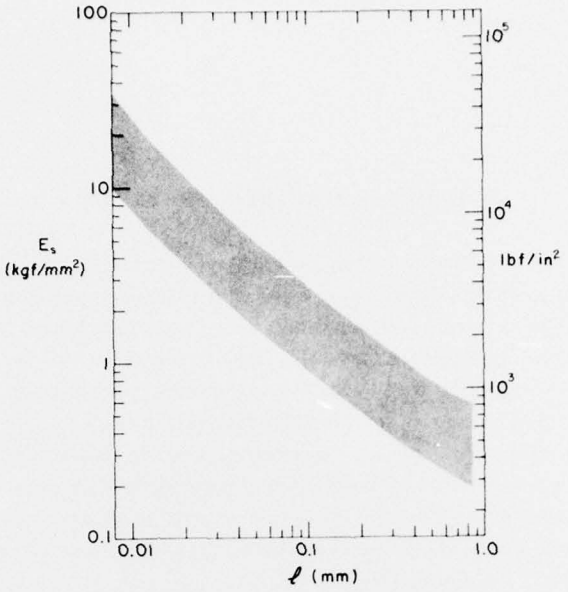

Figure A2. E_s as a function of ℓ, as deduced from machining tests. (Original data from Mazur, 1974.)

APPENDIX B. CONVERSION FACTORS: U.S. CUSTOMARY AND METRIC (SI) UNITS OF MEASUREMENT

Multiply	*By*	*To obtain*
inch	25.40	millimeter
millimeter	3.937×10^{-2}	inch
meter	3.281	foot
millimeter^2	1.550×10^{-3}	inch^2
millimeter^3	6.102×10^{-5}	inch^3
in./s	2.540×10^{-2}	m/s
m/s	1.968×10^{2}	ft/min
pound-force	4.448	newton
newton	0.2248	pound-force
lbf/in.	0.1751	N/mm
kgf/cm	0.9807	N/mm
lbf/in.^{2}	6.895	kN/m^2
MN/m^2	1.450×10^{-2}	lbf/in.^{2}
lbf/in.^{2} = in.-lbf/in.^{3} (specific energy)	6.895×10^{-3}	MJ/m^3
MJ/m^3	1.450×10^{2}	lbf/in.^{2}
kgf-m/cm^3	9.807	MJ/m^3
gram	2.205×10^{-3}	pound
ft-lbf/lb	2.99×10^{-3}	J/g
J/g	3.35×10^{2}	ft-lbf/lb